

MESTRADO
ESPECIALIDADE EM TOXICOLOGIA ANALÍTICA CLÍNICA E FORENSE

Screening of newly synthesized xanthonic derivatives as potential P-glycoprotein inducers/activators: an innovative strategy to fight Alzheimer's disease

Eva Alexandra Gil Martins

M
2018

Screening of newly synthesized xanthonic derivatives as potential P-glycoprotein inducers/activators: an innovative strategy to fight Alzheimer's disease
Eva Alexandra Gil Martins





UNIVERSIDADE DO PORTO

Faculdade de Farmácia, Departamento de Ciências Biológicas

Eva Alexandra Gil Martins

**Screening of newly synthesized xanthonic derivatives as potential
P-glycoprotein inducers/activators: an innovative strategy to fight
Alzheimer's disease**

**Dissertation of the Master's Degree in Analytical, Clinical and Forensic
Toxicology**

Work developed under the supervision of:

Professor Doctor Renata Sofia Araújo da Silva (FFUP)

Doctor Daniel José da Costa Barbosa (i3S)

September 2018

IT IS NOT PERMITTED TO REPRODUCE ANY PART OF THIS DISSERTATION

**DE ACORDO COM A LEGISLAÇÃO EM VIGOR, NÃO É PERMITIDA A REPRODUÇÃO
DE QUALQUER PARTE DESTA DISSERTAÇÃO.**

Work developed in the Toxicology Laboratory, Department of Biological Sciences, Faculty of Pharmacy, University of Porto (FFUP).

This work received financial support from the European Union (FEDER funds POCI/01/0145/FEDER/007728) and National Funds (FCT/MEC, Fundação para a Ciência e a Tecnologia and Ministério da Educação e Ciência) under the Partnership Agreement PT2020 UID/MULTI/04378/2013. The study is a result of the project NORTE-01-0145-FEDER-000024, supported by Norte Portugal Regional Operational Programme (NORTE 2020), under the PORTUGAL 2020 Partnership Agreement (DESIGNBIOTECHEALTH—New Technologies for three Health Challenges of Modern Societies: Diabetes, Drug Abuse and Kidney Diseases), through the European Regional Development Fund (ERDF).

The results presented in this dissertation are part of the following scientific communications:

Abstracts in international peer-review journals:

- **Martins E**, Palmeira A, Carmo H, Sousa E, Lemos A, Pinto M, Bastos ML, Remião F, Silva R (2018). P-gp induction and activation as a potential therapeutic approach in intoxications and/or neurological diseases – *in vitro* and *in silico* studies. Toxicology Letters. (258) Supplement: S270.

Poster communications:

- **Martins E**, Palmeira A, Sousa E, Lemos A, Carmo H, Pinto M, Bastos ML, Remião F and Silva R (2018). P-gp induction and activation by newly synthesized xanthonic derivatives as a potential therapeutic approach in intoxications and neurological diseases. Italian-Spanish-Portuguese Joint Meeting in Medicinal Chemistry (MedChemSicily2018), Palermo, Italy, July 12 - 20, 2018.
- **Martins E**, Palmeira A, Carmo H, Sousa E, Lemos A, Pinto M, Bastos ML, Remião F, Silva R (2018). P-gp induction and activation as a potential therapeutic approach in intoxications and/or neurological diseases – *in vitro* and *in silico* studies. In 54th Congress of European Societies of Toxicology (EUROTOX 2018), Brussels, Belgium, September 2 - 5, 2018.

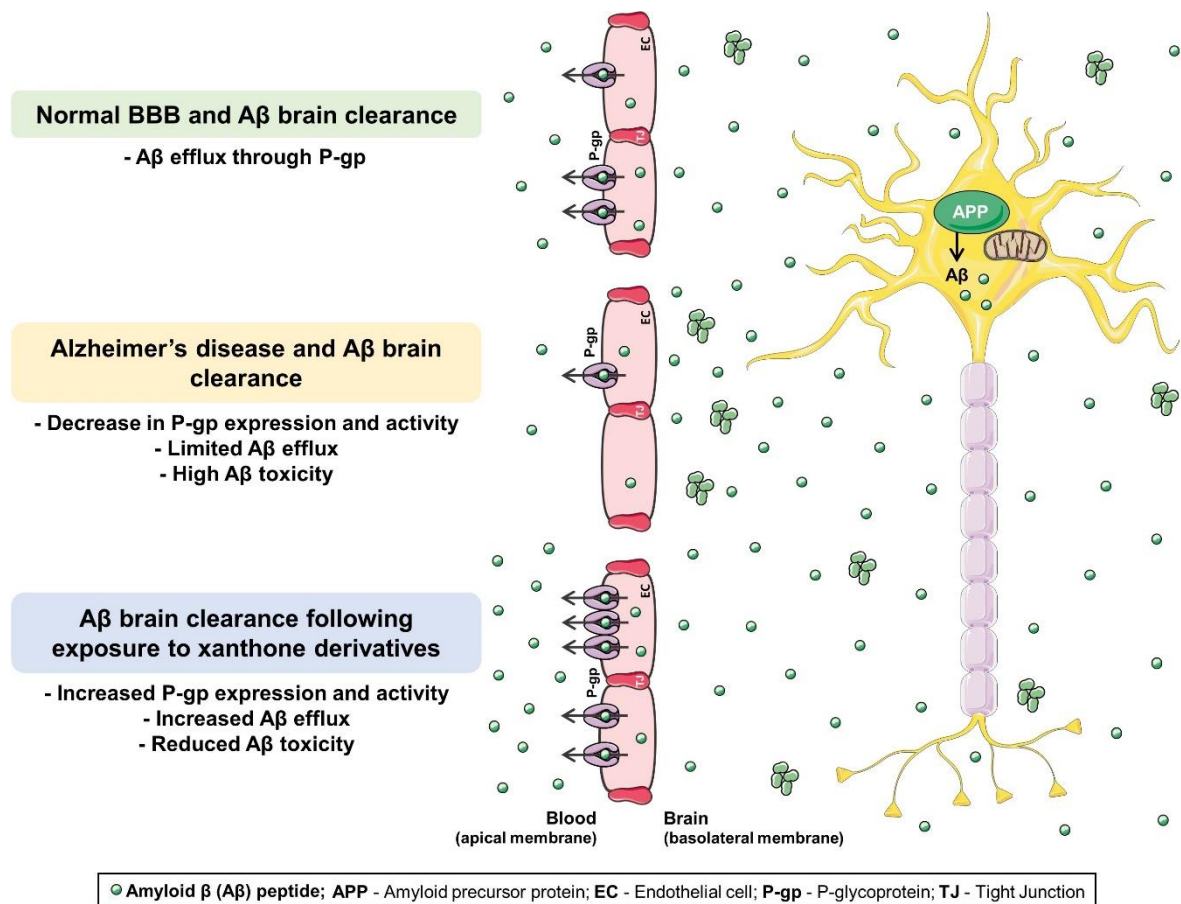
Acknowledgments

A realização desta dissertação de mestrado não seria possível sem os apoios e os incentivos de todos os que me rodearam ao longo desta caminhada. Assim, ficam aqui os meus mais sinceros agradecimentos.

- À professora Renata Silva, orientadora desta dissertação, agradeço todo o apoio, disponibilidade, confiança e estímulo constante. Sinto-me privilegiada por poder presenciar diariamente a pessoa brilhante que é. Obrigada acima de tudo pela amizade.
- Ao Daniel Barbosa, coorientador desta tese, agradeço a total disponibilidade, apoio e paciência. Obrigada pela prontidão com que sempre deste resposta às mais variadas situações inerentes à realização deste trabalho.
- À Vera Silva, por ter sido a minha companheira ao longo deste ano, agradeço toda a ajuda, disponibilidade e simpatia. Obrigada por todas as horas no laboratório e fora dele. Foi tudo mais fácil contigo ao meu lado.
- Aos meus colegas do laboratório e do mestrado de Toxicologia, Ricardo, João, Rita, Brandon e tantos outros, que tornaram esta caminhada muito mais fácil. Obrigada pelos almoços tardios, pelas pausas de café e pela partilha de desesperos.
- Ao Rafa, por ser o meu porto seguro.
- À Patrícia, a irmã que nunca tive, companheira de todas as horas, aventuras e conquistas.
- Ao Cristiano, Patrick, Joka, Vlad, Yin, João, Duarte, Pedro, Daniele, Ângela e Catarina. Obrigada pelos momentos divertidos e pelas inúmeras gargalhadas.
- À Dri, ao João e ao Fred pelos momentos de descontração.
- À Juliana, Cátia, Margarida e Carlos pela boa disposição, ajuda e palavras de incentivo.
- À minha família. Ao meu pai, por todo o apoio ao longo deste percurso e por me ter dado a oportunidade de fazer aquilo que gosto. À minha mãe, os meus êxitos são também teus. À minha tia Iria e ao meu tio Carlos, pela presença, preocupação e por me tratarem como uma filha. Ao meu primo Gui, que me enche de alegria pelo simples facto de existir. À minha madrinha e à minha prima Lili por estarem sempre ao meu lado. À Sílvia e à Joaquina, porque a família vai muito além do laço sanguíneo. À minha Minie, que é o melhor presente do mundo.

É possível que me tenha esquecido de mencionar alguém. Termino assim, agradecendo a toda a gente que de maneira direta ou indireta contribuiu para a finalização deste projeto.

Graphical Abstract



Abstract

ABC (ATP-binding cassette) transporters, the most large and diverse superfamily of proteins in living species, mediate the cellular efflux of endogenous and exogenous substrates, reducing their intracellular accumulation and, therefore, their potential toxicity. **P-glycoprotein** (P-gp), the best studied ABC transporter, as it contributes to the multidrug resistance in neoplastic cells, presents broad substrate specificity, cellular polarized expression in many excretory and barrier tissues (e.g. Blood-Brain Barrier), and great efflux capacity. Thus, it plays a crucial role in the protection of susceptible organs, by significantly decreasing the absorption and distribution of harmful xenobiotics, as well as endogenous substrates, such as the **amyloid beta peptide** (A β). For this reason, P-gp induction and/or activation can be faced as a disease-modulating pathway, including in **Alzheimer's disease**.

Xanthonic derivatives have received increasing interest due to their ability to interact and modulate P-gp expression and transport activity. Thus, in this dissertation, the modulatory effect of six newly synthesized xanthonic derivatives on P-gp function and expression was evaluated in **hCMEC/D3 cells**, a human cerebral microvessel endothelial cell line widely used to mimic the Blood-Brain Barrier. Additionally, the neuroprotective role of the most promissory synthetic xanthonones against the A β -induced cellular toxicity was further explored.

To select a non-cytotoxic working concentration, hCMEC/D3 cells were exposed to the newly synthesized xanthonic derivatives (0 - 50.0 μ M) and their cytotoxicity evaluated, by the NR uptake and MTT reduction assays, 24 h after the exposure. At the concentration that caused no significant toxicity (20.0 μ M), and after 24 h of exposure, several of the tested xanthonic derivatives positively modulated P-gp expression (xanthonones **X4**, **X7**, **X8**, **X9** and **X17**) and activity (xanthonones **X7**, **X9** and **X13**). Furthermore, after a short incubation period of 90 minutes, the synthetic xanthonones **X7**, **X9**, **X13** and **X17** efficiently and immediately increased P-gp activity, without changing the protein expression, thereby suggesting that these compounds acted as P-gp activators. Additional experiments revealed that the synthetic xanthone **X7** protected against the cytotoxic effect induced by the A β peptide, a pathological hallmark of Alzheimer's disease, an effect prevented upon P-gp inhibition with Zosuquidar, a third-generation P-gp inhibitor, thus suggesting a role for P-gp in A β peptide clearance.

In conclusion, the *in vitro* results included in this dissertation suggest P-gp induction/activation as an interesting mechanism for modulating Alzheimer's disease pathogenesis, by increasing A β peptide brain clearance, thus limiting its accumulation and, consequently, its toxicity. Furthermore, these studies also suggest xanthonic

derivatives as a promising class of new compounds with P-gp modulation ability that worth to be further explored

Keywords: P-glycoprotein; Induction; Activation; Xanthones; Amyloid beta peptide; Alzheimer's disease.

Resumo

Os transportadores ABC (*ATP-binding cassette*) representam a maior e mais diversificada superfamília de proteínas presentes em espécies vivas, sendo responsáveis pelo efluxo de substratos endógenos e exógenos, reduzindo, assim, a sua acumulação intracelular, e por consequência, a sua toxicidade. A **glicoproteína P** (P-gp) é o transportador mais estudado desta superfamília, dado que contribui para a resistência a múltiplos fármacos em células neoplásicas, a qual apresenta ampla especificidade de substratos, expressão polarizada em diversos tecidos barreira (como é o caso da barreira hematoencefálica) e grande capacidade de efluxo. Assim, esta proteína desempenha um papel crucial na proteção de órgãos sensíveis, devido à redução da absorção e distribuição de xenobióticos tóxicos, bem como à redução da acumulação de substratos endógenos, como é o caso do **peptídeo beta amiloide** (A β). Por esta razão, a indução e/ou ativação da P-gp pode ser encarada como uma via moduladora de doenças, incluindo a **doença de Alzheimer**.

Os **derivados xantônicos** têm recebido crescente interesse devido à sua capacidade para interagir e modular a expressão e atividade da P-gp. Assim, nesta dissertação, o efeito modulatório de seis novos derivados xantônicos na função e expressão da P-gp foi avaliado em células **hCMEC/D3**, uma linha celular endotelial de microvasos cerebrais humanos, amplamente utilizada para mimetizar a barreira hematoencefálica. Adicionalmente, o papel neuroprotetor das xantonas sintéticas mais promissoras contra a citotoxicidade induzida pelo peptídeo A β foi igualmente explorado.

Para selecionar uma concentração não citotóxica, as células hCMEC/D3 foram expostas aos derivados xantônicos (0 - 50.0 μ M), e a sua citotoxicidade posteriormente avaliada pelos ensaios de incorporação do vermelho neutro e pelo ensaio de redução do MTT, 24 h após a exposição. Numa concentração que não causou toxicidade significativa (20.0 μ M) e após 24 h de exposição, alguns derivados xantônicos modularam positivamente a expressão (xantonas **X4**, **X7**, **X8**, **X9** e **X17**) e atividade (xantonas **X7**, **X9** e **X13**) da P-gp. Além disso, após um curto período de incubação de 90 minutos, as xantonas sintéticas **X7**, **X9**, **X13** e **X17** aumentaram de forma eficiente e imediata a atividade da P-gp, sem alterar a expressão da proteína, sugerindo que estes compostos atuam como ativadores da P-gp. Experiências adicionais revelaram ainda que a xantona sintética **X7** conferiu um efeito protetor contra o efeito citotóxico induzido pelo peptídeo A β , um marcador patológico da doença de Alzheimer, sendo que este efeito foi prevenido pela inibição da P-gp com Zosuquidar, um inibidor de terceira geração, sugerindo um papel para a P-gp na clearance do peptídeo.

Em conclusão, os resultados *in vitro* incluídos nesta dissertação sugerem a indução/ativação da P-gp como um mecanismo importante para modular a patogénese da doença de Alzheimer, aumentando a clearance cerebral do peptídeo A β , limitando assim a sua acumulação, e consequentemente, a sua toxicidade. Além disso, estes estudos sugerem igualmente os derivados xantónicos como uma importante classe de compostos com capacidade de modular a função da P-gp, tendo portanto, potencial para serem explorados.

Palavras chave: Glicoproteína-P; Indução; Ativação; Xantonas; Peptídeo beta amiloide; Doença de Alzheimer.

Table of Contents

Acknowledgments	ix
Graphical Abstract	xi
Abstract	xiii
Resumo	xv
Table of Contents	xvii
Index of Figures	xix
Index of Tables	xxi
Index of Equations	xxiii
Abbreviations List	xxv
1. Introduction	1
1.1. ABC transporters.....	1
1.1.1. P-glycoprotein	2
1.1.1.1. Tissue distribution and physiological role.....	2
1.1.1.2. Structure.....	4
1.1.1.3. Mechanism of drug efflux.....	5
1.1.1.4. Catalytical and transport cycle	6
1.1.1.5. P-glycoprotein substrates	8
1.1.1.6. P-glycoprotein modulation	10
1.1.1.6.1. P-glycoprotein inhibition mechanism and inhibitors.....	10
1.1.1.6.2. P-glycoprotein induction mechanism and inducers	14
1.1.1.6.3. P-glycoprotein activation mechanism and activators.....	17
1.1.1.6.4. Xanthones	19
1.2. Central nervous system and blood brain barrier	20
1.2.1. Involvement of P-glycoprotein in neurodegenerative diseases	21
1.2.1.1. P-glycoprotein and Alzheimer's disease	22
2. Objectives	29
3. Materials and Methods	31
3.1. Materials	31
3.2. Synthesis of xanthones	31
3.3. hCMEC/D3 cell line - general considerations	32
3.3.1. hCMEC/D3 cell culture.....	32
3.3.2. Xanthones, Zosuquidar and Rhodamine 123 cytotoxicity assays	33
3.3.2.1. Neutral red uptake assay.....	34
3.3.2.1.1. General principle	34
3.3.2.1.2. Experimental protocol.....	34

3.3.2.2. MTT reduction assay.....	35
3.3.2.2.1. General principle	35
3.3.2.2.2. Experimental protocol.....	35
3.3.3. Evaluation of P-glycoprotein expression – flow cytometry.....	35
3.3.4. Evaluation of P-glycoprotein transport activity.....	36
3.3.4.1. Rhodamine 123 accumulation in hCMEC/D3 cells pre-exposed to the tested xanthenes	36
3.3.4.2. Rhodamine 123 accumulation assay in hCMEC/D3 in the presence of the tested xanthenes	37
3.3.5. Evaluation of amyloid- β_{42} peptide cytotoxicity.....	38
3.3.6. Evaluation of xanthenes' neuroprotective effects against amyloid- β_{42} peptide cytotoxicity	38
3.3.7. Statistical analysis	39
4. Results and discussion	41
4.1. Synthetic xanthenes are relatively harmless to hCMEC/D3 cells	41
4.2. Synthetic xanthenes at non-cytotoxic concentrations significantly increased P-glycoprotein expression.....	42
4.3. Synthetic xanthenes at non-cytotoxic concentrations significantly increased P-glycoprotein transport activity	44
4.3.1. P-gp transport activity in cells pre-exposed to the tested xanthenes	45
4.3.2. P-gp transport activity in the presence of the tested xanthenes	49
4.4. The pathological hallmark of Alzheimer's disease, amyloid- β_{42} peptide, was toxic to hCMEC/D3 cells	51
4.5. Synthetic xanthenes protected hCMEC/D3 cells against the toxicity caused by amyloid- β_{42} peptide	52
5. Conclusions	57
6. Future perspectives	59
7. References	61
8. Supplementary data.....	69

Index of Figures

Figure 1. Schematic representation of the blood brain barrier (BBB) with P-glycoprotein (P-gp) localization.....	3
Figure 2. Membrane topology proposal for P-glycoprotein (P-gp).....	4
Figure 3. “Hydrophobic vacuum cleaner” and “flippase” models of P-glycoprotein (P-gp) function.	5
Figure 4. Proposed catalytic and transport cycle for P-glycoprotein (P-gp).	7
Figure 5. Chemical structure of a xanthonic scaffold.....	19
Figure 6. Schematic representation of Alzheimer's disease (AD) pathology.	23
Figure 7. Main transporters involved in amyloid- β (A β) peptide transport across the blood brain barrier (BBB).	24
Figure 8. Chemical structure and IUPAC nomenclature of the xanthonic derivatives	31
Figure 9. Brief experimental protocol for cell subculturing and cell seeding.	33
Figure 10. Xanthonic X4, X7, X8, X9, X13 and X17 (0 - 50.0 μ M) cytotoxicity in hCMEC/D3 cells evaluated by the neutral red (NR) uptake assay, 24 h after exposure...	41
Figure 11. Xanthonic X4, X7, X8, X9, X13 and X17 (0 - 50.0 μ M) cytotoxicity in hCMEC/D3 cells evaluated by the MTT uptake assay, 24 h after exposure.....	42
Figure 12. Flow cytometry analysis of P-glycoprotein (P-gp) expression levels in hCMEC/D3 cells exposed to the tested xanthonic (20.0 μ M) for 24 h.....	43
Figure 13. Rhodamine 123 (Rho 123, 0 - 5.0 μ M) cytotoxicity in hCMEC/D3 cells evaluated by the Neutral Red and MTT uptake assays, 24 h after exposure.	44
Figure 14. Zosuquidar (Zos, 0 - 10.0 μ M) cytotoxicity in hCMEC/D3 cells evaluated by the Neutral Red and MTT uptake assays, 24 h after exposure.	45
Figure 15. P-glycoprotein (P-gp) transport activity in hCMEC/D3 cells previously exposed to the tested xanthonic (X, 20.0 μ M) for 24 h and to Rhodamine 123 (Rho 123, 5.0 μ M) for 90 minutes.	47
Figure 16. P-glycoprotein (P-gp) transport activity in hCMEC/D3 cells previously exposed to the tested xanthonic (X, 20.0 μ M) for 24 h and to Rhodamine 123 (Rho 123, 5.0 μ M) for 90 minutes. P-gp activity was measured 48 h after the 24 h exposure period to the tested xanthonic.....	47
Figure 17. P-glycoprotein (P-gp) transport activity in hCMEC/D3 cells previously exposed to the tested xanthonic (X, 20.0 μ M) for 24 h and to Rhodamine 123 (Rho 123, 5.0 μ M) for 90 minutes. P-gp activity was measured 96 h after the 24 h exposure period to the tested xanthonic.....	48

Figure 18. P-glycoprotein (P-gp) activity levels in hCMEC/D3 cells simultaneously exposed to the tested xanthenes (X, 20.0 μ M) and Rhodamine 123 (Rho 123, 5.0 μ M) for 90 minutes. 49

Figure 19. Amyloid- β peptide 42 ($A\beta_{42}$, 0 - 25.0 μ M) cytotoxicity and P-glycoprotein (P-gp) contribution in the $A\beta_{42}$ toxicity [$A\beta_{42}$ (25.0 μ M) + Zos (5.0 μ M)] in hCMEC/D3 cells evaluated by the MTT uptake assay, 24 h after exposure. 52

Figure 20. Amyloid- β peptide 42 ($A\beta_{42}$, 0 - 25.0 μ M) cytotoxicity and the xanthenes (X, 20.0 μ M) neuroprotective effects ($A\beta_{42}$ + X) in hCMEC/D3 cells evaluated by the MTT uptake assay, 24 h after exposure. 54

Figure 21. Amyloid- β peptide 42 ($A\beta_{42}$, 0 - 25.0 μ M) cytotoxicity and P-glycoprotein (P-gp) contribution in the neuroprotective effects conferred by xanthone X7 against $A\beta_{42}$ toxicity [$A\beta_{42}$ + Zos + X7 (20.0 μ M)] in hCMEC/D3 cells evaluated by the MTT uptake assay, 24 h after exposure. 55

Figure S1. Cytotoxicity of the Amyloid- β peptide 42 ($A\beta_{42}$) vehicle in hCMEC/D3 cells evaluated by the MTT uptake assay, 24 h after exposure. 69

Index of Tables

Table 1. P-glycoprotein (P-gp) known substrates.....	8
Table 2. P-glycoprotein (P-gp) known inhibitors.....	12
Table 3. P-glycoprotein (P-gp) known inducers.....	15
Table 4. P-glycoprotein (P-gp) known activators.....	18

Index of Equations

Equation 1. P-gp activity was assessed by the ratio between the amount of Rhodamine 123 (Rho 123) accumulated in the presence of the inhibitor (IA, Zos, 5.0 μ M) and the amount of Rho 123 accumulated in the absence of the inhibitor (NA).....	37
--	----

Abbreviations List

A β – Amyloid- β

ABC transporters – ATP-binding cassette transporters

AD – Alzheimer's disease

ADP – Adenosine 5'-diphosphate

AMT – Adsorptive mediated transcytosis

APOE – Apolipoprotein E

APP – Amyloid precursor protein

ATP – Adenosine 5'-triphosphate

BBB – Blood-brain barrier

BCRP – Breast cancer resistance protein

BCSFB – Blood-cerebrospinal fluid barrier

BSCB – Blood-spinal cord barrier

BECs – Blood vascular endothelial cells

bFGF – Basic fibroblast growth factor

CNS – Central nervous system

CP – Choroid plexus

CYP – Cytochrome P450

DMSO – Dimethyl sulfoxide

Dox – Doxorubicin

ECs – Endothelial cells

FXR – Farnesoid X receptor

GTP – Guanosine-5'-triphosphate

hAPP – Human amyloid precursor protein

HBSS (-/-) – Hank's balanced salt solution without Ca^{2+} and Mg^{2+} salts

HBSS (+/+) – Hank's balanced salt solution with Ca^{2+} and Mg^{2+} salts

hCMEC/D3 – Human cerebral microvessel endothelial cell line D3 clone

IA – Inhibited activity

IP – Intraperitoneal

IV – Intravenous

LRP-1 – Low density lipoprotein receptor-related protein 1

LXR – Liver X receptor

MDR – Multidrug-resistance

mRNA – Messenger ribonucleic acid

MRP1 – Multidrug resistance-associated protein 1

MRP2 – Multidrug resistance-associated protein 2

MRP3 – Multidrug resistance-associated protein 3

MRP4 – Multidrug resistance-associated protein 4

MRP5 – Multidrug resistance-associated protein 5

MRP6 – Multidrug resistance-associated protein 6

MRP7 – Multidrug resistance-associated protein 7

MRP8 – Multidrug resistance-associated protein 8

MRP9 – Multidrug resistance-associated protein 9

MTT – 3-(4,5-dimethylthiazol-2-yl)-2,5-diphenyltetrazolium bromide

NA – Normal activity

NBD – Nucleotide binding domains

NR – Neutral red

PCN – Pregnenolone 16 α -carbonitrile

PBS (-/-) – Phosphate-buffered saline solution without Ca²⁺ and Mg²⁺ salts

PBS (+/+) – Phosphate-buffered saline solution with Ca²⁺ and Mg²⁺ salts

PE – Phycoerythrin

P-gp – P-glycoprotein

PPAR- α – Peroxisome proliferator-activated receptor α

PPAR- γ – Peroxisome proliferator-activated receptor γ

PQ – Paraquat

PSEN1 – Presenilin 1 gene

PSEN2 – Presenilin 2 gene

PXR – Pregnane X receptor

QSAR – Quantitative structure-activity relationship

RAGE – Receptor for advanced glycation end products

Rho 123 – Rhodamine 123

RMT – Receptor mediated transcytosis

SLCs – Solute carriers

TJs – Tight junctions

TMD – Transmembrane domains

TMHs – Transmembrane α -helices

UV – Ultraviolet

X – Xanthone

WT – Wild type

Zos – Zosuquidar

1. Introduction

1.1. ABC transporters

The adenosine 5'-triphosphate (ATP)-binding cassette (ABC) transporters are recognized as one of the most large, diverse and ubiquitous superfamily of proteins in living species, presenting a vital role in many biological processes (1). These pumps are responsible for the influx and efflux of innumerable endogenous and exogenous substrates, from amino acids, sugars and inorganic anions to xenobiotics and their metabolites (2, 3). Thus, they can be classified as importers (influx) or exporters (efflux), but, to date, importers seem to be uniquely present in bacteria (4, 5).

ABC proteins are active transporters since they pump substrates across the biological membranes and against the concentration gradient, thereby preventing their accumulation inside the cell, at the cost of ATP hydrolysis (6). These transporters are typically constituted by two nucleotide binding domains (NBDs) and two transmembrane domains (TMDs), which usually contain six transmembrane α -helices (TMHs) (5, 7). The NBD is located at the cytoplasm and comprises three conserved domains, Walker A and B domains (present in all ATP-binding proteins) and signature C motif (specific to ABC transporters) (3). By contrast, TMDs architecture is variable, determining the specificity of the transporter through substrate binding sites (8). P-glycoprotein (P-gp) (ABCB1/MDR1), multidrug resistance-associated protein 4 (ABCC4/MRP4), multidrug resistance-associated protein 5 (ABCC5/MRP5), multidrug resistance-associated protein 8 (ABCC11/MRP8) and multidrug resistance-associated protein 9 (ABCC12/MRP9) are transporters that exhibit this typical structure (3).

However, not all members of this superfamily present this typical conformation. They can be classified as full transporters, comprising twelve TMHs (divided into two TMDs) and two NBDs as mentioned above, or half transporters, such as breast cancer resistance protein (ABCG2/BCRP), with six TMHs (one TMD) and one NBD, which set as either homodimers or heterodimers to generate a functional transporter (3, 6). Furthermore, they can be full transporters with an extra TMD containing five TMHs, such as multidrug resistance-associated protein 1 (ABCC1/MRP1), multidrug resistance-associated protein 2 (ABCC2/MRP2), multidrug resistance-associated protein 3 (ABCC3/MRP3), multidrug resistance-associated protein 6 (ABCC6/MRP6) and multidrug resistance-associated protein 7 (ABC10/MRP7) (6).

ABC transporters are extremely important in nutrient uptake, cell signalling, and in the transport of a wide range of substrates, therefore having the ability to maintain cellular homeostasis and detoxify against toxic substrates (9). The importance of human ABC proteins function is highlighted under the consequences of their dysfunction, since many

diseases, such as adrenoleukodystrophy, Dubin-Johnson syndrome, cystic fibrosis, Alzheimer's, Stargardt and Tangier diseases or cancer, have been associated with alterations in these transporters (10).

In humans, forty-nine ABC genes have been identified and classified in seven subfamilies, nominated from ABCA to ABCG, according to their phylogenetic analysis. However, only some subfamilies have been fully characterized on their function and biochemistry (2, 11). Well-known members of this superfamily with importance in drug efficacy and toxicity include, multidrug resistance (MDR)-associated proteins (ABCC/MRP), BCRP, and P-glycoprotein (P-gp), the main focus of this dissertation (12).

1.1.1. P-glycoprotein

P-gp is the best characterized efflux pump of the ABC superfamily of transporters, belonging to the ABCB (MDR/TAP) subfamily (13). This protein was first discovered and isolated from colchicine-resistance Chinese hamster ovary cells by Juliano and Ling in 1976 (14). In humans, P-gp is encoded by two MDR genes, *MDR1/ABCB1*, coding to the drug transporter associated with the MDR phenotype, and *MDR3/ABCB4* (or *MDR2*), coding to a protein that functions as a phosphatidylcholine translocase exporting this phospholipid into the bile (15).

Two isoforms of P-gp exist: isoform 1, the longest isoform composed by 1350 amino acids, and isoform 2 (1280 amino acids), which presents a shorter N-terminus as a result of a translation initiation at a downstream start codon (16).

In the following sections P-gp will be used to indicate the human *MDR1/ABCB1* gene product (or *abcb1a/abcb1b* gene products in rodents).

1.1.1.1. Tissue distribution and physiological role

P-gp is present at low expression levels in most human tissues (17), although it is highly expressed in the apical surface of endothelial cells (ECs) of the intestine (enterocytes), liver bile ducts and kidney proximal tubules (18). Considering these locations, it is reasonable to assume that P-gp plays a role in the removal of xenobiotics or endogenous metabolites through phase-III-mediated transport (19, 20).

In the gastrointestinal tract P-gp is highly expressed at the apical surface of enterocytes and plays a crucial defense role against xenobiotics, including orally administered drugs (21). Consequently, P-gp presence in the intestine ECs strongly influences the absorption and bioavailability of numerous orally administered drugs, since P-gp transports drugs back into the intestinal lumen for excretion (22, 23). P-gp

expression in the liver apical membrane of hepatocytes and in kidney tubular cells results in an increased excretion of drugs and other substrates into the bile and urine, respectively (21).

Moreover, P-gp was also found in pancreatic ducts, adrenal gland, placenta, pregnant endometrium, hematopoietic cells, blood-testis-barrier, capillary ECs of the cochlea and vestibule, in the blood-brain barrier (BBB) and in cancer cells, where it plays an important role in the multidrug resistance (MDR) phenomenon in cancer chemotherapy (6, 20).

At the BBB, P-gp is highly expressed at the apical membrane of brain capillary ECs (**Figure 1**), restricting the access of certain xenobiotics to the central nervous system (CNS) (24, 25). Thus, and since the transporter is found oriented to the blood, P-gp presence in these cells limits the entry of its substrates into the brain, conferring, in many cases, pharmacoresistance, especially when its expression is increased (26, 27).

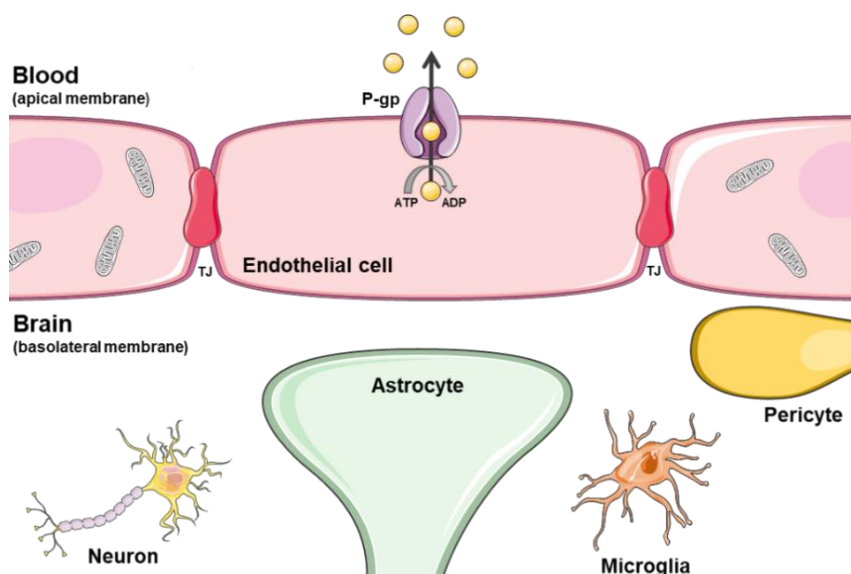


Figure 1. Schematic representation of the blood brain barrier (BBB) with P-glycoprotein (P-gp) localization. TJ (Tight junction). Adapted from (26, 28).

Additionally, tissue localizations suggest that P-gp is associated with the protection of susceptible organs against toxic xenobiotics (18, 25).

Altogether, cellular localization and tissue distribution make P-gp an extremely important protein in the absorption, distribution, metabolism, excretion and transport (ADMET) of drugs which are P-gp substrates, leading in some cases to therapy failure (22).

1.1.1.2. Structure

P-gp is a ~150 kDa protein synthesized in the endoplasmic reticulum (29). This protein is a result of a gene duplication event, where two homologous halves with six TMHs (one TMD) and one NBD each, fused together (**Figure 2**) (18). The two homologous halves are separated by a “linker region” which is highly charged and phosphorylated at several sites by protein kinase C (30).

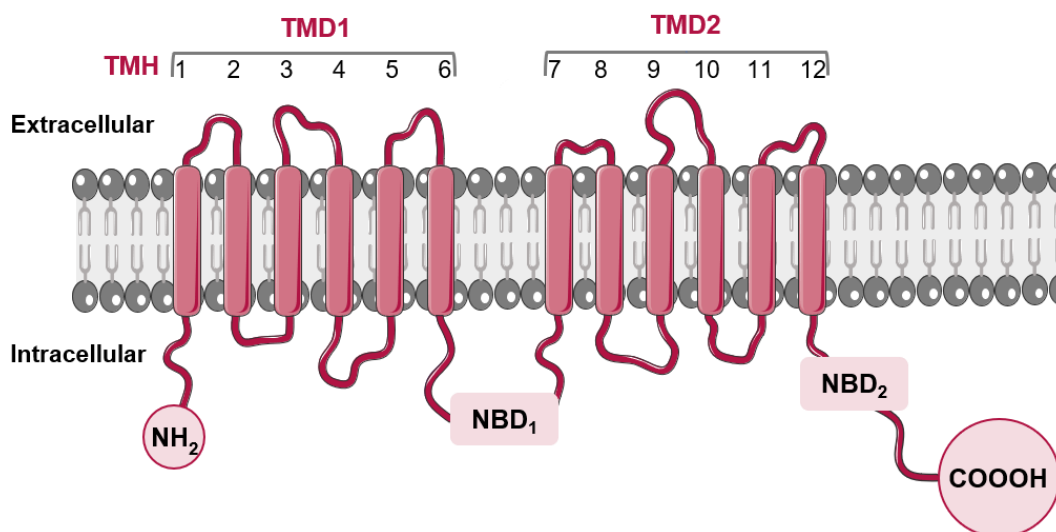


Figure 2. Membrane topology proposal for P-glycoprotein (P-gp). P-gp is a full transporter, with twelve transmembrane α -helices (TMHs), divided in two halves [transmembrane domains (TMD) 1 and 2], each one fused with a cytoplasmic nucleotide binding domain (NBD). N- and C-termini are cytoplasmic. Adapted from (18, 31).

The NBD regions, located in the cytoplasmic membrane side, bind and hydrolyse ATP, producing the energy needed to execute the membrane passage, being the TMHs responsible for creating the pathway of this passage (23). Each NBD contains two sequence motifs designated Walker A and B, which can be found in several proteins that bind and hydrolyse ATP and guanosine-5'-triphosphate (GTP) (18). Walker A motif presents a highly conserved lysine residue, which is implicated in binding the β -phosphate of ATP. On the other hand, Walker B comprises a highly conserved aspartic acid residue that binds Mg^{2+} (32). Furthermore, between the Walker A and B motifs, is located the signature C motif, which is exclusive to the ABC superfamily of transporters (6, 23). Its specific function has not yet been fully determined. However, Walkers A and B and signature C motif seem to be involved in the binding and hydrolysis of nucleotides (18).

1.1.1.3. Mechanism of drug efflux

The precise mechanism by which P-gp combines the ATP hydrolysis with the transport of compounds across the membrane, and the exact interaction site of the substrate with the protein, remains unknown (18). However, there are two proposal models (“hydrophobic vacuum cleaner” and “flippase” models) that are the most accepted, since they are in accordance with the P-gp tertiary structure data, indicating that the substrates enter the pore through the lipid phase of the membrane (15, 18).

In the “hydrophobic vacuum cleaner” model, P-gp recognizes and expels from the inner leaflet of the plasma membrane to the external aqueous medium the hydrophobic compounds, which never enter the cytosol, thus protecting the cells from the exposure to potentially toxic molecules (**Figure 3**) (15, 25). This pumping action increases the drug concentration in the external aqueous phase, and consequently, raises the concentration gradient across the plasma membrane (25).

On the other hand, in the “flippase” model, P-gp substrates are flipped from the inner leaflet either to the outer leaflet of the lipid bilayer or directly to the extracellular environment (**Figure 3**) (15). The substrates crossing occurs slowly, which permits P-gp to generate a concentration gradient, since drug concentration in the outer leaflet is higher (6, 25).

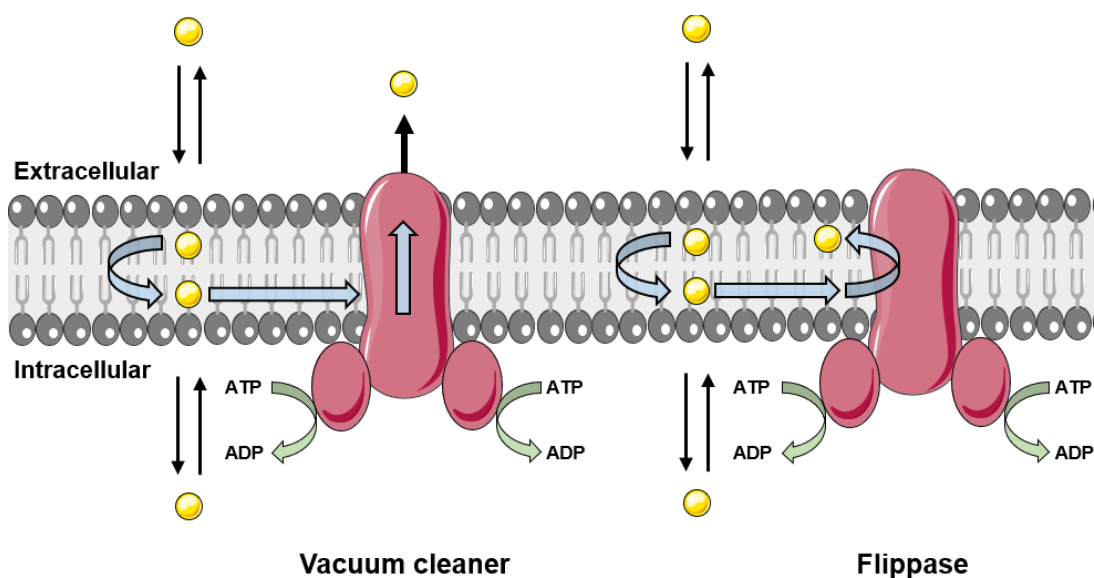


Figure 3. “Hydrophobic vacuum cleaner” and “flippase” models of P-glycoprotein (P-gp) function. In the “hydrophobic vacuum cleaner” P-gp recognizes and expels from the inner leaflet of the plasma membrane to the external aqueous medium the hydrophobic compounds without entering the cytosol. In the “flippase” model P-gp substrates are flipped from the inner leaflet to the outer leaflet of the lipid bilayer or directly to the extracellular environment. ATP (adenosine triphosphate); ADP (adenosine diphosphate). Adapted from (25, 33).

In both cases, prior to the interaction with P-gp, it is assumed that substrates partitioning into the lipid phase. This fact helps to explain the broad substrate specificity of this carrier, since the main determinant of specificity is the capacity of a substrate to intercalate into the lipid bilayer, with the resultant interaction with the substrate-binding site in minor importance (15, 18). However, the two presented models are difficult to distinguish experimentally (15).

1.1.1.4. Catalytical and transport cycle

As previously mentioned, P-gp is dependent on the hydrolysis of ATP at the two cytoplasmic NBDs, which are composed by three highly conserved motifs (Walker A, Walker B and signature C motifs) (23).

Presently, it is accepted that the NBDs must dimerize to hydrolyse ATP (34). The NBDs are organised in a head-to-tail arrangement, with two ATP molecules bound along the interface, forming the so-called “ATP sandwich dimer” (34). In detail, each ATP binding site is constituted by the Walker A and B motifs of one NBD subunit and the signature C motif of the other NBD subunit (35). However, it is not yet understood how ATP hydrolysis is coordinated between the two NBDs or how this energy is used to transport substrates (18).

P-gp presents an atypical high level of basal ATPase activity, which is observed in the apparent absence of substrates. Additionally, some drugs inhibit and others stimulate P-gp ATPase activity, and it is usual to observe a biphasic pattern of inhibition at high concentrations and stimulation at low concentrations (25).

P-gp catalytic cycle comprises several steps, including nucleotide and drug binding, nucleotide hydrolysis and drug translocation (33). **Figure 4** schematizes a proposal for the P-gp catalytic cycle. It is commonly recognized that P-gp exists in two main conformations during the catalytic cycle: “inward-facing” and “outward-facing” conformation (18, 36). In the “inward-facing” conformation the high affinity drug binding pocket is exposed to the cytoplasmic side and the NBDs are separated. Differently, in the “outward-facing” conformation the low affinity drug binding site is exposed to the extracellular space and the NBDs closely interact (37). Inward to outward facing conformation transition seems to require ATP binding/hydrolysis, while subsequent ATP hydrolysis and/or product release involving one or both NBD seems to rearrange the transporter to the ground state (inward facing conformation), restarting the transport cycle (37, 38).

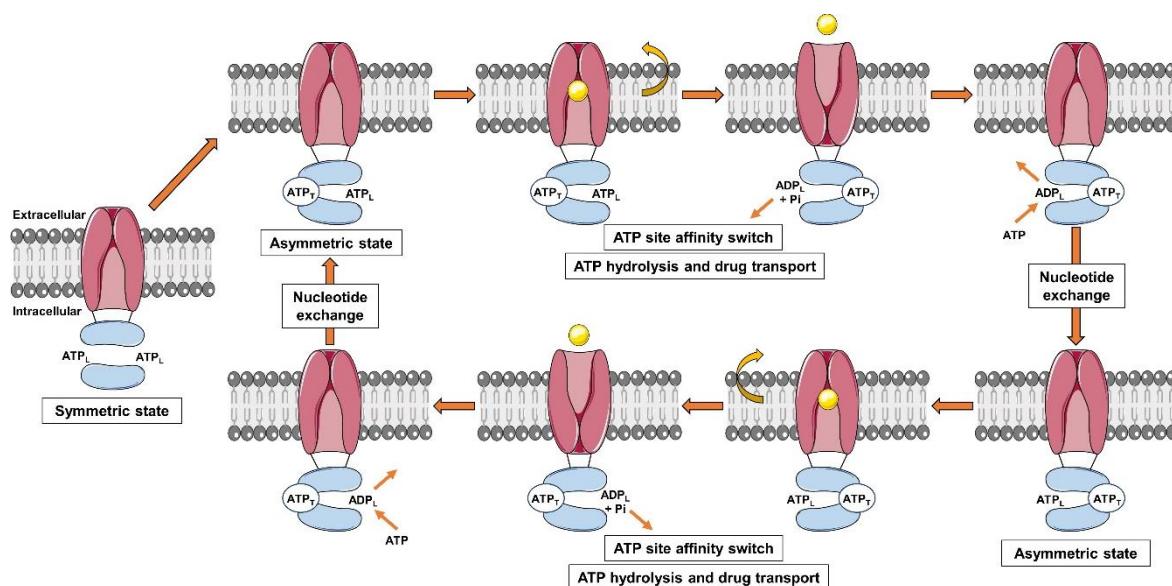


Figure 4. Proposed catalytic and transport cycle for P-glycoprotein (P-gp). In the symmetric state with two adenosine 5'-triphosphate (ATP) molecules (ATP_L) both halves are open. If the pump is catalytically active, this state develops to the asymmetric state where one ATP molecule is tightly bound (ATP_T) in the nucleotide binding domain 1 (NBD₁), closing this NBD dimer interface. The firmly bound ATP molecule is impaired to enter the transition state and suffers hydrolysis, providing the energy for the drug (yellow sphere) transport from the transporter binding pocket to the opposite face of the membrane (ATP and drug binding can occur in a random order). ATP hydrolysis converts the tightly bound ATP into adenosine 5'-diphosphate (ADP) and phosphate (Pi), which are loosely bound (ADP_L), resulting in the opening of the dimer interface in NBD₁. The other catalytic site simultaneously changes to the high affinity state, leading in tight binding of the second ATP molecule and closure of the nucleotide binding domain 2 (NBD₂) dimer interface. Firstly, Pi dissociates from the cycle, followed by ADP, which is substituted by another loosely ATP molecule bound (nucleotide exchange), to reach the asymmetric occluded state again. Then, a second round of ATP hydrolysis and drug transport begins at the NBD₂. At all points of the catalytic cycle, P-gp is in an asymmetric state, directing that the two NBDs alternate during catalysis. Adapted from (36).

Recently, the human P-gp cryo-electron microscopy structure in an outward-facing conformation was reported, in which two ATP molecules are bound between the two NBDs. Additionally, the substrate-binding site, located in the transmembrane domain, was reported to be open to the outside of the cell, but compressed, and no substrate is bound, suggesting that ATP binding, rather than ATP hydrolysis, promotes the transition to the outward-facing conformation and the substrate release. Furthermore, it was also proposed that the subsequent ATP hydrolysis, which may occur at only one of the two catalytic sites stochastically, resets the transporter to the inward-facing conformation. The proposed model reinforces the dynamic nature of P-gp, which enables the translocation of a large variety of substrates and prompts new perspectives in the prediction and screening of new substrates, inhibitors and activators (31).

1.1.1.5. P-glycoprotein substrates

P-gp can export a large number of chemical- and structurally different compounds, including chemotherapeutic drugs, steroids, immunosuppressive agents, natural products, calcium channel blockers, pesticides, among others (**Table 1**) (18, 21, 39). These compounds are usually amphipathic, relatively hydrophobic and nonpolar often containing aromatic rings and a positively charged nitrogen atom. Moreover, P-gp substrates can significantly vary in size, structure and function, extending from small molecules (amino acids, organic cations, carbohydrates), to macromolecules (proteins, polysaccharides) (18, 23, 25). This wide range of substrates is in agreement with the P-gp protective role in the efflux of an extensive number of compounds (6).

Table 1. P-glycoprotein (P-gp) known substrates (endogenous, exogenous and experimentally used) Adapted from (21, 39).

P-gp endogenous substrates
A β peptides, Bile acids, Bilirubin, Inflammatory mediators, Lipids, Steroids;
P-gp exogenous substrates (by pharmacotherapeutic classes)
<p>Antibacterial agents (actinomycin D, amoxicillin, clarithromycin, doxycycline, erythromycin, gramicidin A, grepafloxacin, levofloxacin, minocycline, rifampicin, sparfloxacin, tetracycline, valinomycin)</p> <p>Antifungal agents (itraconazole, ketoconazole)</p> <p>Antiretrovirals (amprenavir, atazanavir, darunavir, indinavir, lopinavir, maraviroc, nelfinavir, ritonavir, saquinavir)</p> <p>Anthelmintics (abamectin, ivermectin)</p> <p>Muscle relaxants (vecuronium)</p> <p>Antiemetics (domperidone, ondansetron)</p> <p>Antiepileptics and Anticonvulsants (carbamazepine, felbamate, gabapentin, lamotrigine, levetiracetam, phenobarbital, phenytoin, topiramate)</p> <p>Antipsychotics (chlorpromazine, trans-flupentixol, trifluoperazine)</p> <p>Antidepressants (amitriptyline, doxepin, nortriptyline, paroxetine, venlafaxine)</p> <p>Narcotic analgesics (fentanyl, meperidine, morphine, oxycodone, pentazocine)</p> <p>Other Nervous System Drugs (disulfiram, methadone, riluzole)</p> <p>Cardiotonics (digitoxin, digoxin, quinidine)</p> <p>Antiarrhythmics (amiodarone, diltiazem, propafenone, quinidine)</p> <p>Antihypertensives (azidopine, celiprolol, debrisoquine, losartan, nicardipine, nifedipine, nimodipine, prazosin, propranolol, reserpine, talinolol, verapamil)</p> <p>Lipid modifying agents (lovastatin, simvastatin)</p> <p>Anticoagulant agents (dabigatran)</p>

P-gp exogenous substrates (by pharmacotherapeutic classes) (cont.)
<p>Gastric secretion modifiers (cimetidine, ranitidine) Antidiarrheals (loperamide) Antidiabetics (berberine) Anti-gout agents (colchicine) Antihistamines (fexofenadine, terfenadine) Antineoplastic drugs <u>Anthracenes</u> (bisantrene, mitoxantrone) <u>Anthracyclines</u> (daunorubicin, doxorubicin) <u>Antimetabolites</u> (methotrexate) <u>Cyclin-dependent kinase inhibitors</u> (seliciclib) <u>Taxanes</u> (docetaxel, paclitaxel) <u>Topoisomerase I inhibitors</u> (irinotecan, topotecan) <u>Topoisomerase II inhibitors</u> (etoposide, teniposide) <u>Tyrosine kinase inhibitors</u> (gefitinib, imatinib, mesylate, nilotinib, tandutinib) <u>Vinca alkaloids</u> (catharanthine, vinblastine, vincristine) Immunomodulators (cyclosporin A, sirolimus, tacrolimus, valspodar) Steroid Hormones (aldosterone, corticosterone, cortisol, dexamethasone, hydrocortisone, methylprednisolone) Nature products (curcuminoids, flavonoids, Rhei Rhizoma extract) Pesticides (cypermethrin, endosulfan, fenvalerate, methyl parathion, paraquat)</p>
P-gp substrates used experimentally (by class of compounds)
<p>Drugs (Colchicine, Digoxin, Mercaptopurine, Methotrexate, Quinidine) Fluorophores (^{99m}Tc] Sestamibi, Calcein-AM, CDCF, FITC, Hoechst 33342, NBD-CSA, Rho 123, Rhodamine 6G) Pesticides (Paraquat) Others (Aβ protein, cAMP, cGMP, N-methyl-quinidine)</p>

A β (Amyloid- β), CDCF (Carboxydichlorofluorescein), cAMP (Cyclic adenosine monophosphate), cGMP (Cyclic guanosine monophosphate), FITC (Fluorescein isothiocyanate), NBD-CSA (N-(4-nitrobenzofurazan-7-yl)-D-Lys8]-cyclosporine A), Rho 123 (Rhodamine 123).

Since P-gp is imperative in drug pharmacokinetics and in drug resistance, many studies have attempted to clarify the common set of molecular attributes that determine substrate specificity. By now, the precise mechanism by which P-gp interacts with its substrates is not well defined (40). However, it is of enormous importance to determine P-gp substrate specificity, since drug targeting and design of new drugs would be more successful, as well as to overcome the MDR phenomenon. Despite the efforts, the design of effective compounds has been difficult due to P-gp poly-specificity in substrate recognition (15, 18, 23). In 1998, Seelig et al. demonstrated that a compound to interact with P-gp must comprise either two electron donor groups, with a spatial separation of $2.5 \pm 0.3 \text{ \AA}$, two electron donor groups, with a spatial separation of $4.6 \pm 0.6 \text{ \AA}$, or three electron donor groups with a spatial separation of the outer two groups of $4.6 \pm 0.6 \text{ \AA}$ (41).

Following studies found that P-gp rate limiting step and substrate interaction is the partition into the lipid bilayer, and that the number and strength of the hydrogen bonds formed between the substrate and P-gp is the decisive factor in the dissociation of the P-gp-substrate complex (23, 42).

More recently, computational models, such as quantitative structure-activity relationship (QSAR), docking techniques and pharmacophore models, were developed to predict potential P-gp substrates. These *in silico* models replaced the obsolete *in vitro* assays, since they are faster and more economic (18, 23). Cianchetta et al. recognized a pharmacophore model where P-gp recognition elements are two hydrophobic groups, 16.5 Å apart, and two bond-acceptor groups, 11.5 Å apart (43). More efficient *in silico* models to predict P-gp substrates are emerging, using a Particle Swarm algorithm and a Support Vector Machine approach, which show an average accuracy higher than 90% (18, 44).

Other studies revealed some physicochemical characteristics, such as molecular weight, lipophilicity (log-P value of 2.92 or higher), surface area (eighteen atom-long or longer molecular axis) and hydrogen-binding activity (at least one tertiary basic nitrogen atom) that can be crucial in the substrate binding ability (23, 45, 46).

Additionally, there is an overlap in substrate specificity between P-gp and other ABC transporters (MRP1, MRP2, BCRP) and cytochrome P450 (CYP) 3A enzymes (specially CYP3A4) (47). Moreover, P-gp and CYP3A4 also overlap in tissue distribution, suggesting that they act as a synergetic defence mechanism against the intrusion of harmful compounds (23, 48).

1.1.1.6. P-glycoprotein modulation

Beyond substrates, there are other compounds that can interact with P-gp, directly or indirectly, modulating its expression and/or activity, which are known as modulators (25). P-gp modulators are structurally diverse and can be divided in three groups: inhibitors, inducers and activators (18). In the following sections, an overview of all modulators (inhibitors, inducers and activators) will be discussed.

1.1.1.6.1. P-glycoprotein inhibition mechanism and inhibitors

P-gp was originally associated with the MDR phenomenon, which is one of the most important mechanism responsible for the failure of chemotherapy (14, 15). MDR is a well-known therapeutic problem, where cancer cells exposed to one type of drug develop cross resistance to many others structurally and functionally unrelated compounds (49).

Consequently, many strategies have been improved to surpass the difficulties related with MDR and drug delivery, being the direct inhibition of P-gp one of the best studied mechanism (25, 50). Inhibitors, which block the drug efflux function of P-gp, increasing the drug absorption and the drug penetration in protective barriers, are being widely developed in order to make them more efficient and specific (18, 25). Most P-gp inhibitors share chemical features, such as aromatic ring structures, a secondary or tertiary amino group and high lipophilicity (23). P-gp can be inhibited by: blocking the substrate binding-site(s) either competitively, non-competitively or allosterically; interposing with ATP hydrolysis; and changing the integrity of cell membrane lipids. Most P-gp inhibitors act as competitive or noncompetitive compounds and by binding to drug interaction sites resulting in allosteric changes (49, 50). Nevertheless, they all have the same aim, which is to improve drugs bioavailability and absorption, and consequently therapeutic efficacy (23). These inhibitors are classified into four generations depending on their potency, selectivity and drug-drug interaction potential (49).

First-generation inhibitors comprise pharmacological active compounds, which were in clinical use for other therapeutic applications (49, 50). In this class are included verapamil (first reported P-gp inhibitor), cyclosporin-A, reserpine, among others, as listed in **Table 2**. Many of these compounds are also P-gp substrates and act by competing for efflux with other substrates (18). However, the clinical use of these inhibitors was hindered, since the concentration needed to inhibit P-gp could not be safely used due to their toxicity (51).

In order to improve the safety profile in these compounds, analogues of first-generation inhibitors were developed, thus appearing the second- and third- generation inhibitors (15). Second-generation inhibitors resulted from structural modifications of the first-generation inhibitors in order to enhance their P-gp inhibitory activity and simultaneously reduce their other P-gp unrelated activities (49). Dexverapamil (R-isomer of verapamil) and valspodar (cyclosporin-D analogue) are some examples (**Table 2**) (18). Despite having a higher P-gp affinity, they also inhibit other ABC transporters leading to drug-drug interactions (50).

The third-generation group is constituted by the most selective and potent P-gp inhibitors. They were developed with the purpose to enhance MDR tumors treatment with high specificity for P-gp inhibition and low toxicity (49). Furthermore, these compounds were developed using QSAR and combinatorial chemistry, and demonstrated an approximately 10-fold higher potency when compared to first- and second- generation inhibitors (50). In the third-generation inhibitors are included tariquidar and elacridar, which despite being more effective than first- and second- generation inhibitors also inhibit BCRP; and zosuquidar (Zos), a highly specific P-gp blocker that can inhibit the transporter

at a nanomolar range, both *in vitro* and *in vivo* (**Table 2**). Also, Zos has shown to have lower affinity for CYP3A4 than for P-gp, meaning lower drug-drug interactions than the observed in other generation's inhibitors. Nevertheless, unexpected side effects in clinical trials and pharmacokinetic interactions have limited their clinical use (18).

Table 2. P-glycoprotein (P-gp) known inhibitors. Adapted from (39, 49).

P-gp inhibitors	Compounds by pharmacotherapeutic classes
1st Generation	<p>Antibacterial agents (azithromycin, brefeldin A, cefoperazone, ceftriaxone, erythromycin, metronidazole, monensin, salinomycin)</p> <p>Antifungal agents (aureobasidin A, econazole, itraconazole, ketoconazole)</p> <p>Antiretrovirals (concanamycin A, ritonavir)</p> <p>Antischistosomal agents (hycanthone)</p> <p>Scabicial Agents (benzyl alcohol)</p> <p>Anesthetics (chloroform, propofol)</p> <p>Antiemetics (benzquinamide)</p> <p>Antipsychotics (chlorpromazine, haloperidol, loxapine, perospirone, perphenazine, prochlorperazine, trans-flupentixol, trifluoperazine)</p> <p>Antidepressants (amoxapine, sertraline)</p> <p>Stimulants (Methiopropamine)</p> <p>Other Nervous System Drugs (lomerizine)</p> <p>Antiarrhythmics (amiodarone, bepridil, felodipine, isradipine, nifedipine, propafenone, quinidine, diltiazem)</p> <p>Antihypertensives (mibefradil, nicardipine, nifedipine, nimodipine, nitrendipine, prazosin, doxazosin, reserpine, verapamil)</p> <p>Anticoagulant agents (dipyridamole)</p> <p>Peripheral vasodilators (pentoxifylline)</p> <p>Other Vasodilators (vardenafil)</p> <p>Antihistamines (azelastine)</p> <p>Antineoplastic drugs</p> <p style="padding-left: 20px;"><u>Antiandrogens</u> (bicalutamide)</p> <p style="padding-left: 20px;"><u>Tyrosine kinases inhibitors</u> (erlotinib, gefitinib, lapatinib)</p> <p style="padding-left: 20px;"><u>Others</u> (lonafarnib, mitotane, tamoxifen, tesmilifene, tipifarnib)</p> <p>Immunomodulators (cyclosporin A, sirolimus, tacrolimus)</p> <p>Steroid Hormones (medroxyprogesterone, methylprednisolone, mifepristone (RU486), progesterone, tirilazad)</p> <p>Natural products (curcumin)</p> <p>Anti-inflammatory (ibuprofen, indomethacin, tetrandrine, zomepirac)</p> <p>Analgesics (quinine)</p> <p>Non-hormonal steroid derivative (RU49953)</p> <p>Others (bafilomycin, cotinine, diethyl ether, deverapamil, dihydrotychantonol A, emopamil, nigericin, NS398, SB4723, SB4769, SC236)</p>
P-gp inhibitors	Compounds by first generation origin
2nd Generation	<p>BIBW22BS (dipyridamole)</p> <p>Biricodar (tacrolimus)</p> <p>CGP 42700 (staurosporine)</p>

P-gp inhibitors	Compounds by first generation origin (cont.)
2nd Generation (cont.)	Cinchonine (quinidine/quinine) Dexniguldipine (niguldipine) Dexverapamil (verapamil) Dofequidar (ciprofloxacin/levofloxacin) Hydro-cinchonine (quinidine/quinine) KR-30031 (verapamil) MM36 (verapamil) PAK-104P (niguldipine) Quinine homodimer Q2 (quinidine/quinine) Ro 44-5912 (verapamil) S9788 (almitrine) Stipiamide homodimer (stipiamide) Timcodar (tacrolimus) Toremifene (tamoxifen) tRA-96023 (paclitaxel) Valspodar or PSC833 (cyclosporine) WK-X-34 (tetrandrine)
P-gp inhibitors	Compounds developed using QSAR and combinatorial chemistry
3rd Generation	CBT-1, DP7, elacridar (GF120918), laniquidar, OC 144-093, PGP-4008, tariquidar (XR9576), zosuquidar (LY-335979);
P-gp inhibitors	Compounds by class
4th Generation	Dual ligands (aminated thioxanthenes - 1-[2-(1H-benzimidazol-2-yl) ethanamine]-4-propoxy-9H-thioxanthen-9-one) Natural products <u>Alkaloids</u> (ellipticine, pervilleine F) <u>Cannabinoids</u> (cannabidiol) <u>Coumarins</u> (conferone, cnidiadin, praeruptorin A, rivulobirin A) <u>Diterpenes</u> (10-DAB, euphodendroidin D, euphopotlandols A and B, jolkinol B, pepluanin A, portlanquinol, taxuyunnanine-C) <u>Flavonoids</u> (baicalein, DMC, heptamethoxyflavone, nobiletin, quercetin, sinensetin, tangeretin, TMF) <u>Ginsenosides</u> (20S-Ginsenoside, 20S-ginsenoside Rg ₃) <u>Lignans</u> (nirtetralin, schisandrin A and B, silibinin, xanthonolignoid trans-(+/-)-kielcorin C) <u>Polyenes</u> (pentadeca-(8,13)-dien-11-yn-2-one) <u>Sesquiterpenes</u> (dihydro- β -agarofuran) <u>Taccalonolides</u> (taccalonolides A) <u>Triterpenes</u> (β -amyirin, ABA, balsaminoside B, glycyrrhetic acid, karavelagenin C, oleanolic acid, papyriferic acid, sipholenol A, sipholenone E, uvaol) Peptidomimetics (peptide 15, reversin 121, reversin 125, XR9051) Surfactants and lipids (cremophor EL, dodecyl sodium sulfate, nonidet P40, PEG-300, pluronic p85, span-80, triton X-100, tween-20)

10-DAB (10-deacetylbaicatin III), ABA (Alisol B 23-acetate), DMC (2',4'-Dihydroxy-6'-methoxy-3',5'-dimethylchalcone), PEG-300 (Poly(ethylene glycol) 300), TMF (3',4',7-trimethoxyflavone);

More recently, fourth generation inhibitors are arising, focusing in new strategies and techniques hopefully to accomplish a P-gp inhibitor of excellence. This generation includes surfactants, lipids, compounds extracted from natural origins and derivatives, peptidomimetics and agents combining transport inhibition with another beneficial biological activity (dual ligands), among others (**Table 2**) (18, 49).

Overall, at a molecular level, the exact mechanism by which these inhibitors exert their action is not yet well understood, making the design of new efficient and specific templates a challenging process (6). However, the recently proposed molecular structure of human P-gp in the ATP-bound outward-facing conformation can prompt the development of new and potent P-gp inhibitors and may help to better understand their mechanisms of inhibition (31).

1.1.1.6.2. *P-glycoprotein induction mechanism and inducers*

Cells that experience short-term exposure to a variety of environmental/chemical insults adapt by upregulating drug efflux pumps, such as P-gp. P-gp induction results from the increase of the human *MDR1* mRNA levels, since *MDR1* gene transcription is induced, consequently resulting in an exacerbation of the MDR phenotype (18, 23).

MDR1 expression can be upregulated by an increase in gene transcription or mRNA stabilization (52). Transcription of a specific gene is determined by their accessibility and complexity, by several response elements in the promoter sequence, and by transcription factors available to interact with them, which rely on the intracellular environment and extracellular signals (53). A redundant network of *MDR1* regulation guarantees the fast appearance of resistance in cells subjected to chemical stress. The total understanding of the molecular mechanisms through which the *MDR1* gene is activated can lead to an effective silencing or intensification of its transcriptional activation, consequently overcoming the MDR phenomenon, or decreasing the intracellular concentration of toxic xenobiotics, correspondingly (18, 52).

Regulation of ABC transporters gene expression comprises the contribution of many nuclear receptors, including liver X receptor (LXR), farnesoid X receptor (FXR), pregnane X receptor (PXR), and peroxisome proliferator-activated receptors α and γ (PPAR- α and PPAR- γ) (23). Moreover, PXR is the main known nuclear receptor in P-gp induction and can be activated by many unrelated compounds. Once P-gp is co-expressed with PXR in several tissues (brain, liver or intestine), P-gp induction mediated by PXR activation can disturb the pharmacokinetics profile of P-gp substrates and, therefore, affect the intracellular accumulation and toxicity of these compounds (18, 54).

P-gp can be induced by a variety of distinct compounds, such as colchicine, doxorubicin, dexamethasone, insulin, morphine, retinoic acid, verapamil, high levels of glutamate, among many others listed in **Table 3**. Furthermore, P-gp is also induced by environmental factors such as X-irradiation, ultraviolet (UV) irradiation and heat shock (39).

In 2006, Dinis-Oliveira et al. demonstrated, using Wistar rats, that dexamethasone (100 mg/kg, IP) administration, 2 h after intoxication with the toxic P-gp substrate paraquat (PQ, 25 mg/kg, IP), significantly reduced the lung PQ accumulation to about 40% when compared to the group exposed uniquely to PQ, and this result was associated to tissue healing as a result of the induction of *de novo* synthesis of P-gp at the lungs. Moreover, P-gp involvement was confirmed using a competitive P-gp inhibitor, verapamil (10 mg/kg, IP), which, administrated 1 h before dexamethasone, blocked its protective effects leading to an increase in lung PQ concentration and, therefore, a toxicity exacerbation. So, P-gp induction caused an increase in PQ elimination from lung cells, an increase in its fecal excretion and consequently, an increase in the animal survival rate (55). Additionally, Silva et al. using Caco-2 cells as an *in vitro* model proved that doxorubicin (Dox) increased P-gp expression as soon as 6 h after exposure to 5, 10, 50 and 100 μM (147, 186, 312 and 365 % when compared to controls (100%), correspondingly) and 48 h after exposure to 1 μM [204% when compared to control (100%)]. Also, this increase in P-gp expression was accompanied by an increase in the efflux pump activity after exposure to 50 and 100 μM Dox for 6 h (126 and 132 % when compared to control (100%), respectively) and to 0.5 - 10 μM exposure for 48 h [between 128 and 136 % when compared to control (100%)] (56). This increment in P-gp expression and activity was translated in cell protection against the cytotoxicity induced by PQ (56, 57).

In conclusion, P-gp induction can be faced as a possible approach on reducing the intracellular accumulation of toxic compounds and, therefore, reducing their potential toxicity.

Table 3. P-glycoprotein (P-gp) known inducers. Adapted from (18, 23).

P-gp inducers by pharmacotherapeutic class
Antibacterial agents (actinomycin D, doxycycline, erythromycin, rifampicin)
Antifungal agents (clotrimazole, trichostatin A)
Antiretrovirals (abacavir, amprenavir, atazanavir, darunavir, efavirenz, indinavir, lopinavir, nelfinavir, nevirapine, ritonavir, saquinavir)
Anthelmintics (ivermectin, ivermectin)
Antimalarial agents (artemisinin)
Antiprotozoal agents (emetine)
Antiepileptics and Anticonvulsants (carbamazepine, pentylenetetrazol, phenobarbital, phenytoin)

P-gp inducers by pharmacotherapeutic class (cont.)

Antipsychotics (phenothiazine)

Anxiolytics, sedative and hypnotics (midazolam)

Antidepressants (desvenlafaxine, nefazodone, trazodone, venlafaxine)

Dopaminomimetic drugs (bromocriptine)

Stimulants (caffeine)

Narcotic analgesics (morphine, oxycodone)

Cardiotonics (digoxin)

Antiarrhythmics (amiodarone, diltiazem, quinidine)

Antihypertensives (ambrisentan, bosentan, celiprolol, nifedipine, nifedipine, propranolol, reserpine, reserpine, verapamil)

Diuretic (spironolactone)

Lipid modifying agents (atorvastatin)

Drugs used in erectile dysfunction (sildenafil, tadalafil)

Antidiabetics (berberine)

Anti-gout agents (colchicine, probenecid)

Antihistamines (R-cetirizine)

Analgesics (capsaicin)

Anti-inflammatory (diclofenac, fenbufen, indomethacin, meloxicam, mepirizole, nimesulide, sulindac)

Antineoplastic drugs

Alkylating agent (chlorambucil, cisplatin, cyclophosphamide, ifosfamide)

Anthracenes (mitoxantrone, MX2)

Anthracyclines (daunorubicin, doxorubicin, epirubicin, idarubicin)

Anti-androgens (flutamide)

Antimetabolites (cytarabine, fluorouracil, hydroxyurea, methotrexate)

Others (daidzein, tamoxifen)

Taxanes (paclitaxel, docetaxel)

Topoisomerase I inhibitors (topotecan)

Topoisomerase II inhibitors (etoposide)

Tyrosine kinases inhibitors (erlotinib, gefitinib, nilotinib, sorafenib, vandetanib)

Vinca alkaloids (vinblastine, vincristine)

Immunomodulators (cyclosporin A, sirolimus, tacrolimus)

Endogenous hormones (insulin)

Steroid Hormones (aldosterone, betamethasone, budesonide, ciclesonide, corticosterone, dexamethasone, β - estradiol, ethinylestradiol, fluticasone, methylprednisolone, mifepristone, prednisolone)

Natural products

Alkaloids (piperine)

Catechin (epigallocatechin-3-gallate)

Curcumins (curcuma extracts, curcumin, tetrahydrocurcumin)

Diterpenes (ginkgolide-A, ginkgolide-B)

Flavonoids (chrysin, apigenin, catechin, eriodictyol, flavone, genistein, myricetin, naringenin, quercetin, tangeretin, taxifolin, isoxanthohumol)

Others (oleocanthal, ouabain, retinoic acid, γ -tocotrienol, isosafrole)

Phytochemicals (hyperforin, hypericin, *Hypericum perforatum* (Saint John's-wort))

Polyphenols (norathyriol)

P-gp inducers by pharmacotherapeutic class (cont.)
<p>Natural products (cont.)</p> <p><u>Quinones</u> (rhinacanthin-C)</p> <p><u>Xanthonoids</u> (mangiferin)</p> <p>Toxins (aflatoxin B₁)</p> <p>Synthetic xanthonoids</p> <p><u>Chiral aminated thioxanthonoids</u> ((R)-1-((1-Hydroxypropan-2-yl) amino)-4-propoxy-9H-thioxanthen-9-one [ATx 2 (-)])</p> <p><u>Dihydroxylated xanthonoids</u> (3,4-Dihydroxy-9H-xanthen-9-one (X1), 1,2-Dihydroxy-9H-xanthen-9-one (X2), 1,3-Dihydroxy-9H-xanthen-9-one (X3), 2,3-dihydroxy-9H-xanthen-9-one (X4), 3,6-dihydroxy-9H-xanthen-9-one (X5))</p> <p><u>Thioxanthonic derivatives</u> (1-[(3-hydroxypropyl) amino]-4-propoxy-9H-thioxanthen-9-one (TX 1), 1-chloro-4-hydroxy-9H-thioxanthen-9-one (TX 2), 1-[2-(1,3-benzodioxol-5yl) ethyl] amino-4-propoxy-9H-thioxanthen-9-one (TX3), 1-[(2-methylpropyl) amino]-4-propoxy-9H-thioxanthen-9-one (TX 4), 1-(propan-2-ylamino) -4-propoxy-9H-thioxanthen-9-one (TX 5))</p> <p>Others [6,16α-dimethylpregnenolone, 2-AAF, AAAF, asiatic acid, BAP, BEP beclomethasone, benzo(a)pyrene, benzo(e)pyrene, bilirubin, cadmium chloride, cembratriene, cholate, CITCO, cyanidin, cycloheximide, dimethylformamide, dimethylsulfoxide, LY191401, N-OH-AAF, PAF, parthenolide, PCN, PMA, RedRif, sodium arsenate, sodium butyrate, SR-12813, taurocholate, TCDD, TPA, triactyloleandomycin, trimethoxybenzoylyohimbine, depsipeptides (FR901228, FK228, NSC630176)]</p>
Others
<p>Heat Shock</p> <p>UV-irradiation</p> <p>X-irradiation</p>

2-AAF (2-Acetylaminofluorene), AAAF (N-acetoxy-2-acetylaminofluorene), BAP (benzo(a)pyrene), BEP (benzo(e)pyrene), CITCO (6-(4-chlorophenyl)-imidazo[2,1-b][1,3]thiazole-5-carbaldehyde-O-(3,4-dichlorobenzyl)oxime), N-OH-AAF (N-hydroxy-2-(acetyl amino)fluorene), PAF (platelet-activating factor), PCN (pregnenolone 16 α -carbonitrile), PMA (Phorbol 12-myristate 13-acetate), RedRif (reduced rifampicin derivative), TCDD (2,3,7,8-Tetrachlorodibenzo-p-dioxin), TPA (12-O--tetradecanoylphorbol-13-acetate).

1.1.1.6.3. P-glycoprotein activation mechanism and activators

More recently, a new group of compounds that interacts with P-gp has emerged and gained recognition, since they have the capacity to immediately increase P-gp activity without interfering with its protein expression. This class of compounds is known as P-gp activators (58, 59).

It is very important to differentiate P-gp induction and P-gp activation. P-gp induction corresponds to an increase in the transporter expression and, therefore, an increase in the carrier activity is expected. Contrarily, P-gp activation leads to a P-gp conformational change caused by the binding of the activator to the protein, thus stimulating the transport of a substrate bound to another binding site (39, 58). This mechanism suggests that P-gp contains at least two positively cooperative sites for drug binding and transport (18).

Since it is a new concept, the number of identified P-gp activators is still limited. Some examples for this class of compounds are listed in **Table 4** and include a synthetic derivative of rifampicin (a reduced derivative, RedRif), dehydroxylated xanthenes and thioxanthonic derivatives, obtained by chemical synthesis (59-62).

Vilas-Boas et al., using RBE4 cells, demonstrated that RedRif significantly increased P-gp expression and activity at 24 and 72 h, conferring protection against PQ (a P-gp toxic substrate) induced cytotoxicity. This P-gp activity increase occurred even at time points at which no increase in protein content was observed, thus being consistent with an activation mechanism, which was further confirmed by docking studies (59).

Therefore, similar to P-gp induction, P-gp activation seems to be a promising strategy for modulating, in a faster way, the efflux of harmful compounds, acting as an antidotal pathway. In this dissertation, special focus is given to xanthonic derivatives as modulators of P-gp activity and the studies reported in the literature concerning the activation effect of these compounds will be further explored in the following section.

Table 4. P-glycoprotein (P-gp) known activators. Adapted from (18, 58, 60, 63-65).

P-gp activators (by class of compounds)
<p>Chiral aminated thioxanthenes: (S)-1-((1-Hydroxypropan-2-yl) amino)-4-propoxy-9H-thioxanthen-9-one [ATx 1 (+)], (R)-1-((1-Hydroxypropan-2-yl) amino)-4-propoxy-9H-thioxanthen-9-one [ATx 2 (-)], (S)-1-((2-Hydroxypropyl) amino)-4-propoxy-9H-thioxanthen-9-one [ATx 3 (+)], (R)-1-((2-Hydroxypropyl) amino)-4-propoxy-9H-thioxanthen-9-one [ATx 4 (-)], (S)-1-((1-Hydroxy-4-methylpentan-2-yl) amino)-4-propoxy-9H-thioxanthen-9-one [ATx 5 (+)], (R)-1-((1-Hydroxy-4-methylpentan-2-yl) amino)-4-propoxy-9H-thioxanthen-9-one [ATx 6 (-)], (S)-1-((1-Hydroxy-3-methylbutan-2-yl) amino)-4-propoxy-9H-thioxanthen-9-one [ATx 7 (+)], (R)-1-((1-Hydroxy-3-methylbutan-2-yl) amino)-4-propoxy-9H-thioxanthen-9-one [ATx 8 (-)];</p> <p>Dihydroxylated xanthenes: 3,4-Dihydroxy-9H-xanthen-9-one (X1), 1,2-Dihydroxy-9H-xanthen-9-one (X2), 1,3-Dihydroxy-9H-xanthen-9-one (X3), 2,3-dihydroxy-9H-xanthen-9-one (X4), 3,6-dihydroxy-9H-xanthen-9-one (X5);</p> <p>Reduced rifampicin (RedRif);</p> <p>Thioxanthonic derivatives: 1-[(3-hydroxypropyl) amino]-4-propoxy-9H-thioxanthen-9-one (TX 1), 1-chloro-4-hydroxy-9H-thioxanthen-9-one (TX 2), 1-[2-(1,3-benzodioxol-5yl) ethyl] amino-4-propoxy-9H-thioxanthen-9-one (TX3), 1-[(2-methylpropyl) amino]-4-propoxy-9H-thioxanthen-9-one (TX 4), 1-(propan-2-ylamino) -4-propoxy-9H-thioxanthen-9-one (TX 5);</p> <p>Others (Bergamottin, Epicatechin, Imidazobenzothiazoles, Kaempferol, QB102, QB11, Quercetin)</p>

1.1.1.6.4. Xanthones

Xanthones (dibenzo- γ -pyrones) are a natural and organic class of compounds found in plants, fungi, lichens and bacteria as secondary metabolites, in which the chemical structure of the xanthonic scaffold is well-studied (**Figure 5**) (66). It is possible to create an enormous number of derivatives from a xanthonic scaffold by adding different side chains to the backbone. These molecules have a vast list of known benefits, such as anti-allergic, anti-inflammatory, anti-tumor, anticonvulsant properties, among others (67, 68). Thus, these compounds have evoking special interest to medicinal chemistry investigators that considered them as “privileged structures” (69), mostly due to their interaction ability with a diverse range of biomolecules and to their notable biological activity in a broad spectrum of disease states. Nevertheless, the xanthone-drug transporter interaction mechanism remains allusive (62).

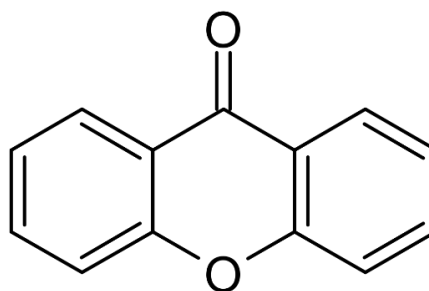


Figure 5. Chemical structure of a xanthonic scaffold (drawn with chemdraw professional 15.0).

Xanthones and thioxanthones (sulfur analogs of xanthones) derivatives have been synthesized and tested *in vitro* as potential inhibitors and/or activators of P-gp (60-62). Silva et al. conducted two studies in Caco-2 cells where five newly dehydroxylated xanthones and five thioxanthonic derivatives were screened as potential modulators of P-gp expression and activity. They found a significant increase in P-gp expression and activity in cells exposed to all tested (thio)xanthonic derivatives for 24 h, thus behaving as P-gp inducers. Additionally, these compounds also rapidly increased P-gp activity without increasing its expression, showing therefore a P-gp activation behavior. In addition, these studies also evaluated the potential protective effects of (thio)xanthones against the cytotoxicity caused by the P-gp substrate, PQ. All dehydroxylated xanthones and four out of five thioxanthonic derivatives were found to significantly reduce PQ cytotoxicity, highlighting the relevance of P-gp modulation in cell protection against toxic substrates (61, 62).

Furthermore, Lopes et al. evaluated the capacity of four enantiomeric pairs of newly synthesized chiral aminated thioxanthones to modulate P-gp expression and/or activity in

Caco-2 cells, revealing that all the tested compounds immediately (simultaneous incubation of the tested xanthenes and Rhodamine 123) increased, in a significant manner, the P-gp activity, when compared to control cells (between 114 and 132 % increase). Most of the compounds also increased P-gp activity after a pre-incubation with the tested xanthenes for 24 h (between 147 and 176 % increase when compared to control cells). However, this increase in the efflux pump activity was not the reflection of an increased P-gp expression, since only one thioxanthone significantly augmented P-gp expression by 36%, when compared to control cells, after 24 h of incubation. Therefore, these results highlight that P-gp activity can be increased without an increase in P-gp expression (60).

In summary, xanthenes are promising compounds once they act as P-gp inducers and/or activators, thus conferring protection against toxic substrates. Accordingly, they might be faced as possible antidotes in cases of intoxications or as disease-modifying drugs in several pathologies/diseases.

1.2. Central nervous system and blood brain barrier

The central nervous system (CNS) plays a major role in the functioning of the human body, consuming at least 20% of the oxygen uptake (70). Being the most sensitive system, it requires special care, having for this purpose three essential structural elements: the blood-cerebrospinal fluid barrier (BCSFB), the arachnoid barrier and the blood-brain barrier (BBB), that work together to protect and maintain the CNS homeostasis (40, 71).

The epithelial cells of choroid plexus and the arachnoid membrane form the BCSFB, which along with the BBB, maintain the homeostasis of the CNS and the uptake of nutrients (71, 72).

Furthermore, the blood-arachnoid barrier represents the interaction between the blood vessels and the avascular arachnoid epithelial layer, sealing the CNS from the rest of the body without significant influence in the blood-CNS exchanges (71, 73).

Lastly, the BBB is present in all organisms that have a well-developed CNS and it is an essential structure for its operation. Functioning as a selective and dynamic barrier between the blood and the CNS, it provides nutrients to the brain, restricts the permeability to hydrophobic molecules and is responsible for the efflux of brain metabolites and other potentially harmful molecules (71, 72). In the brain and spinal cords of humans, it is composed of ECs with tight junctions (TJs), which form the brain capillary walls, representing the principal blood-brain exchange and the most important path for drugs to access the brain cells (**Figure 1**) (71). Deeply TJs are a particularity of the BBB,

significantly reducing the ECs permeability and limiting the diffusion between the vascular system and the brain, being valued to prevent the entry of at least 98% of all therapeutic drugs into the brain (74-76). Moreover, cells like pericytes, astrocytes, microglia and neurons can also be found associated with brain capillaries, as well as drug metabolizing enzymes, such as various forms of CYP, epoxide hydrolase, glutathione S-transferase and UDP-glucanoyltransferase families (77).

Despite not having pores or fenestrae, the BBB presents many paths for permeation, such as transcellular passive diffusion for lipid soluble non-polar molecules (78); solute carriers (SLCs) for, per example, glucose and amino acids transport (79, 80); endocytic routes for macromolecules as peptides and proteins via two different paths, a receptor mediated (RMT) or an adsorptive mediated (AMT) transcytosis (71); and ATP-binding cassette (ABC) transporters, actively effluxing a miscellaneous number of lipid soluble compounds out of the CNS (28). The BBB also prevents the entry from the blood of immune mediators and cell components, acting as an immune privileged local with a low neutrophil infiltration comparing to other sites (71, 81). However, in cases of trauma or pathologic conditions, neutrophils can overcome and damage the BBB, giving brain access to other cells, including leukocytes, macrophages and monocytes, as they transverse the BBB by diapedesis or by the opening of the TJs (82).

As previously stated, P-gp is expressed at the BBB in the brain ECs (**Figure 1**) and, being orientated to the blood, this efflux protein limits the entry of its substrates into the brain, conferring in many cases pharmacoresistance, especially when its expression is increased, and in other cases lack of CNS protection, particularly when its expression is decreased (26, 27).

Given the magnitude of the BBB in the proper functioning of the brain, it is reasonable to consider that a disruption in P-gp function at the BBB could progress to brain dysfunction and neurological diseases.

1.2.1. Involvement of P-glycoprotein in neurodegenerative diseases

Neuropathologies are a current problem in medicine and research, since there is a growing number of CNS diseases emerging and, in most cases, a poorly effective therapeutic response. ABC transporters play an essential role in many neuropathologies for two major reasons: (1) they reduce drug efficacy, since many therapeutic agents are substrates for ABC transporters; (2) some CNS diseases alter the expression and function of ABC transporters (28). Some neurodegenerative diseases, including epilepsy, Creutzfeldt-Jakob disease, amyotrophic lateral sclerosis, multiple sclerosis, Parkinson's disease and Alzheimer's disease, the most studied neurodegenerative disorder and the

main focus of this thesis, are tightly linked to the dysfunction of ABC transporters, particularly P-gp (83).

1.2.1.1. P-glycoprotein and Alzheimer's disease

Alzheimer's disease (AD), firstly named by the psychiatrist Alois Alzheimer in 1901, is currently the most prevalent cause of dementia, being characterized by a progressive decline in cognitive function and behavioral conduct (84, 85).

Two forms of AD are presently considered: (1) sporadic/late onset, representing the majority of the cases, usually in individuals over 65 years old; (2) familial/early onset, usually in individuals under 65 years old, accounting for 0,1% of the total disease cases (84). The late onset of the disease develops as a result of three main factors: (1) age, which is the supreme risk factor; (2) family history, individuals with a first degree relative have a higher risk to develop the disease; (3) the $\epsilon 4$ allele form of the apolipoprotein E (APOE), being by now the only reliably genetic risk identified (84, 86). Furthermore, environmental and lifestyle factors can also contribute to the development/progression of the disease (85, 87). For the early onset form, mutations in three specific genes are involved in the development of the disease, the amyloid precursor protein (APP) and the presenilin 1 (PSEN1) and presenilin 2 (PSEN2) genes (84, 88). Individuals inheriting a mutation in the APP gene, causing an increase in all amyloid- β ($A\beta$) peptides production, or in the PSEN1 gene, which leads to abnormal production of $A\beta_{42}$ peptides, are certain to develop the disease. Nevertheless, individuals who inherit a mutation in the PSEN2 gene, which results in an abnormal production of $A\beta_{42}$ peptides, have a 95% chance of developing the pathology. These mutations play a role in APP breakdown, generating harmful forms of amyloid plaques. Furthermore, those who inherit any of the mentioned mutations tend to develop the AD symptoms before 65 years old (85, 86).

This neurodegenerative disease presents a multifaceted pathogenesis as schematized in **Figure 6**, including accumulation of the $A\beta$ peptide outside neurons, with extracellular senile plaques formation and atypical aggregation of tau protein (tau tangles) inside neurons. $A\beta$ plaques supposedly contribute to cell death by interfering with the neurons communication at the synapses, while tau tangles block the nutrients and other essential molecules transport inside neurons (85, 89, 90). In addition, it is also characterized by high levels of $A\beta$ oligomers, increased oxidative stress, inflammation of cerebral blood vessels, reduced brain weight and loss of neurons (91).

$A\beta$ accumulation is, by far, the best described pathogenic event. $A\beta$ descends from a larger transmembrane protein, the amyloid precursor protein (APP), and is normally produced in healthy individuals (92), where it has physiological roles (antimicrobial activity

regulation of cholesterol transport, protection against oxidative stress) (93-95). There are several isoforms of A β , with A β_{40} and A β_{42} being the most relevant for AD pathology (96).

Two main theories are at the basis for this neurodegenerative disease. The A β cascade hypothesis states that oligomeric A β species accumulation in the CNS is the essential event in AD development (97). The second theory, the neurovascular hypothesis of AD, tries to identify the cause for this accumulation (98). Therefore, the neurovascular hypothesis suggests that this CNS A β accumulation can result from three core events: (1) decrease/lack of A β degradation, (2) diminished A β clearance, and (3) increased influx of A β species across the BBB (99).

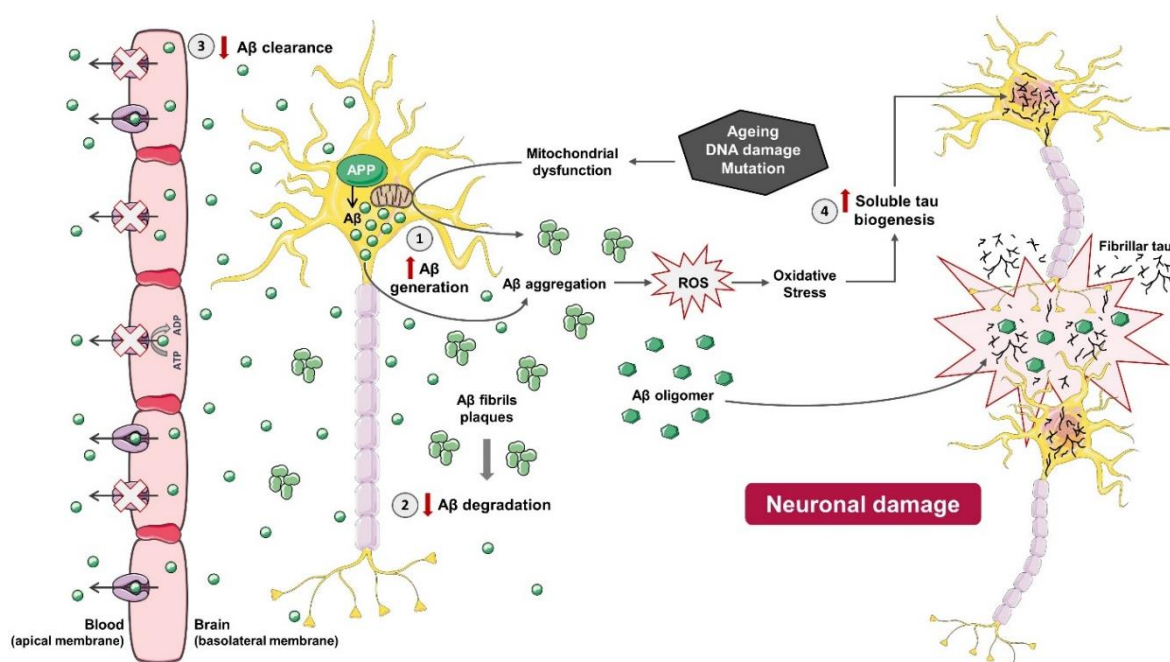


Figure 6. Schematic representation of Alzheimer's disease (AD) pathology. This disease presents a multifaceted pathogenesis, with amyloid- β (A β) peptide accumulation as the major cause of the disease. This peptide is descendant from the amyloid precursor protein (APP), being released into the extracellular environment where it forms fibrillar plaques and A β oligomers, that if not degraded are toxic to the adjacent synapses. In addition, atypical aggregation of tau protein resulting from oxidative stress caused by A β aggregation also contributes to neuronal damage. Four main factors are involved in AD: (1) excessive production of A β ; (2) lack degradation of A β fibrillar plaques; (3) decrease in A β clearance; and (4) increase of tau protein biogenesis. Adapted from (100-102).

In 2010, Mawuenyega et al. compared the relationship between the human CNS production and clearance of A β (A β_{40} and A β_{42}) in healthy individuals and individuals with symptomatic AD. The average rate production of A β_{40} and A β_{42} did not differ between the control and AD groups. However, they found a reduced A β_{40} and A β_{42} clearance capacity (for A β_{40} : 5.2%/hour for AD individuals *versus* 7.0%/hour for controls; and for A β_{42} : 5.3%/hour for AD individuals *versus* 7.6%/hour for controls), leaving evident the possibility of an A β clearance impairment in the late onset form of AD (103). Moreover, the A β

clearance mechanisms include astrocyte-mediated enzymatic degradation (104), removal via the CSF bulk flow (105) and, the most influent, active efflux across the BBB, which is accomplished by the ABC efflux transporters (P-gp, **Figure 7**) (106) and by the low density lipoprotein receptor-related protein 1 (LRP-1) (107). LRP-1 is present at the basolateral membrane of the BBB, where it promotes the A β passage from the brain into capillary cells (**Figure 7**). Moreover, A β can suffer influx into the brain via the receptor for advanced glycation end products (RAGE, **Figure 7**). Therefore, it is essential to continuously remove and/or degrade A β species from the brain in order to avoid their brain accumulation and potential neurotoxicity (108, 109).

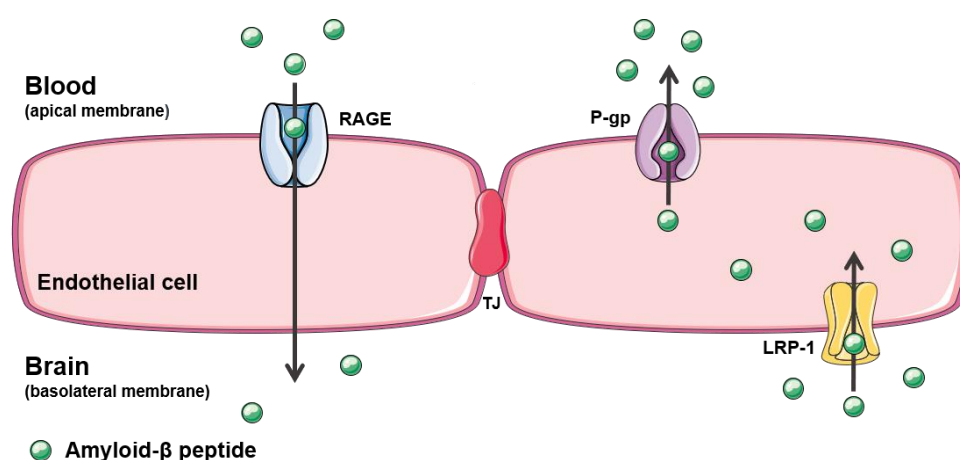


Figure 7. Main transporters involved in amyloid- β (A β) peptide transport across the blood brain barrier (BBB). Low density lipoprotein receptor-related protein 1 (LRP-1), present at the basolateral membrane of the BBB, promotes the A β traffic from the brain into endothelial cells. P-glycoprotein (P-gp), present at the apical membrane of the BBB, promotes the active efflux of A β from endothelial cells into the systemic circulation (blood). On the other hand, the receptor for advanced glycation end products (RAGE) facilitates A β return to the brain interstitial fluid. Adapted from (91, 108).

In the last few years, several studies have shown clear evidence of ABC transporters, mostly P-gp, involvement in A β efflux (110-121). In 2001, Lam et al. reported for the first time, using HEK293 cells transiently transfected with pHaMDR1/A and with APP695 harboring the Swedish double mutation (K269sw), that pharmacological inhibition of P-gp (RU486 and RU49953) significantly reduced A β secretion in a fast and dose-dependent manner, demonstrating that P-gp participates in the A β efflux (115). One year later, Vogelgesang et al. found in tissue samples from the brain medial temporal lobe, that A β_{40} and A β_{42} accumulation was inversely correlated with P-gp expression, with a most striking inverse relationship for A β_{40} . Using immunohistochemical assays, the group revealed that 44% of the individuals without detectable P-gp expression had A β_{40} -positive plaques in the cerebral cortex, when compared to those with moderate and strong P-gp expression (19 and 15 %, respectively) (119). In 2005, Cirrito et al., using wild type (WT) and *mdr1a/b*^{-/-} double knockout mice (P-gp null) injected with [¹²⁵I]A β_{40} and [¹²⁵I]A β_{42} , showed

that P-gp null animals retained significantly more A β ₄₀ and A β ₄₂ into the brain, when compared to control animals (31% of injected A β ₄₀ was transported across the BBB in WT mice versus 14% in P-gp null mice and 16% of A β ₄₂ was transported in Pgp WT mice versus 6% in Pgp-null mice). Furthermore, using APP^{sw} mice (with human APP overexpression), the group revealed that 8 h after P-gp inhibition with XR9576 (80mg/kg, IV) A β _{1-x} levels in brain interstitial fluid increased almost 30%, when compared to control animals, establishing a connection between A β transport and P-gp (112). Additionally, a study performed by Kuhnke et al. using MDR1-transfected LLC cells, yielded extra evidence for P-gp relevance in A β clearance from the brain, highlighting P-gp as a putative target to prevent/treat AD. Also, the group demonstrated, using fluorescence-labeled peptides and isolated inside-out membrane vesicles from LLC-MDR1 cells, that A β ₄₀ and A β ₄₂ transport is ATP-dependent (114). Later in 2010, Hartz et al. demonstrated a reduced P-gp expression (approximately 60% decrease) and transport activity (70% decrease) in 12-week-old mice overexpressing human amyloid precursor protein (hAPP), when compared to wild type littermates. Furthermore, at this time point, transgenic mice showed human A β accumulation in the brain without signs of cognitive impairment. However, after one daily injection of a PXR activator (pregnenolone 16 α -carbonitrile (PCN), 25 mg/kg, IP) for 7 days, this reduction in P-gp expression and activity in hAPP mice was prevented and correlated with a decreased brain A β levels. Thus, the authors suggested a new therapeutic strategy for AD, which, by targeting signals that upregulate P-gp at the BBB, in early stages of the disease, can modulate A β accumulation and clearance (113). Moreover, Abuznait et al. demonstrated, using LS-180 cells as an *in vitro* model, a 10-35% decrease in [¹²⁵I]A β ₄₀ intracellular accumulation in cells exposed to different recognized P-gp inducers [rifampicin (50 μ M), dexamethasone (50 μ M), caffeine (50 μ M), verapamil (50 μ M), hyperforin (100 nm), β -estradiol (50 μ M) and pentylenetetrazol (50 μ M)], for 48 h, when compared to control cells. These results highlighted the importance of P-gp upregulation in A β clearance, which can be an effective pathway in slowing or halting AD progression (110). Van Assema et al., using (R)-[¹¹C] verapamil and positron emission tomography, provided the first direct evidence for compromised P-gp transport at the human BBB in late onset AD, suggesting that AD pathogenesis may be related to reduced P-gp function (117). Moreover, the same group found a direct correlation between aging and decreased P-gp at the human BBB (118). Still, in 2012, an interesting study performed by Qosa et al., demonstrated using C57BL/6 mice as an *in vivo* model, an upregulation of P-gp and LRP-1 at the BBB after rifampicin and caffeine exposure. Western blot and quantitative analysis showed that rifampicin (20 mg/kg, IP) and caffeine (40 mg/kg, IP) augmented P-gp expression by at least 2.7-fold and at least 1.5-fold, respectively, when compared to control animals, and LRP-1

expression by at least 1.9-fold and 1.2-fold compared to control animals, correspondingly. Furthermore, this upregulation mediated by rifampicin and caffeine was associated with BBB enhanced $A\beta_{40}$ clearance (about 20% increase), which was correlated with the P-gp and LRP-1 transporters (116). The same group, in 2014, developed the first mathematical model describing $A\beta$ clearance across the BBB, also providing an insight into interspecies' differences between mouse and human $A\beta$ clearance at the BBB (122). Wang et al., showed that in *mdr1a* knockout mice (P-gp deficient), $A\beta$ accumulation into the brain was aggravated in comparison to wild type animals, providing evidence that a deficit in the P-gp transporter can lead to an extra $A\beta$ accumulation in the mice brain (120). In the last year, Bruckmann et al. studied the influence of P-gp sited at the BBB on the efficiency of $A\beta$ immunization (reduces cerebral $A\beta$ deposits). To this end, they analyzed the brain of male APP/PS1+/-P-gp mice with intact P-gp (n=8) and APP/PS1+/-P-gp mice lacking functional P-gp (n=8), after $A\beta_{42}$ immunization. In immunized mice with intact P-gp, a significant decrease in soluble and insoluble $A\beta_{40}$ and $A\beta_{42}$ was observed. Immunization also reduced $A\beta$ plaque burden. On the other hand, in immunized APP/PS1+/-P-gp mice lacking functional P-gp, only the soluble form of $A\beta_{42}$ showed a significant reduction. Besides, a stronger intracerebral amyloid angiopathy was found after immunization. Thus, these results indicate that the absence of P-gp results in a significant perturbation in $A\beta$ clearance. Moreover, they suggested that P-gp upregulation can be an improvement in the treatment/prevention of AD, by enhancing $A\beta$ immunization efficiency (111). Recently, Zhang et al., using male APP/PS1 mice as an *in vivo* model of AD, showed that P-gp expression (western blot analysis) was significantly downregulated in the brain of AD mice, an effect reverted by ibuprofen [chow containing ibuprofen (375 ppm) for 5 months]. The expression of inflammatory factors [TNF- α and IL-1 β mRNA (qRT-PCR analysis) and NF- κ B protein expression levels (ELISA analysis)] was also increased in the brain of AD mice when compared to control mice. Likewise, ibuprofen treatment suppressed the expression of those inflammatory factors, which could restore P-gp expression and function, leading to an increase in $A\beta$ efflux and, thereby, improve AD condition. Furthermore, AD mice presented more $A\beta$ plaques (immunohistochemistry analysis) when compared to control and ibuprofen-treated AD mice, suggesting that ibuprofen treatment might reverse the downregulation of P-gp expression and function induced by $A\beta$ via suppressing inflammation in AD mice brain (121).

Beyond the previously mentioned studies relating P-gp with $A\beta$ clearance, there are still other studies attempting to demonstrate that $A\beta$, by itself, downregulates P-gp (123-125). Kania et al., using the hCMEC/D3 cell line as an *in vitro* model, reported a significant decrease in P-gp expression, at both protein and mRNA levels, after $A\beta_{42}$ peptide exposure (5.0 μ M for 48 h). Considering that the most likely explanation for $A\beta$ effects on

P-gp is the reduction in the Wnt/ β -catenin pathway (implicated in the regulation of P-gp expression), a Wnt agonist (Wnt3a) was used, which counteracted the decrease in P-gp expression caused by the A β (124). Nonetheless, A β concentrations used in those studies may be above the concentrations normally found in humans. Thus, the effects of A β on P-gp expression need further clarification (91, 126).

In summary, although there are many studies associating AD with P-gp dysfunction, additional studies are still needed to provide mechanistic insights into the role of this peptide in AD pathogenesis, to further develop a more efficient, novel preventive or therapeutic strategy for AD.

2. Objectives

The unquestionable importance of P-gp in the efflux of a wide range of substrates, its expression in many excretory and barrier tissues (e.g. BBB), and its broad substrate specificity make this protein essential in modulating the pharmacokinetic processes. Thus, it acts as a defense mechanism against toxic substrates, such as harmful xenobiotics (PQ), as well as endogenous substrates ($A\beta$), significantly reducing their absorption, and, consequently, their toxicity.

P-gp is implicated in many different diseases, playing an essential role in many neuropathologies, such as Alzheimer's disease. Since in AD P-gp is downregulated (111, 113, 119), this protein can be faced as a potential target pathway, through modulating mechanisms such as induction and activation, in order to enhance the efflux of $A\beta$, a P-gp substrate that accumulates in AD pathology.

Considering that xanthonic derivatives are known to interact with P-gp, thereby modulating its expression and/or activity (60-62), this dissertation aims to gain insight into the putative contribution of P-gp modulation by these compounds on AD. Thus, by using the hCMEC/D3 cell line as an *in vitro* model of the human BBB, the following specific objectives were explored:

- The potential P-gp induction or/and activation by six new xanthonic derivatives obtained by chemical synthesis;
- The putative toxic effect of the $A\beta_{42}$ peptide (a biomarker of AD pathogenesis);
- The contribution of P-gp modulation by the newly synthesized xanthonic derivatives against the cytotoxic effect induced by the $A\beta_{42}$ peptide;

3. Materials and methods

3.1. Materials

EndoGRO MV Basal Medium kit and lithium chloride (LiCl) were acquired from Merck Millipore (Darmstadt, Germany). Neutral red (NR) solution, 3-[4,5-dimethylthiazol-2-yl]-2,5 diphenyl tetrazolium bromide (MTT), resveratrol, rhodamine 123 (Rho 123) and zosuquidar (Zos) were obtained from Sigma (St. Louis, MO, USA). Reagents used in hCMEC/D3 cell culture, such as heat-inactivated fetal bovine serum (FBS), 0,25% trypsin/1 mM EDTA, antibiotic (10,000 U/mL penicillin, 10,000 µg/mL streptomycin), rat tail collagen type I, Hank's balanced salt solution (HBSS) and phosphate-buffered saline solution (PBS), were purchased from Gibco Laboratories (Lenexa, KS, USA). Triton™ X-100 detergent solution was acquired from Thermo Fisher Scientific (Waltham, MA, USA). Basic fibroblast growth factor (bFGF) was obtained from Invitrogen (Carlsbad, CA, USA). P-gp monoclonal antibody (clone UIC2) conjugated with phycoerythrin (PE) was purchased from Abcam (Cambridge, United Kingdom). Human Aβ₄₂ was purchased from AnaSpec (Fremont, CA, USA). All the reagents used were of analytical grade or the highest grade available.

3.2. Synthesis of xanthenes

The six tested xanthenes (X4, X7, X8, X9, X13 and X17) used in this work were synthesized in the Organic and Pharmaceutical Chemistry Laboratory, Department of Chemical Sciences, Faculty of Pharmacy, University of Porto. The following figure (**Figure 8**) illustrates the chemical structure and the IUPAC nomenclature of the tested xanthonic derivatives.

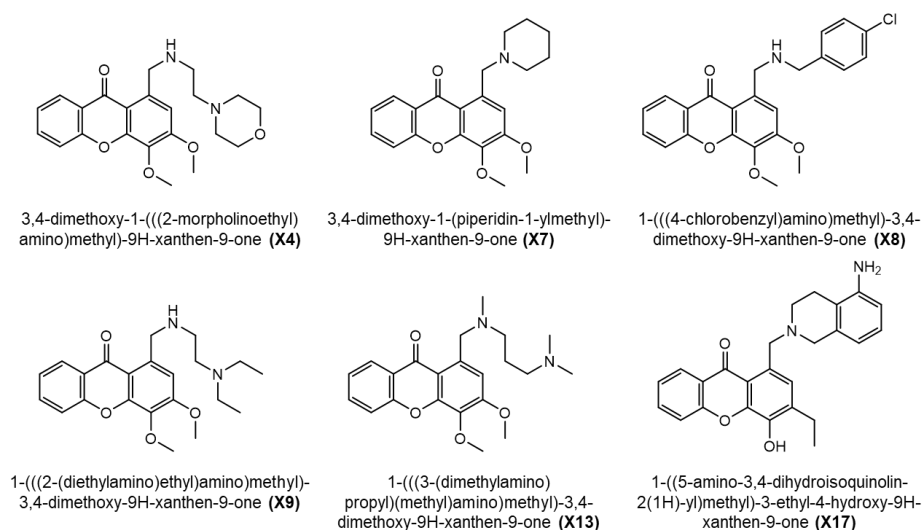


Figure 8. Chemical structure and IUPAC nomenclature of the xanthonic derivatives (drawn with chemdraw professional 15.0).

3.3. hCMEC/D3 cell line - general considerations

The hCMEC/D3 cell line was developed from human temporal lobe microvessels isolated from tissue in a cortectomy performed on an epileptic patient (127). Cellular immortalization was then achieved by transduction with the catalytic unit of human telomerase (hTERT) and SV40 T antigen, through a lentiviral vector system (128).

hCMEC/D3 cell line is widely used as a model for the human BBB, since it preserves most of the functional and morphological characteristics of the blood vascular endothelial cells (BECs), demonstrating BBB physiognomies, such as the expression of chemokine receptors, adhesion molecules, endothelial markers (cluster of differentiation 31), vascular endothelial cadherin and von Willebrand factor, and expression of efflux transporters, such as P-gp, BCRP and MRP1 (127). Moreover, this cell line presents the formation of tight junctions (TJs), a stable karyotype and the formation of capillary tubes in matrix. In culture, they maintain contact-inhibited monolayers and can be subcultured until the 35th passage without changes in growth and endothelial marker characteristics (129). Therefore, hCMEC/D3 cell line is a valuable *in vitro* model to study the human BBB drug transport (127).

3.3.1. hCMEC/D3 cell culture

Human cerebral microvessel endothelial cell line clone D3 (hCMEC/D3) was cultured in 75 cm² flasks (T75), using EndoGRO MV Basal Medium, supplemented with EndoGRO-LS Supplement (0.2%), recombinant human epidermal growth factor [(rh EGF), (5 ng/ml)], L-Glutamine (10 mM), hydrocortisone hemisuccinate (1 µg/ml), heparin sulphate (0.75 U/ml), and ascorbic acid (50 µg/ml), and heat-inactivated fetal bovine serum (5%), all components of EndoGRO MV Basal Medium kit, lithium chloride [(LiCl), (10 mM)], resveratrol (10 µM) and antibiotics (100 U/mL penicillin and 100 µg/mL streptomycin). For culturing, bFGF (1ng/mL) was added to the medium just prior to use.

The cells used for the experiments were taken between passage 29 and 35. All cultureware was previously coated, for 1 h at 37°C, with rat tail collagen type I (0,1 mg/mL) and washed twice with HBSS (-/-) right before use, avoiding surface dry. Cells were maintained in a 5% CO₂-95% air atmosphere at 37°C, and the medium was changed every 2-3 days. Cultures were passaged weekly by trypsinization (0.25% trypsin/1 mM EDTA). In all experiments, the cells were seeded at a density of 25,000 cells/cm² (cells were counted using a Neubauer chamber and a trypan blue solution) and used when confluence was reached. A protocol for hCMEC/D3 cells trypsinization and seeding is shown in **Figure 9**.

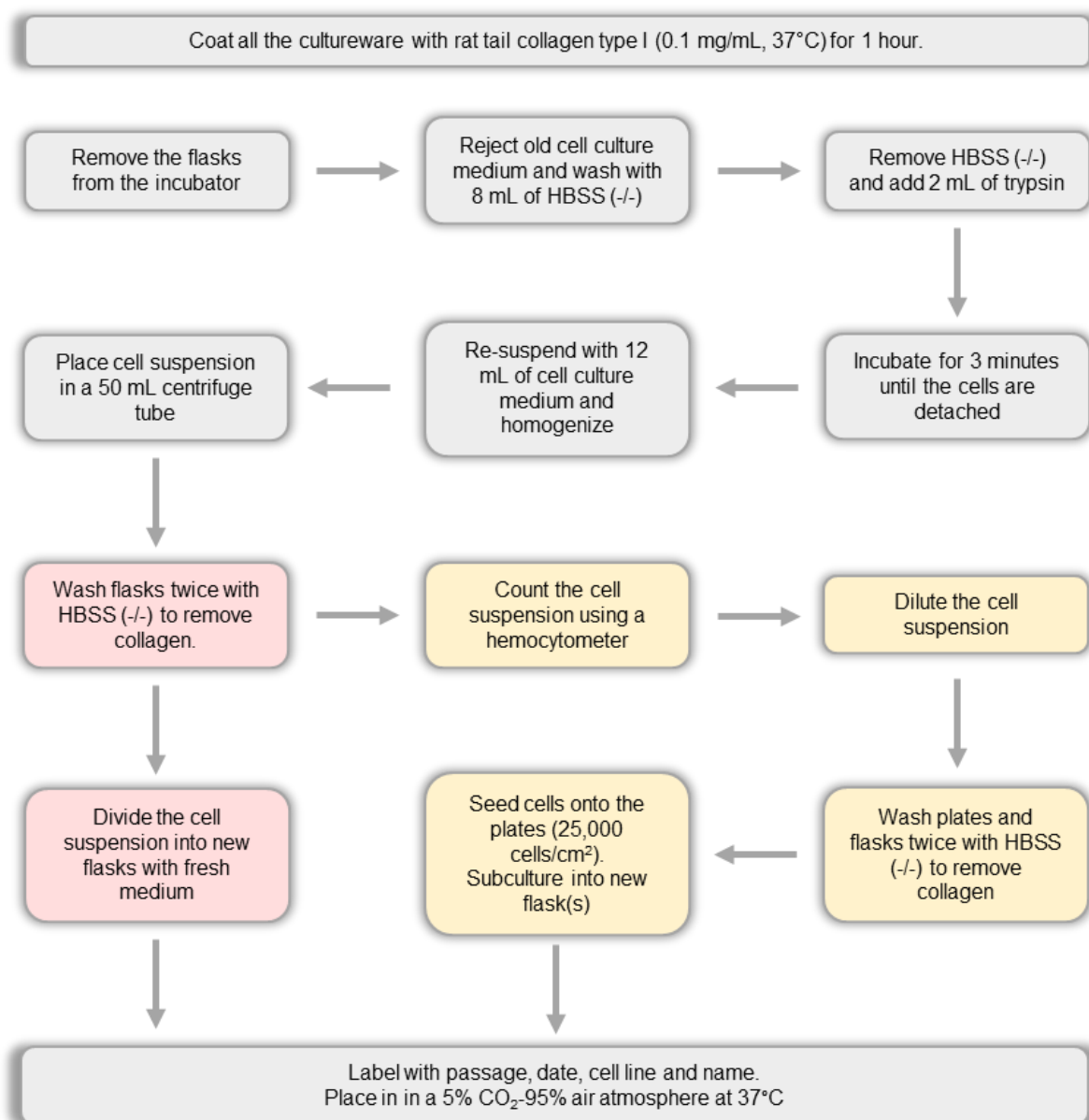


Figure 9. Brief experimental protocol for cell subculturing (pink) and cell seeding (yellow).

3.3.2. Xanthones, Zosuquidar and Rhodamine 123 cytotoxicity assays

Cells were seeded in 96-well plates previously coated with 50 μ L rat tail collagen type I (0,1 mg/mL, for 1 h at 37°C) at a density of 25,000 cells/cm² (100 μ L of a 80,000 cells/mL cell suspension: 8,000 cells/well) and exposed to the tested compounds after reaching confluence (three days after seeding). Xanthones (0 - 50.0 μ M), Zosuquidar (Zos, 0 - 10 μ M) and Rhodamine 123 (Rho 123, 0 - 5.0 μ M) cytotoxicity was evaluated 24 h after exposure by the neutral red (NR) uptake and the MTT reduction assays.

3.3.2.1. Neutral red uptake assay

3.3.2.1.1. General principle

The neutral red (NR) uptake assay is a very simple colorimetric method used to estimate the cell cytotoxicity or viability, based on the ability of viable cells to incorporate and bind the supravital neutral red dye into the lysosomes (130, 131).

NR is a weak cationic dye with the ability to penetrate the cell membrane by non-ionic passive diffusion, binding with anionic sites and/or phosphate groups through electrostatic hydrophobic interactions in the lysosomes, where it accumulates. Since the characteristic lysosome proton gradient allows the dye to become charged and retained in the lysosomal matrix, the cells aptitude to preserve pH gradients directly influences the NR uptake, as a pH gradient reduction or cell death unfeasible the dye retention. Therefore, the quantity of dye retained in the lysosomes is directly proportional to the number of viable cells in culture. Subsequently, the dye is extracted from the viable cells by an acidified ethanol solution and quantified using a spectrophotometer (132).

Moreover, lysosomal membrane damage or variations in cell surface can also alter the NR uptake, allowing the distinction between viable, damaged and dead cells, based on their lysosomal specific capacity to incorporate the dye. Thus, the lysosome integrity and the associated binding of the neutral red dye, make this method a sensitive indicator for cell viability (132).

3.3.2.1.2. Experimental protocol

At the selected time point (24 h), the cell culture medium was removed, and the cells were incubated with 100 μ L of fresh culture medium with 50 μ g/mL NR, for 3.5 h at 37 $^{\circ}$ C, in a humidified, 5% CO₂-95% air atmosphere. After the incubation period, the cell culture medium was removed, and the dye was extracted with 100 μ L of absolute ethyl alcohol/distilled water (1:1) with 5% acetic acid. Afterwards, plates were gently shaken in a microtiter-plate shaker until a homogeneous solution was formed and the absorbance measured at 540 nm in a multiwell plate reader (PowerWaveX BioTek Instruments, Vermont, US).

Cytotoxicity was evaluated by the percentage of NR uptake relative to control cells (0 μ M). At least four independent experiments were performed, in triplicate.

3.3.2.2. MTT reduction assay

3.3.2.2.1. General principle

The MTT reduction assay is a quick colorimetric method to estimate cellular viability and cytotoxicity based on the mitochondrial activity of viable cells (133).

MTT (3-[4,5-dimethylthiazol-2-yl]-2,5 diphenyl tetrazolium bromide) is a water-soluble dye and a yellow tetrazolium salt. Mitochondrial dehydrogenases of viable cells cleave the tetrazolium ring, reducing the tetrazolium dye into purple and water-insoluble formazan crystals, which can be solubilized in an organic solvent. Thus, it is predictable that formazan formation is directly proportional to the number of metabolically viable cells, making this method an effective and easy way of assessing cells cytotoxicity (134, 135).

3.3.2.2.2. Experimental protocol

After the incubation period (24 h), the cell culture medium was removed, 100 μ L of fresh cell culture medium containing 0.5 mg/mL MTT were added and cells were incubated at 37 °C in a humidified, 5% CO₂-95% air atmosphere for 3.5 h. After this incubation period, the cell culture medium was removed, and the formed formazan crystals solubilized with 100 μ L of DMSO. Plates were then gently shaken in a microtiter-plate shaker until a homogeneous solution was formed and the absorbance was measured at 550 nm in a multi-well plate reader (PowerWaveX, BioTek Instruments, VT, USA). The percentage of MTT reduction relative to that of control cells (0 μ M) was used as the cytotoxicity measure. At least four independent experiments were performed, in triplicate.

3.3.3. Evaluation of P-glycoprotein expression – flow cytometry

hCMEC/D3 cells were seeded onto 24-well plates previously coated with 100 μ L rat tail collagen type I (0.1 mg/mL, for 1 h at 37°C), at a density of 25,000 cells/cm² (500 μ L of a 95,000 cells/mL cell suspension: 47,500 cells/well) and, after three days, when confluence was reached, the cells were exposed to the tested xanthenes, at a non-cytotoxic concentration (20.0 μ M), in fresh cell culture medium. Twenty-four hours after exposure, cells were washed with HBSS (-/-) and harvested by trypsinization (0,25% trypsin/1 Mm EDTA) to obtain a cell suspension. The cell suspension was transferred to eppendorf tubes, centrifuged (300g for 5 minutes, at 4°C) and re-suspended in PBS (+/+) buffer (pH 7.4) containing 10% heat-inactivated FBS and the P-gp antibody (UIC2 clone conjugated with PE - 5 μ l for 10⁶ cells.). After 1 h of incubation at room temperature, in the dark, and under gentle shaking, the cells were washed twice with PBS (-/-) buffer (pH 7.4),

centrifuged (300g for 5 minutes at 4°C) and kept on ice until the analysis. Cells were then re-suspended with ice-cold PBS (-/-) buffer immediately before the cytometer analysis. Cells were analyzed in a BD Accuri™ C6 flow cytometer (BD Biosciences, CA, USA), with the FCS Express™ analysis software.

The fluorescence of the UIC2-PE-antibody was measured by a 585 ± 40 nm band-pass filter (FL2 detector). The logarithmic fluorescence was recorded and displayed as a single parameter histogram and based on the acquisition of data for at least 20,000 cells. The parameter used for comparison was the mean of fluorescence intensity (MFI), calculated as percentage of control (0 μ M). The cells autofluorescence (unlabeled cells with or without the tested xanthenes) was also evaluated in every experiment in order to eliminate its potential contribution to the analyzed fluorescence signals. Mouse IgG2a-PE was used as an isotype-matched negative control to estimate non-specific binding of the PE-labeled anti-P-glycoprotein antibody [UIC2-PE]. At least six independent experiments were performed in duplicate.

3.3.4. Evaluation of P-glycoprotein transport activity

P-gp activity was evaluated through two different experimental protocols, both using Rho 123 (5.0 μ M) as a fluorescent P-gp substrate. In the first protocol, the accumulation of Rho 123 was evaluated in hCMEC/D3 cells previously exposed to the tested xanthenes for 24 h, thus assessing to eventual alterations in P-gp activity due to the possible effects on P-gp expression caused by the xanthenes.

On the other hand, in the second protocol, the accumulation of Rho 123 was evaluated in the presence of the tested xanthonic derivatives, allowing a direct detection of alterations in P-gp activity without affecting its protein expression.

In both protocols, the incubation with the fluorescent P-gp substrate was performed in the presence and absence of Zos (5.0 μ M), a third-generation P-gp inhibitor.

3.3.4.1. Rhodamine 123 accumulation in hCMEC/D3 cells pre-exposed to the tested xanthenes

hCMEC/D3 cells were seeded onto 24-well plates previously coated with 100 μ L rat tail collagen type I (0.1 mg/mL, for 1 h at 37°C), at a density of 25,000 cells/cm² (500 μ L of a 95,000 cells/mL cell suspension: 47,500 cells/well). After three days in culture, when confluence was reached, the cells were exposed to the tested xanthenes, at a non-cytotoxic concentration (20.0 μ M) in fresh cell culture medium. Cells were processed after an incubation period of 24 h or, alternatively, the medium was replaced by new cell culture

medium without the tested compounds, and cells were processed 24 h or 72 h later (48 h or 96 h after starting the exposure to the tested compounds) under normal or inhibited P-gp conditions:

- Rho 123 accumulation under normal P-gp conditions (NA): cells were maintained in HBSS (+/+) for 30 minutes, and then exposed to Rho 123 (5.0 μ M) for 90 minutes.
- Rho 123 accumulation under inhibited P-gp conditions (IA): the cells were exposed to Zos [5.0 μ M in HBSS (+/+)] for 30 minutes, and then exposed to Rho 123 (5.0 μ M) for 90 minutes. This allows a maximal Rho 123 accumulation inside the cells.

Afterwards, the medium was removed, the cells (NA and IA) were washed twice with PBS (-/-) buffer (pH 7.4) and lysed with 1% Triton X-100 for 30 minutes. After this incubation period, the Rho 123 intracellular fluorescence was measured at excitation/emission wavelengths of 485/528 nm, in a multi-well plate reader (PowerWaveX, BioTek Instruments, VT, USA). The ratio between the mean fluorescence intensity (MFI) of Rho 123 accumulation under inhibited P-gp conditions (IA) and Rho 123 accumulation under normal P-gp conditions (NA) was used (**Equation 1**). Results were expressed as percentage of control cells (0 μ M). At least six independent experiments were performed in triplicate.

$$\text{Rho 123 accumulation} = \frac{\text{MFI of Rho 123 accumulation under conditions of inhibition (IA)}}{\text{MFI of Rho 123 accumulation under normal conditions (NA)}}$$

Equation 1. P-gp activity was assessed by the ratio between the amount of Rhodamine 123 (Rho 123) accumulated in the presence of the inhibitor (IA, Zos, 5.0 μ M) and the amount of Rho 123 accumulated in the absence of the inhibitor (NA). MIF (mean fluorescence intensity).

3.3.4.2. Rhodamine 123 accumulation assay in hCMEC/D3 in the presence of the tested xanthenes

hCMEC/D3 cells were seeded onto 24-well plates previously coated with 100 μ L rat tail collagen type I (0.1 mg/mL, for 1 h at 37°C), at a density of 25,000 cells/cm² (500 μ L of a 95,000 cells/mL cell suspension: 47,500 cells/well). Four days after seeding, cells were processed under normal or inhibited P-gp conditions:

- Rho 123 accumulation under normal P-gp conditions (NA): the cells were incubated with the tested xanthenes (20.0 μ M) prepared in HBSS (+/+) for 30 minutes, and then incubated with Rho 123 (5.0 μ M) for 90 minutes.
- Rho 123 accumulation under inhibited P-gp conditions (IA): cells were simultaneously exposed to the tested xanthenes (20.0 μ M) and to Zos (5.0 μ M), both prepared in HBSS (+/+), for 30 minutes, and then incubated with Rho 123 (5.0 μ M) for 90 minutes. This allows a maximal Rho 123 accumulation inside the cells.

After this incubation period, the medium was removed, cells (NA and IA) were washed twice with PBS (-/-) buffer (pH 7.4) and lysed with 1% Triton X-100 for 30 minutes. Afterwards, the Rho 123 intracellular fluorescence was measured at excitation/emission wavelengths of 485/528 nm, in a multi-well plate reader (PowerWaveX, BioTek Instruments, VT, USA). The ratio between the mean fluorescence intensity (MFI) of Rho 123 accumulation under inhibited P-gp conditions (IA) and Rho 123 accumulation under normal P-gp conditions (NA) was used (**Equation 1**). Results were expressed as percentage of control cells (0 μ M). At least five independent experiments were performed in triplicate.

3.3.5. Evaluation of amyloid- β_{42} peptide cytotoxicity

The peptide was dissolved in sterile water at a concentration of 1 g/L (221.5 μ M). A β_{42} aliquots were stored at -20°C until use.

hCMEC/D3 cells were seeded in 96-well plates previously coated with 50 μ L rat tail collagen type I (0,1 mg/mL, for 1 h at 37°C) at a density of 25,000 cells/cm² (100 μ L of a 80,000 cells/mL cell suspension: 8,000 cells/well) and exposed after reaching confluence (three days after seeding) to A β_{42} at 25.0 μ M. A β_{42} (0 - 25.0 μ M) cytotoxicity was evaluated 24 h after exposure by the previously described MTT reduction assay. At least three independent experiments were performed in duplicate. To confirm P-gp involvement in A β_{42} cytotoxicity (25.0 μ M), this procedure was repeated in the presence of a P-gp inhibitor. Therefore, a well-known and potent third-generation P-gp inhibitor, Zos (5.0 μ M) was used and its effect on A β_{42} -mediated cytotoxicity was also evaluated by the MTT reduction assay, performed as previously described. At least three independent experiments were performed in duplicate.

3.3.6. Evaluation of xanthenes' neuroprotective effects against amyloid- β_{42} peptide cytotoxicity

The neuroprotective efficiency of the new synthesized xanthenes was evaluated in the presence of A β_{42} . hCMEC/D3 cells were seeded in 96-well plates previously coated with 50.0 μ L rat tail collagen type I (0,1 mg/mL, for 1 h at 37°C) at a density of 25,000 cells/cm² (100 μ L of a 80,000 cells/mL cell suspension: 8,000 cells/well) and exposed after reaching confluence (three days after seeding) to A β_{42} (25.0 μ M) in the presence or absence of the studied xanthenes (20.0 μ M). At least four independent experiments were performed in duplicate. To confirm P-gp contribution in the xanthenes (20.0 μ M) protective effects, this

procedure was repeated in the presence of Zos (5.0 μM) and A β_{42} peptide (25.0 μM). At least two independent experiments were performed in duplicate.

3.3.7. Statistical analysis

GraphPad Prism 7 for Windows (GraphPad Software, San Diego, CA, USA) was used to perform all statistical calculations. Three tests were performed to evaluate the normality of the data distribution: Kolmogorov-Smirnov, D'Agostino & Pearson omnibus, and Shapiro-Wilk normality tests. For data with parametric distribution, One-way ANOVA was used for statistical comparisons, followed by the Dunnett's multiple comparisons test, the Tukey's multiple comparisons test or by the Holm-Sidak's multiple comparisons test. For data with only two groups (e.g. Rho 123 cytotoxicity), the statistical comparisons were made using the unpaired *t* test. In all cases, *p* values lower than 0,05 were considered significant.

4. Results and Discussion

4.1. Synthetic xanthenes are relatively harmless to hCMEC/D3 cells

Xanthenes cytotoxicity was evaluated by the NR uptake and MTT reduction assays, 24 h after exposure, to select a non-cytotoxic working concentration to be used in the subsequent studies. As shown in **Figure 10**, xanthenes **X8**, **X9** and **X17** caused a significant decrease in cells viability, as measured by the NR uptake assay, at the highest tested concentration of 50.0 μM [the NR uptake significantly reduced to 86, 89 and 81 %, respectively, when compared to control cells (0 μM , 100%)]. For the other tested compounds, no significant cytotoxicity was detected for any of the tested concentrations (0 - 50.0 μM) and up to 24 h of exposure.

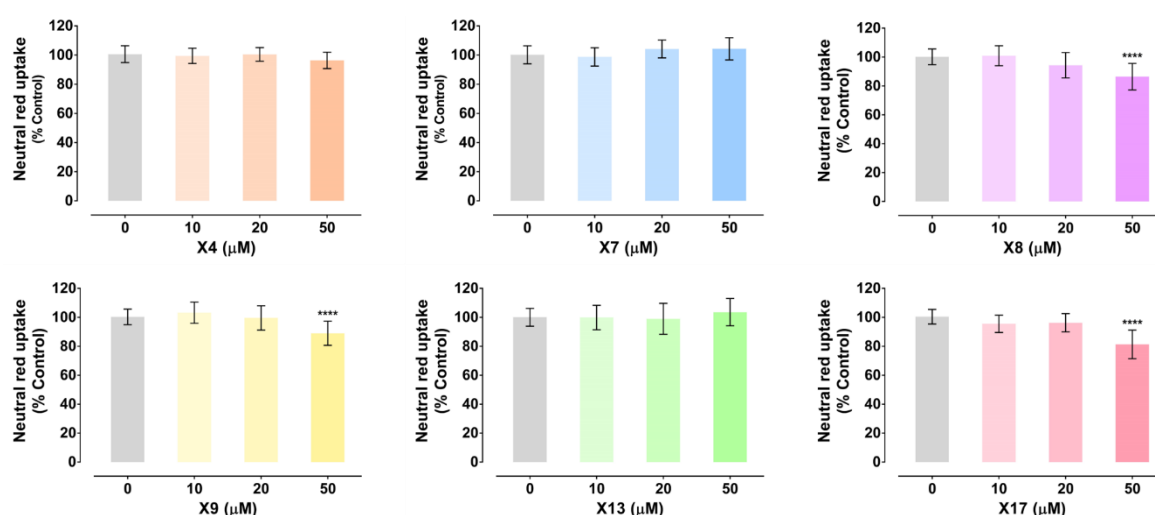


Figure 10. Xanthenes X4, X7, X8, X9, X13 and X17 (0 - 50.0 μM) cytotoxicity in hCMEC/D3 cells evaluated by the neutral red (NR) uptake assay, 24 h after exposure. Results are presented as mean \pm SD from at least 3 independent experiments (performed in triplicate). Statistical comparisons were made using the parametric method of one-way ANOVA, followed by Dunnett's multiple comparisons test; [**** $p < 0.0001$ vs. Control (0 μM , 100%)].

In what concerns to the MTT reduction assay, and as shown in **Figure 11**, xanthenes **X4**, **X7** and **X17** caused a significant decrease in mitochondrial function at the highest tested concentration of 50.0 μM [the MTT reduction significantly decreased to 92, 96 and 81 %, respectively, when compared to control cells (0 μM , 100%)]. At the 20.0 μM concentration, a small but significant decrease in mitochondrial function was also detected for the xanthenes **X4** and **X7**, to 94 and 96 % when compared to control cells (0 μM , 100%), respectively. For the xanthenes **X8**, **X9** and **X13**, no significant cytotoxicity was detected for any of the tested concentrations (0 - 50.0 μM) and up to 24 h of exposure.

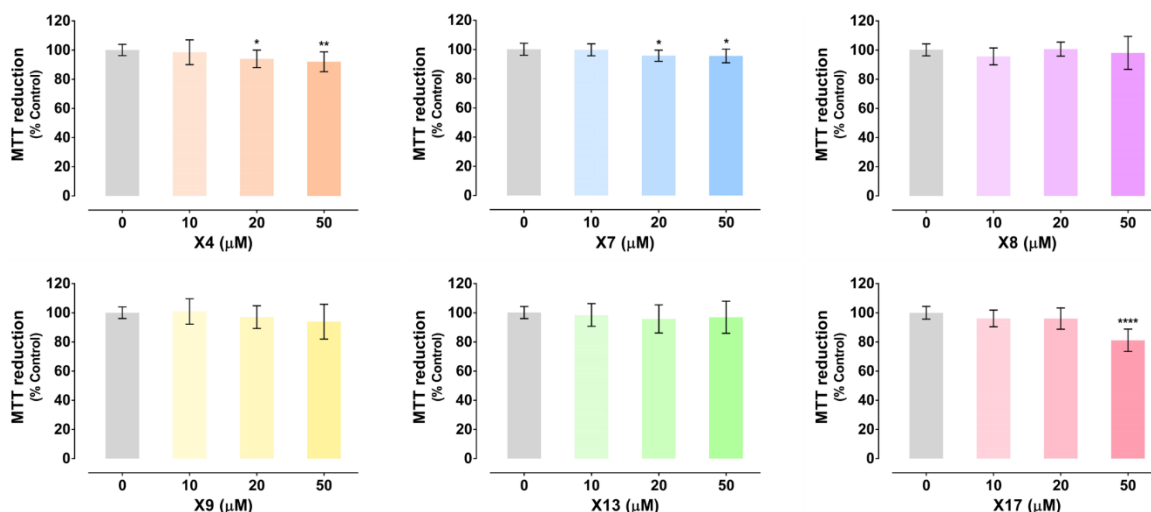


Figure 11. Xanthenes X4, X7, X8, X9, X13 and X17 (0 - 50.0 μM) cytotoxicity in hCMEC/D3 cells evaluated by the MTT uptake assay, 24 h after exposure. Results are presented as mean \pm SD from at least 3 independent experiments (performed in triplicate). Statistical comparisons were made using the parametric method of One-way ANOVA, followed by the Dunnett's multiple comparisons test; [* $p < 0.5$; ** $p < 0.01$; **** $p < 0.0001$ vs. Control (0 μM , 100%)].

Differences in sensibility between methods could explain the slightly different results obtained from the NR and MTT assays.

Previous studies have reported significant increases in both P-gp expression and activity for similar xanthonic derivatives, at a 20.0 μM non-cytotoxic concentration (60-62). Thus, according to the obtained results, the concentration of 20.0 μM was selected for the subsequent P-gp modulation experiments.

4.2. Synthetic xanthenes at non-cytotoxic concentrations significantly increased P-glycoprotein expression

To evaluate the effect of the tested compounds on P-gp expression, hCMEC/D3 cells were exposed for 24 h to the synthetic xanthenes (20.0 μM), and further analyzed by flow cytometry, using a P-gp monoclonal antibody (UIC2) conjugated with PE. As shown in **Figure 12**, the tested xanthenes **X4**, **X7**, **X8**, **X9** and **X17** significantly increased P-gp expression to 293, 242, 410, 305 and 209 %, respectively, as compared with control cells (Control, 100%). Accordingly, **X8** demonstrated to be the most efficient P-gp inducer among the tested compounds. The synthetic xanthone **X13**, at the concentration of 20.0 μM , did not caused a significant alteration in P-gp expression relative to control cells in the adopted experimental conditions (24 h after exposure).

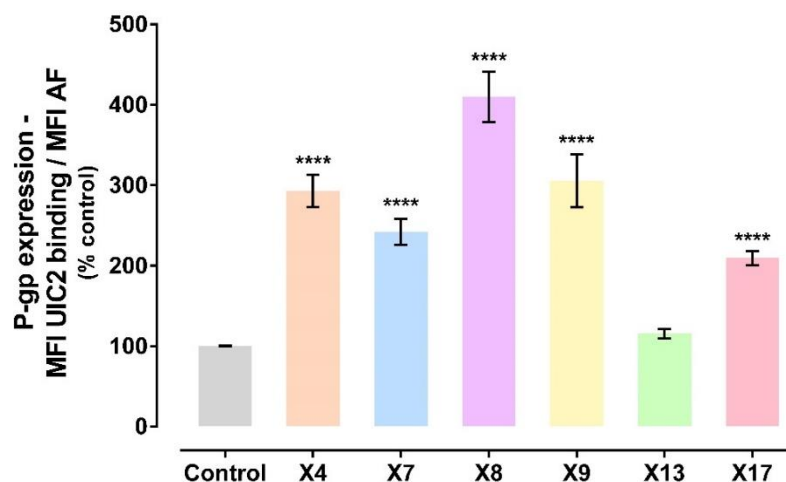


Figure 12. Flow cytometry analysis of P-glycoprotein (P-gp) expression levels in hCMEC/D3 cells exposed to the tested xanthenes (20.0 μ M) for 24 h. Results are presented as mean \pm SD from at least 6 independent experiments (performed in duplicate). Statistical comparisons were made using the parametric method of One-way ANOVA, followed by the Dunnett's multiple comparisons post hoc test. [**** p < 0.0001 vs. Control (0 μ M, 100%)].

Previous studies have demonstrated the ability of other synthetic thioxanthenes and xanthenes, including dihydroxylated xanthonic derivatives, to significantly increase P-gp expression, although in more modest magnitudes (60-62). Silva et al. demonstrated, for the first time, in 2014, a significant increase in P-gp expression in Caco-2 cells following the exposure to five dihydroxylated xanthenes at a non-cytotoxic concentration of 20.0 μ M (X1, X2, X3, X4 and X5) for 24 h, as analyzed by flow cytometry using a P-gp monoclonal antibody (UIC2) conjugated with fluorescein isothiocyanate (FICT). On average, the studied xanthenes significantly increased P-gp expression by approximately 140%, when compared to control cells (100%) (62). Using the same *in vitro* model, Silva et al. also reported a significant increase in P-gp expression, ranging from 120 to 208 % of control cells (100%), for five thioxanthonic derivatives (TX1, TX2, TX3 TX4 and TX5, at 20.0 μ M for 24 h), as measured by flow cytometry, and further confirmed by western blot analysis for the most potent P-gp inducer (TX5) (61). Recently, Lopes et al. evaluated the influence of eight chiral aminated thioxanthenes (at a non-cytotoxic concentration of 20.0 μ M and also after 24 h of exposure) on P-gp expression in Caco-2 cells, by flow cytometry (using a P-gp monoclonal antibody (UIC2) conjugated with PE). It was demonstrated an increase of 36% in P-gp expression for one thioxanthonic derivative (ATX2), as compared with control cells (60). Altogether, these results reveal the potential of xanthonic and thioxanthonic derivatives to positively modulate P-gp expression. However, since the expression values found for the xanthonic derivatives used in this dissertation showed

exacerbated magnitudes, these should be further confirmed using other analytical techniques, such as western blot and immunocytochemistry.

4.3. Synthetic xanthenes at non-cytotoxic concentrations significantly increased P-glycoprotein transport activity

Based on previous studies (59, 61, 62), two different approaches were used to measure P-gp transport activity, by using the well-known P-gp fluorescent substrate, Rho 123 and a third generation P-gp inhibitor, Zos. To select a non-cytotoxic concentration of Rho 123 and Zos to be used in the P-gp activity assays, hCMEC/D3 cells were exposed to Rho 123 and Zos for 24 h and compounds' cytotoxicity was then evaluated by the NR uptake and the MTT reduction assays. As demonstrated in **Figure 13**, 24 h of exposure to 5.0 μM Rho 123 did not show significant cytotoxicity to hCMEC/D3 cells, relative to control cells (0 μM , 100%), as measured by both the NR uptake and MTT reduction assays.

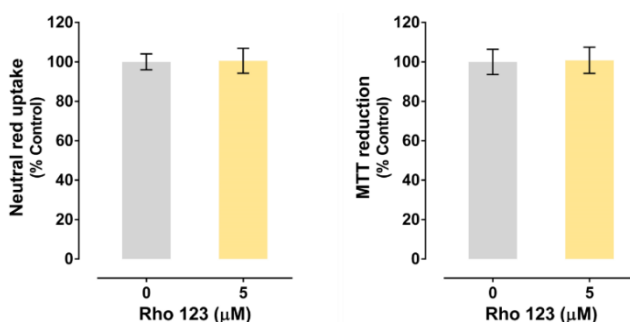


Figure 13. Rhodamine 123 (Rho 123, 0 - 5.0 μM) cytotoxicity in hCMEC/D3 cells evaluated by the Neutral Red and MTT uptake assays, 24 h after exposure. Results are presented as mean \pm SD from at least 3 independent experiments (performed in triplicate). Statistical comparisons were made using the unpaired *t* test.

In what concerns to Zos, and as measured either by the NR uptake or by the MTT reduction assays, 24 h of exposure to the 10.0 μM concentration of Zos significantly reduced cell viability by 39 (NR assay) and 6% (MTT assay), when compared to control cells (0 μM , 100%) (**Figure 14**). Nevertheless, 5.0 μM Zos did not cause significant toxicity to hCMEC/D3 cells, as compared to control cells (0 μM , 100%), an effect observed in both assays.

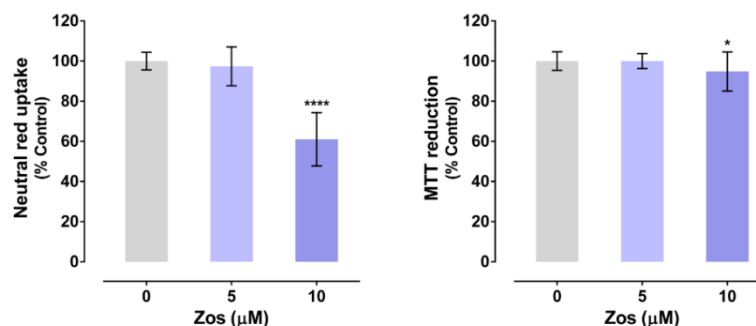


Figure 14. Zosuquidar (Zos, 0 - 10.0 µM) cytotoxicity in hCMEC/D3 cells evaluated by the Neutral Red and MTT uptake assays, 24 h after exposure. Results are presented as mean ± SD from at least 4 independent experiments (performed in triplicate). Statistical comparisons were made using the parametric method of One-way ANOVA, followed by Dunnett's multiple comparisons test [*p < 0.5; ****p < 0.0001 vs. Control (0 µM, 100%)].

Based on these results (**Figure 13** and **Figure 14**), P-gp transport activity assays were performed with Rho 123 and Zos at the concentration of 5.0 µM, which is in line with other studies reported in the literature (127, 136, 137).

4.3.1. P-gp transport activity in cells pre-exposed to the tested xanthenes

In the first approach for P-gp transport activity evaluation, Rho 123 (5.0 µM) accumulation was assessed in hCMEC/D3 cells previously exposed to the tested xanthenes (20.0 µM) for 24 h. This approach allows to detect variations in P-gp transport activity due to alterations on P-gp protein expression. Furthermore, this approach has an important impact in the evaluation of the modulatory potential of new compounds since some reports suggest that alterations in P-gp expression do not linearly translate into similar changes in P-gp transport activity (56, 60, 138, 139), which could be due to an insufficient time to guarantee complete protein function or incomplete membrane targeting. In fact, Silva et. al observed in Caco-2 cells that the strong increases in P-gp expression levels after the exposure to Dox (with increases reaching 646% after 24 h of incubation with 100.0 µM Dox) were not translated in proportional increases in P-gp transport activity (150% increase after a 24 h incubation period with 100.0 µM Dox) (56). In accordance, Wongwanakul et al. found that Caco-2 cells treated with 3.0 µM Dox for 1 and 7 days, significantly increased P-g expression up to 2.15-fold and 3.76-fold over control cells, respectively. However, P-gp activity did not accompanied these increases in protein expression, revealing no significant alterations at any of the tested Dox concentrations (1.0, 3.0 and 10.0 µM) and up to 7 days of incubation (140). Vilas-Boas et al. found that the age-dependent increase in P-gp expression observed in human lymphocytes isolated from whole blood samples was not accompanied by a correspondent increase in protein transport activity, reinforcing the need to assess both P-

gp expression and activity (139). Additionally, Silva et. al, using Caco-2 cells as an *in vitro* model, further demonstrated a concentration-dependent increase in P-gp expression induced by colchicine, a known P-gp substrate and inducer (129, 135, 145, 150, 154 and 183 % increase after 24 h of exposure to 0.5, 1.0, 5.0, 10.0, 50.0 and 100.0 μ M colchicine, correspondingly) with no significant changes in the protein transport activity. These results suggest that P-gp incorporation at the cell membrane does not guarantee protein function (138). Furthermore, knowing that the success of adopting P-gp induction as a potential therapeutic approach, both in intoxications by toxic xenobiotics that are P-gp substrates and in the reduction of the accumulation of toxic endogenous compounds, such as the A β peptide, is remarkably dependent on the activity of the newly synthesized protein, the evaluation of P-gp transport activity is of utmost importance.

Therefore, and based on the previously mentioned studies, hCMEC/D3 cells were exposed to the synthetic xanthenes for 24 h and immediately processed for P-gp transport activity. Alternatively, after 24 h of exposure to the synthetic xanthenes, the cell culture medium was replaced by new medium without the tested compounds, and the cells processed for P-gp transport activity 24 or 72 h later (48 h or 96 h after starting the exposure the tested compounds). This strategy allows to evaluate if more time is needed for the protein incorporation in the cell membrane and/or to ensure its complete protein function.

As shown in **Figure 15**, hCMEC/D3 cells pre-exposed to the xanthenes **X7**, **X9** and **X13** for 24 h, and further analyzed, show small but significant increases in P-gp transport activity to 109, 108 and 107 %, respectively, as compared to control cells (Control, 100%). For the other tested compounds, no significant changes in P-gp transport activity were detected. For xanthenes **X7** and **X9** the increases in P-gp transport activity may be related to the increased P-gp expression (**Figure 12**). However, as formerly reported, these increases in P-gp activity were not proportional to the remarkable increases observed in P-gp expression 24 h after exposure. Furthermore, although xanthone **X8** demonstrated to be the most promisor P-gp inducer (**Figure 12**) it did not translate into any significant alteration in P-gp transport activity. On the other hand, although xanthone **X13** did not cause significant alterations in P-gp expression, it induced a slight but significant increase in the protein activity, suggesting no direct correlation between P-gp expression and transport activity, as reported in other studies (56, 60, 138, 139).

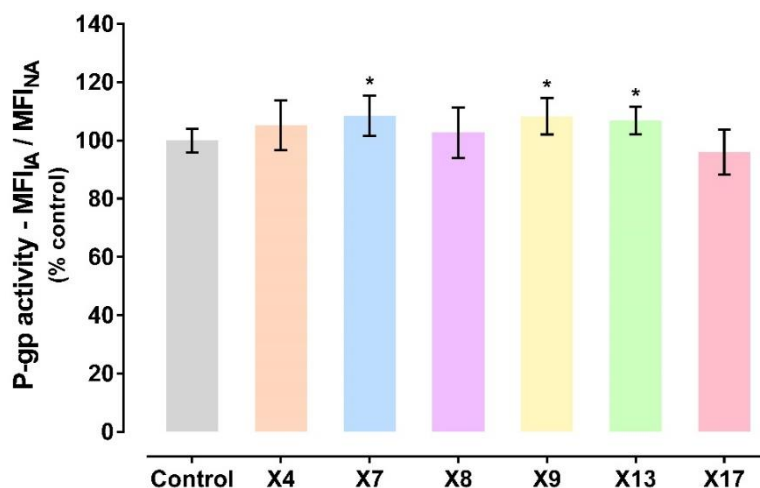


Figure 15. P-glycoprotein (P-gp) transport activity in hCMEC/D3 cells previously exposed to the tested xanthenes (X, 20.0 μ M) for 24 h and to Rhodamine 123 (Rho 123, 5.0 μ M) for 90 minutes. P-gp activity was immediately measured after the 24 h of the xanthenes exposure. Results are presented as mean \pm SD from at least 3 independent experiments (performed in triplicate). Statistical comparisons were made using the parametric method of One-way ANOVA, followed by Dunnett's multiple comparisons test; [*p < 0.5 vs. Control (0 μ M, 100%)].

In hCMEC/D3 cells exposed to the synthetic xanthenes (20.0 μ M) for 24 h and let to recover for another period of 24 h, in fresh cell culture medium without the tested compounds, only the xanthenes **X7** and **X9** significantly increased P-gp transport activity to 110 and 109 %, respectively, when compared to control cells (Control, 100%) (**Figure 16**). Interestingly, the observed increases in P-gp transport activity were similar to the observed for these xanthone derivatives immediately after the 24 h exposure period to the compounds (**Figure 15**). For the xanthenes **X4**, **X8**, **X13** and **X17** this exposure paradigm did not cause significant alterations on P-gp transport activity.

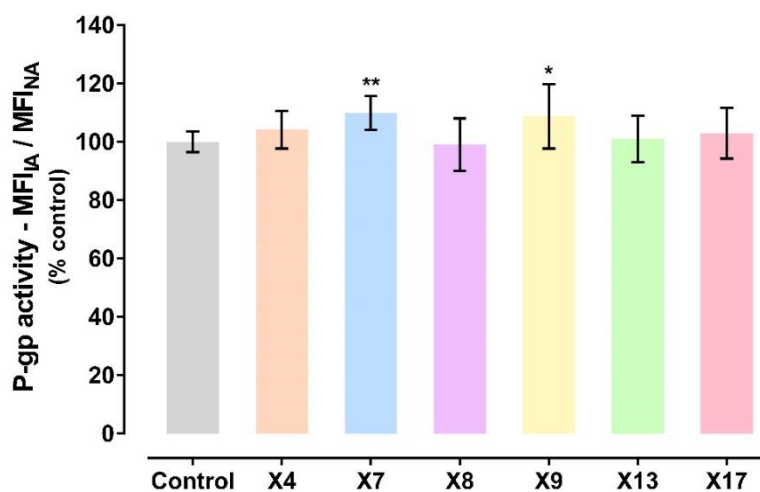


Figure 16. P-glycoprotein (P-gp) transport activity in hCMEC/D3 cells previously exposed to the tested xanthenes (X, 20.0 μ M) for 24 h and to Rhodamine 123 (Rho 123, 5.0 μ M) for 90 minutes. P-gp activity was measured 48 h after the 24 h exposure period to the tested xanthenes. Results are presented as mean \pm SD from at least 3 independent experiments (performed in triplicate). Statistical comparisons were made using the parametric method of One-way ANOVA, followed by Dunnett's multiple comparisons test; [*p < 0.5; **p < 0,01 vs. Control (0 μ M, 100%)].

Lastly, in hCMEC/D3 cells exposed to the xanthenes (20.0 μM) for 24 h and let to recover for a period of 72 h, in fresh cell culture medium without the tested compounds, none of the tested xanthone derivatives caused significant effects on P-gp transport activity, as compared to control cells (Control, 100%) (**Figure 17**).

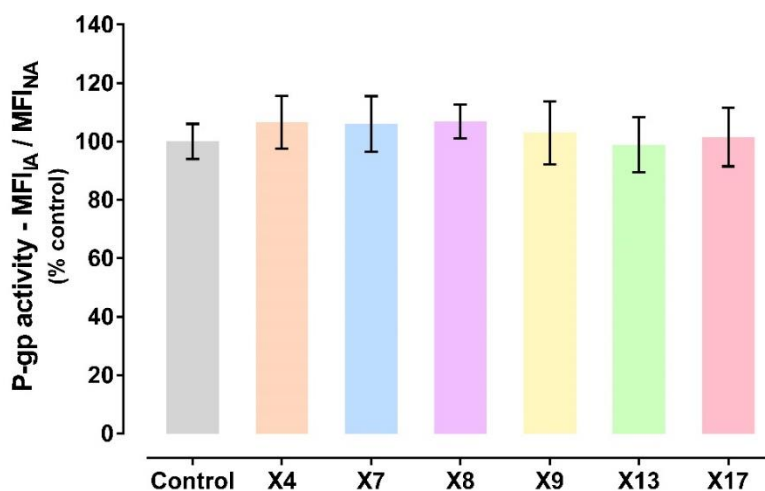


Figure 17. P-glycoprotein (P-gp) transport activity in hCMEC/D3 cells previously exposed to the tested xanthenes (X, 20.0 μM) for 24 h and to Rhodamine 123 (Rho 123, 5.0 μM) for 90 minutes. P-gp activity was measured 96 h after the 24 h exposure period to the tested xanthenes. Results are presented as mean \pm SD from at least 3 independent experiments (performed in triplicate). Statistical comparisons were made using the parametric method of One-way ANOVA, followed by Dunnett's multiple comparisons test.

Additionally, the significant increases in P-gp expression observed in cells pre-exposed to the xanthenes **X4**, **X8** and **X17** were not correlated with alteration in P-gp transport activity, since no significant increases in Rho 123 efflux were observed. The results demonstrate that, although the *de novo* synthesized P-gp is already incorporated into the plasma membrane (since it is recognized by the UIC2 antibody, which targets an external epitope of human P-gp), it may not be fully functional. Furthermore, it may be also speculated that, since the conformational epitope recognized by the UIC2 antibody corresponds to a transient conformational state present during the catalytic cycle for substrate transport (141), the observed increases in P-gp expression may be related to an increased UIC2 reactivity. However, as the incubation with the UIC2 antibody occurs always in the absence of the tested compounds, since the media is removed, and the cells are washed twice prior to the trypsinization, the increases in fluorescence intensity should only reflect an increased cell surface P-gp expression. Moreover, studies performed in Caco-2 cells, 24 h after exposure to the xanthonic derivatives under study demonstrated a significant increase in P-gp expression (as evaluated by flow cytometry using the same antibody), which were accompanied by proportional increases in the pump transport activity, also 24 h after exposure (unpublished results).

4.3.2. P-gp transport activity in the presence of the tested xanthenes

In the second approach for P-gp transport activity evaluation, Rho 123 (5.0 μM) accumulation was assessed in the presence of the tested xanthenes (20.0 μM) during the accumulation phase of the fluorescence substrate, which occurred for 90 minutes. This approach allows to detect the xanthenes' immediate effects on the pump transport activity, as a consequence of a P-gp direct activation. As shown in **Figure 18**, xanthenes **X7**, **X9**, **X13** and **X17** significantly increased P-gp activity to 121, 120, 121 and 113 % of control cells (Control, 100%), respectively. This indicates that these xanthenes, even though in a modest way, have the capacity to directly activate P-gp, thereby behaving as P-gp activators.

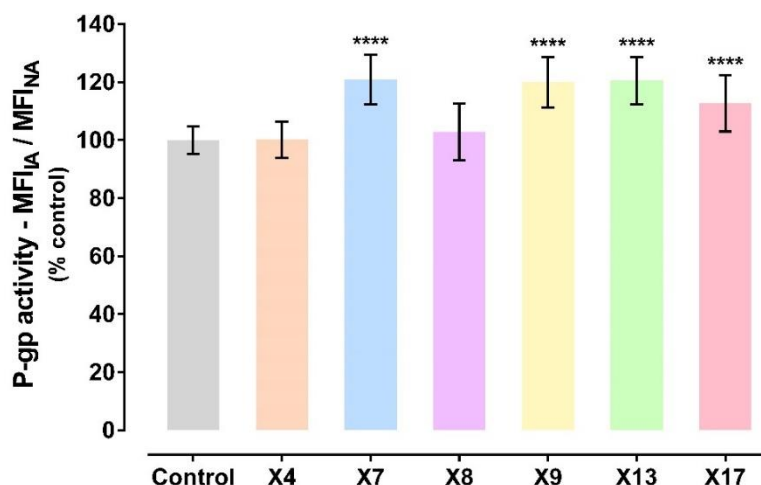


Figure 18. P-glycoprotein (P-gp) activity levels in hCMEC/D3 cells simultaneously exposed to the tested xanthenes (X, 20.0 μM) and Rhodamine 123 (Rho 123, 5.0 μM) for 90 minutes. Results are presented as mean \pm SD from at least 5 independent experiments (performed in triplicate). Statistical comparisons were made using the parametric method of One-way ANOVA, followed by the Dunnett's multiple comparisons post hoc test. [**** $p < 0.0001$ vs. Control (0 μM , 100%)].

Despite being a relatively new concept, growing evidences have indicated P-gp direct activation by (thio)xanthonic derivatives (60-62). In fact, a rapid activation of P-gp has been reported for five dihydroxylated xanthenes and five thioxanthonic derivatives (61, 62). In these studies, Rho 123 (1.0 μM) efflux in the presence of the tested (thio)xanthonic derivatives (20.0 μM) was measured in Caco-2 cells, by flow cytometry, revealing increases ranging from 112 to 124 % for dihydroxylated xanthenes, and from 125 to 198 % for thioxanthonic derivatives, when compared to control cells (100%) (61, 62). Accordingly, Lopes et al. demonstrated that eight chiral thioxanthenes (20.0 μM) significantly increased P-gp activity between 114 and 132 %, when compared to control cells (100%) (60). Since Rho 123 accumulation measurements were performed with the tested compounds present only during the Rho 123 accumulation phase (45 minutes for the dihydroxylated xanthenes and thioxanthenes, and 60 minutes to the chiral

thioxanthenes), the increase in P-gp activity was not related to an increased protein expression, given the short incubation period (60-62).

Furthermore, although this concept of P-gp modulation is relatively new and few studies have focused on P-gp activation (**Table 4**), it is known for a long time that there are compounds that bind to P-gp and stimulate the transport of a substrate bound on another binding site (142). Indeed, Shapiro and Ling proposed that, regarding drug binding and transport, P-gp contains at least two positively cooperative sites, the H site and the R site, where Hoechst-33342 and Rho 123, both P-gp substrates, bound, respectively. Therefore, the binding of a drug at the R site stimulates the transport of Hoechst 33342 at the H site and the binding of a drug at the H site stimulates the transport of Rho 123 at the R site (142). Later, Stertz et al. investigated the P-gp modulating properties of 27 different imidazobenzothiazoles and imidazobenzimidazoles demonstrating that most of the tested compounds stimulated P-gp-mediated daunorubicin and Rho 123 efflux in a concentration-dependent manner, though some of the compounds also displayed weak inhibitory effects (58). In these study, it was proposed that these compounds bind to the P-gp H site and activate the efflux of specific substrates of the R site in a positive cooperative manner, whereas binding of H-type substrates is competitively inhibited. The proposed hypothesis was further confirmed by the observation that these modulators do not influence the hydrolysis of ATP or its affinity towards P-gp (58).

Considering that xanthenes **X7**, **X9** and **X13** acted as P-gp activators (**Figure 18**), it could be speculated that the significant increases in P-gp transport activity observed in hCMEC/D3 cells pre-exposed to these compounds (**Figure 15**, **Figure 16** and **Figure 17**) might result from a residual amount of compound that may remained inside the cells after the incubation period (24 h) and the subsequent washing procedures, which, in turn, could be causing a direct activation of the pump.

Altogether, these results seem to indicate that the observed increases in P-gp transport activity induced by some of the tested xanthenes may be due to the direct pump activation caused by the compounds that remained intracellularly (since they disappeared in the longer 72 h incubation that occurred after the 24 h of exposure to the tested compounds), and that the 72 h recovery period may not be sufficient for the newly synthesized protein to be fully functional, or the induction effect of the tested compounds may lead to the *de novo* synthesis of a nonfunctional protein. Therefore, the obtained data further reinforce the need to fully understand the mechanisms underlying P-gp induction, as well as the importance of determining both P-gp expression and activity in the evaluation of P-gp modulatory potential of new compounds. Furthermore, in the future, the effect of the tested xanthenes on P-gp expression will be also evaluated in cells exposed

for 24 h and allowed to recover in fresh cell culture medium for 72 h in order to access if P-gp protein expression levels remain remarkably high or return to basal levels.

P-gp activation is, thus, defined as the phenomenon in which an immediate increase in P-gp activity occurs without changing its protein expression, leading to the recent recognition of a new class of compounds that interact with P-gp and that are known as P-gp activators (18). Therefore, this phenomenon of P-gp direct activation has potential for clinical practice, since it allows to quickly reduce the intracellular accumulation of potentially harmful P-gp substrates.

4.4. The pathological hallmark of Alzheimer's disease, amyloid- β_{42} peptide, was toxic to hCMEC/D3 cells

As previously stated, brain deposition of A β , namely A β_{42} , is considered a pathological hallmark for AD, thereby representing the most targeted biomarker in drug development. Thus, to ascertain the cytotoxic effect of A β_{42} peptide, hCMEC/D3 cells were exposed to human purified A β_{42} peptide (25.0 μ M) and the peptide cytotoxicity assessed by the MTT reduction assay, after 24 h of exposure. As shown in **Figure 19**, A β_{42} peptide caused a significant decrease in cell mitochondrial function in about 30%, when compared to control cells (0 μ M, 100%), revealing the A β_{42} 's ability to cause brain toxicity. No significant decrease in the MTT reduction was observed for the A β_{42} peptide vehicle, 24 h after exposure (**Figure S1**). In accordance, Oliveira et al. reported, in SH-SY5Y cells, that the exposure to A β_{42} peptide (25.0 μ M for 48 h) resulted in a 28% decrease in cell viability, as compared to control cells (143). Additionally, Marín-Argany et al. also found a decrease in mitochondrial activity, as measure by the MTT reduction assay, in SH-SY5Y cells exposed to A β_{42} peptide for 24 h, with the highest 20.0 μ M concentration reaching around 55% of reduction in mitochondrial function, when compared to control cells (144). Moreover, Zhu et al. demonstrated, in cultured primary rat basal forebrain cholinergic neurons, a concentration-dependent increase in A β_{42} cytotoxicity (about 60, 48, 30 and 20% decrease in cell viability after 72 h of exposure to 1.0, 2.0, 5.0 and 10.0 μ M A β_{42} , respectively, as compared to control) (145). These results reinforce the A β_{42} ability to induce neurotoxicity.

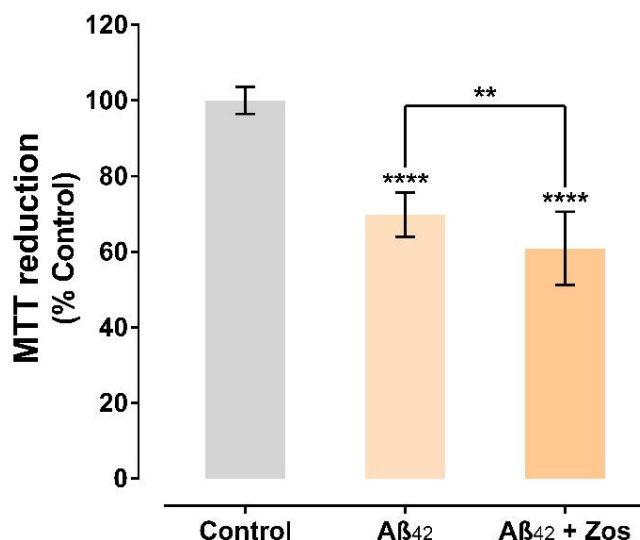


Figure 19. Amyloid- β peptide 42 ($A\beta_{42}$, 0 - 25.0 μ M) cytotoxicity and P-glycoprotein (P-gp) contribution in the $A\beta_{42}$ toxicity [$A\beta_{42}$ (25.0 μ M) + Zos (5.0 μ M)] in hCMEC/D3 cells evaluated by the MTT uptake assay, 24 h after exposure. Results are presented as mean \pm SD from at least 3 independent experiments (performed in duplicate). Statistical comparisons were made using the parametric method of One-way ANOVA, followed by Tukey's multiple comparisons test [$**p < 0.01$; $****p < 0.0001$ vs. Control (0 μ M, 100%)].

Further, to evaluate P-gp potential contribution to $A\beta_{42}$ peptide-induced cytotoxicity, the formerly mentioned assay was repeated in the presence of Zos (5.0 μ M), a third generation P-gp inhibitor. Since Zos blocks P-gp efflux (137, 146) and $A\beta_{42}$ is a P-gp substrate (111, 112, 114, 119), it is expected that the simultaneous exposure to $A\beta_{42}$ and Zos, significantly decreases cell viability. As seen in **Figure 19**, the simultaneous incubation of $A\beta_{42}$ peptide and Zos significantly reduced cell mitochondrial activity by 39% (when compared to 30% reduction for $A\beta_{42}$ alone), when compared to control cells (Control, 100%), as measured by the MTT reduction assay. This demonstrates a role for P-gp in $A\beta_{42}$ efflux, and, consequently on its toxicity.

4.5. Synthetic xanthenes protected hCMEC/D3 cells against the toxicity caused by amyloid- β_{42} peptide

P-gp modulation, either by increasing its expression or its activity, is a mechanism suggested to revert/prevent intoxications caused by xenobiotics that are P-gp substrates (61, 62, 147). Zerín et al. demonstrated, in alveolar A549 cells, a significant amelioration of PQ-induced cytotoxicity by methylprednisolone in a time- (12 - 72 h) and concentration- (100 - 800 μ g/mL) dependent manner (at 72 h, the viability of cells treated with 800 μ g/mL methylprednisolone and 300.0 μ M of PQ improved to 45.1 ± 3.1 %, when compared to 12.1 ± 1.3 % cell viability observed in cells not treated with methylprednisolone and only with the herbicide), being this effect associated with P-gp induction [6 h after 200 μ g/mL

exposure to methylprednisolone, P-gp mRNA levels increased to approximately 200% when compared to control cells (100%)] (147). Additionally, recent *in vitro* studies further reported a significant protection for dihydroxylated xanthenes (20.0 μM) and thioxanthonic derivatives (20.0 μM) against the cytotoxicity induced by PQ, 24 h after exposure, in Caco-2 cells, as traduced by a significant increase in the EC_{50} values of the PQ cell death curves (EC_{50} values in μM : PQ = 1.260; PQ + X1 = 1,620; PQ + X2 = 1.392 PQ + X3 = 1.509; PQ + X4 = 1.520 and PQ + X5 = 1.714 for dihydroxylated xanthenes and PQ = 1.204; PQ + TX1 = 1.262; PQ + TX2 = 1.517; PQ + TX3 = 1.359; PQ + TX4 = 1.378 and PQ + TX5 = 1.749 for thioxanthenes). Supporting a role for P-gp in this protection, simultaneous incubation of dihydroxylated xanthenes (20.0 μM) or thioxanthenes (20.0 μM) with PQ and the P-gp inhibitor, elacridar (Ela, 10.0 μM) for 24 h, prevented the (thio)xanthenes protective effects (EC_{50} values in μM : PQ + Ela = 906.0; PQ + X1 + Ela = 805.9; PQ + X2 + Ela = 726.9; PQ + X3 + Ela = 890.3; PQ + X4 + Ela = 876.7 and PQ + X5 + Ela = 877.5 for dihydroxylated xanthenes and PQ + Ela = 985.1; PQ + TX1 + Ela = 1.124 ; PQ + TX2 + Ela = 968.0; PQ + TX3 + Ela = 1.047; PQ + TX4 + Ela = 1.126 and PQ + TX5 + Ela = 1.279 for thioxanthenes) (61, 62). Further, these results were also demonstrated *in vivo* by Dinis-Oliveira et al., where it was found a relationship between the induction of P-gp induced by dexamethasone and the decreased levels of PQ at the rats lungs, and the corresponding increases in the herbicide faecal excretion, thus reducing its toxicity (detailed study in section 1.1.1.6.2 P-glycoprotein induction mechanism and inducers) (55). These results support a role for P-gp in cell protection against harmful substrates.

Since P-gp is also responsible for the transport of endogenous compounds, including $\text{A}\beta$ peptide, its modulation can be suggested as a strategy to modify AD pathogenesis. As previously reported, this disease is characterized by a P-gp deficit and consequent $\text{A}\beta$ peptide accumulation into the brain. Thus, to verify if the formerly observed increases in P-gp expression and activity caused by the xanthonic derivatives under study could translate in cell protection against $\text{A}\beta_{42}$ -induced toxicity, hCMEC/D3 cells were exposed to $\text{A}\beta_{42}$ peptide (0 - 25.0 μM), in the presence or in the absence of the xanthenes **X7** and **X13** (20.0 μM). Xanthenes **X7** and **X13** were selected for these experiments, since they showed to work as the most promisor P-gp direct activators among the tested compounds, resulting in a 21% increase in protein transport activity, when compared to control cells (**Figure 18**). As shown in **Figure 20**, simultaneous exposure to the xanthone **X7** and $\text{A}\beta_{42}$ peptide significantly protected hCMEC/D3 cells against the cytotoxic effects caused by $\text{A}\beta_{42}$ peptide (from 70% of cell mitochondrial activity in the absence of the xanthone **X7** to 79% in the presence of the xanthone **X7**). In its turn, xanthone **X13** did not

confer significant protection to hCMEC/D3 cells, when simultaneously incubated with A β ₄₂ and in comparison, to cells incubated with A β ₄₂ alone (**Figure 20**).

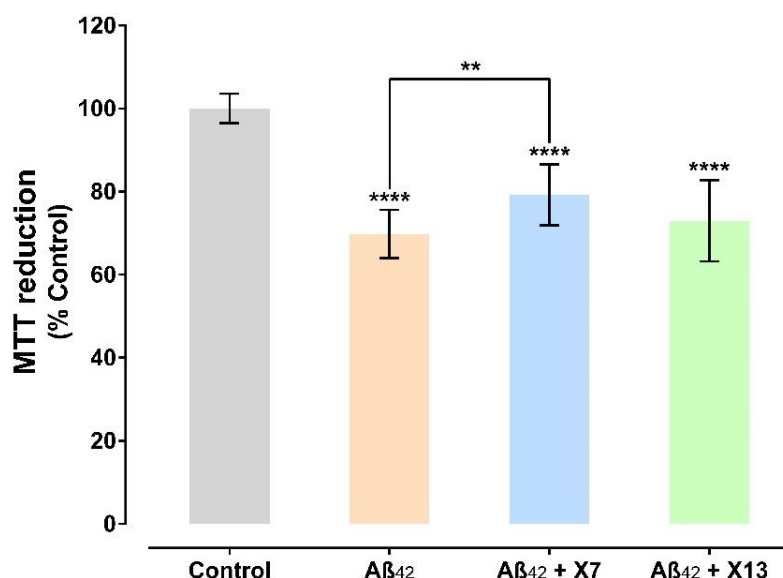


Figure 20. Amyloid- β peptide 42 (A β ₄₂, 0 - 25.0 μ M) cytotoxicity and the xanthenes (X, 20.0 μ M) neuroprotective effects (A β ₄₂ + X) in hCMEC/D3 cells evaluated by the MTT uptake assay, 24 h after exposure. Results are presented as mean \pm SD from at least 4 independent experiments (performed in duplicate). Statistical comparisons were made using the parametric method of One-way ANOVA, followed by Tukey's multiple comparisons test; [** p < 0.01; **** p < 0.0001 vs. Control (0 μ M, 100%)].

To further unequivocally confirm a role for P-gp contribution in the neuroprotective effects described in **Figure 20**, the previously assay was repeated in the presence of Zos (5.0 μ M). As pictured in **Figure 21**, simultaneous exposure to xanthone **X7**, A β ₄₂ peptide and Zos did not confer any significant protection against the toxic effects caused by A β ₄₂ peptide alone. This indicates that the protective effects of the xanthone **X7** against A β ₄₂ toxicity were dependent on P-gp, thereby supporting a role for P-gp in A β ₄₂ peptide clearance from the brain, which is in line with previous reports (111, 112, 114, 119). In accordance with the previous presented results (**Figure 19**), **Figure 21** further reinforced P-gp involvement in A β ₄₂ toxic effects, as A β ₄₂ cytotoxicity significantly decreased when the peptide incubation was performed under Zos-mediated P-gp inhibition.

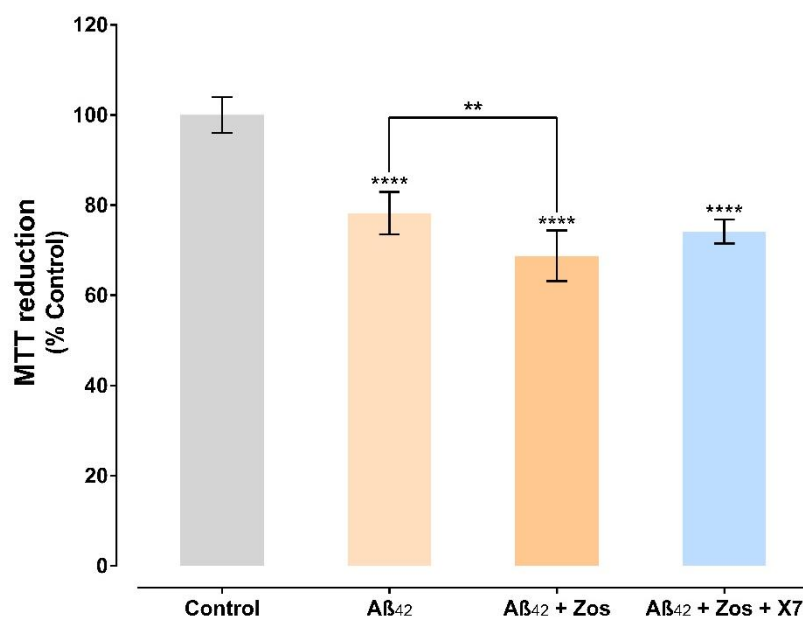


Figure 21. Amyloid- β peptide 42 ($A\beta_{42}$, 0 - 25.0 μ M) cytotoxicity and P-glycoprotein (P-gp) contribution in the neuroprotective effects conferred by xanthone X7 against $A\beta_{42}$ toxicity [$A\beta_{42}$ + Zos + X7 (20.0 μ M)] in hCMEC/D3 cells evaluated by the MTT uptake assay, 24 h after exposure. Results are presented as mean \pm SD from at least 2 independent experiments (performed in duplicate or triplicate). Statistical comparisons were made using the parametric method of One-way ANOVA, followed by Holm-Sidak's multiple comparisons test; [** p < 0.01; **** p < 0.0001 vs. Control (0 μ M, 100%)].

To the best of our knowledge this is the first experimental report that correlates positive P-gp modulation by xanthonic derivatives and their influence on $A\beta_{42}$ cytotoxicity. However, previous studies already used P-gp modulation to increase $A\beta$ efflux (110, 116, 148).

Accordingly, studying the olive oil derived oleocanthal, Abuznait et al. demonstrated, using bEnd3 cells (as a BBB mouse model) and western blot analysis, that oleocanthal treatment significantly increased the expression of P-gp (1.2 - 1.35-fold increase after exposure to 0.50 - 50.0 μ M of oleocanthal for 72 h) and LRP-1 (1.25 - 1.30-fold increase after exposure to 0.50 - 50.0 μ M of oleocanthal for 72 h), which was confirmed by both immunofluorescence studies (2.8-fold increase for P-gp and 2.2-fold increase for LRP-1 when compared to control cells, after exposure to 25.0 μ M of oleocanthal for 72 h) and *in vivo* studies (1.30-fold increase for P-gp and 1.25-fold increase for LRP-1 when compared to control, after C57BL/6 mice IP administration of oleocanthal (10 mg/kg/day) twice a day for 2 weeks). Furthermore, the group analyzed $A\beta_{40}$ clearance 24 h after the last injection, showing an increase of about 18% in oleocanthal-treated mice when compared to control mice. However, this increase in clearance was not totally associated with the two transporters, which possibly suggested the contribution of other mechanisms (148). Furthermore, the same group had already reported that seven known P-gp inducers significantly reduced 125 I- $A\beta_{40}$ intracellular accumulation (approximately 10 - 35 % when

compared to control cells) via P-gp up-regulation (see section 1.2.1.1 P-glycoprotein and Alzheimer's disease) (110). Additionally, Qosa et al. demonstrated that BBB P-gp upregulation induced by rifampicin and caffeine improved A β ₄₀ clearance, and that this effect could partially clarify the protective effects of the two compounds in AD (see section 1.2.1.1 P-glycoprotein and Alzheimer's disease) (116). Thus, positive modulation of P-gp at the BBB could have impact on AD pathogenesis.

5. Conclusions

The results included in this dissertation demonstrate that the synthetic xanthonic derivatives **X4**, **X7**, **X8**, **X9**, **X13** and **X17** did not show significant toxicity towards hCMEC/D3 cells, after 24 h of exposure, for concentrations up to 20.0 μM . The majority of the compounds (xanthenes **X7**, **X9**, **X13** and **X17**) showed the capacity to immediately increase the protein activity, acting as P-gp activators. Additionally, all the synthetic xanthenes tested, except xanthone **X13**, increased P-gp expression in a significant and robust way. However, this increase in protein expression did not translate into similar increases in protein activity, since only xanthenes **X7**, **X9** and **X13** demonstrated to slightly interfere with P-gp transport activity in cells pre-exposed to the tested xanthenes for 24 h. Nevertheless, at the last time point studied (96 h after starting the xanthenes exposure) none of the xanthenes produced significant effects on P-gp transport activity.

$\text{A}\beta_{42}$ peptide exposure reduced the cell mitochondrial activity by 30%. In addition, xanthone **X7** protected hCMEC/D3 cells against $\text{A}\beta_{42}$ -induced cytotoxicity, as traduced by the significant increase in mitochondrial function for cells co-exposed to $\text{A}\beta$ peptide and xanthone **X7** (79%), as compared to cells only exposed to $\text{A}\beta_{42}$ peptide (70%). Additionally, this neuroprotective effect of xanthone **X7** was dependent on P-gp, as co-exposure to $\text{A}\beta$ peptide, xanthone **X7**, and the P-gp inhibitor Zos prevented this protection.

In conclusion, the work included in this dissertation provides insights into the role of P-gp on $\text{A}\beta_{42}$ clearance from the brain. Thus, induction and/or activation of P-gp, by improving $\text{A}\beta$ efflux, thereby reducing its intracellular accumulation and, consequently, its toxicity, could have impact on AD pathogenesis. Furthermore, and given the demonstrated *in vitro* potential of these xanthonic derivatives as P-gp activators, they represent a promising source of new derivatives with P-gp modulation ability that worth to be further explored.

6. Future perspectives

In this dissertation, synthetic xanthenes were shown to significantly increase P-gp expression, as evaluated by flow cytometry. However further western blot and/or immunocytochemistry analysis of P-gp expression in hCMEC/D3 cells exposed to the tested synthetic xanthenes would be useful to further confirm the P-gp expression data obtained by flow cytometry.

In the continuity of this project, measurement of P-gp ATPase activity would be useful to demonstrate whether these xanthonic derivatives are P-gp substrates.

Additionally, *in vivo* translation of the *in vitro* data, showing a role for P-gp induction and/or activation in preventing A β ₄₂ toxicity, would have valuable impact in understanding the P-gp's role in the pathogenesis of AD.

The results included in this dissertation provide direct evidence that xanthonic derivatives have a role in modulating P-gp function by increasing its expression and/or activity. Nevertheless, based on these observations, new xanthonic derivatives can be synthesized and tested, which could reveal new perspectives for AD treatment/prevention, and also for the treatment of poisonings caused by toxic P-gp substrates.

7. References

1. Higgins CF. ABC transporters: from microorganisms to man. *Annu Rev Cell Biol.* 1992;8(1):67-113.
2. Vasiliou V, Vasiliou K, Nebert DW. Human ATP-binding cassette (ABC) transporter family. *Hum Genomics.* 2009;3(3):281-90.
3. Dean M, Hamon Y, Chimini G. The human ATP-binding cassette (ABC) transporter superfamily. *J Lipid Res.* 2001;42(7):1007-17.
4. Beis K. Structural basis for the mechanism of ABC transporters. *Biochem Soc Trans.* 2015;43(5):889-93.
5. Lewinson O, Livnat-Levanon N. Mechanism of action of ABC importers: conservation, divergence, and physiological adaptations. *J Mol Biol.* 2017;429(5):606-19.
6. Sharom FJ. ABC multidrug transporters: structure, function and role in chemoresistance. *Pharmacogenomics.* 2008;9(1):105-27.
7. Chang G. Multidrug resistance ABC transporters. *FEBS Lett.* 2003;555(1):102-5.
8. Higgins CF. ABC transporters: physiology, structure and mechanism--an overview. *Res Microbiol.* 2001;152(3-4):205-10.
9. Gottesman MM, Ambudkar SV. Overview: ABC transporters and human disease. *J Bioenerg Biomembr.* 2001;33(6):453-8.
10. Wilkens S. Structure and mechanism of ABC transporters. *F1000Prime Rep.* 2015;7.
11. Miller DS. ABC transporter regulation by signaling at the blood-brain barrier: relevance to pharmacology. *Adv Pharmacol.* 2014;71:1-24.
12. Borst P, Elferink RO. Mammalian ABC transporters in health and disease. *Annu Rev Biochem.* 2002;71:537-92.
13. DeGorter MK, Xia CQ, Yang JJ, Kim RB. Drug transporters in drug efficacy and toxicity. *Annu Rev Pharmacol Toxicol.* 2012;52:249-73.
14. Juliano RL, Ling V. A surface glycoprotein modulating drug permeability in Chinese hamster ovary cell mutants. *Biochim Biophys Acta.* 1976;455(1):152-62.
15. Hennessy M, Spiers JP. A primer on the mechanics of P-glycoprotein the multidrug transporter. *Pharmacol Res.* 2007;55(1):1-15.
16. Georges E, Bradley G, Garipey J, Ling V. Detection of P-glycoprotein isoforms by gene-specific monoclonal antibodies. *Proc Natl Acad Sci U S A.* 1990;87(1):152-6.
17. Thiebaut F, Tsuruo T, Hamada H, Gottesman MM, Pastan I, Willingham MC. Cellular localization of the multidrug-resistance gene product P-glycoprotein in normal human tissues. *Proc Natl Acad Sci U S A.* 1987;84(21):7735-8.
18. Silva R, Vilas-Boas V, Carmo H, Dinis-Oliveira RJ, Carvalho F, de Lourdes Bastos M, et al. Modulation of P-glycoprotein efflux pump: induction and activation as a therapeutic strategy. *Pharmacol Ther.* 2015;149:1-123.
19. Doring B, Petzinger E. Phase 0 and phase III transport in various organs: combined concept of phases in xenobiotic transport and metabolism. *Drug Metab Rev.* 2014;46(3):261-82.
20. Eckford PD, Sharom FJ. ABC efflux pump-based resistance to chemotherapy drugs. *Chem Rev.* 2009;109(7):2989-3011.
21. Kim RB. Drugs as P-glycoprotein substrates, inhibitors, and inducers. *Drug Metab Rev.* 2002;34(1-2):47-54.

22. Leslie EM, Deeley RG, Cole SP. Multidrug resistance proteins: role of P-glycoprotein, MRP1, MRP2, and BCRP (ABCG2) in tissue defense. *Toxicol Appl Pharmacol.* 2005;204(3):216-37.
23. Zhou SF. Structure, function and regulation of P-glycoprotein and its clinical relevance in drug disposition. *Xenobiotica.* 2008;38(7-8):802-32.
24. Beaulieu E, Demeule M, Ghitescu L, Beliveau R. P-glycoprotein is strongly expressed in the luminal membranes of the endothelium of blood vessels in the brain. *Biochem J.* 1997;326 (Pt 2):539-44.
25. Sharom FJ. The P-glycoprotein multidrug transporter. *Essays Biochem.* 2011;50(1):161-78.
26. Miller DS, Bauer B, Hartz AM. Modulation of P-glycoprotein at the blood-brain barrier: opportunities to improve central nervous system pharmacotherapy. *Pharmacol Rev.* 2008;60(2):196-209.
27. Schinkel AH. P-Glycoprotein, a gatekeeper in the blood-brain barrier. *Adv Drug Deliv Rev.* 1999;36(2-3):179-94.
28. Mahringer A, Fricker G. ABC transporters at the blood-brain barrier. *Expert Opin Drug Metab Toxicol.* 2016;12(5):499-508.
29. Chen CJ, Chin JE, Ueda K, Clark DP, Pastan I, Gottesman MM, et al. Internal duplication and homology with bacterial transport proteins in the *mdr1* (P-glycoprotein) gene from multidrug-resistant human cells. *Cell.* 1986;47(3):381-9.
30. Higgins CF, Callaghan R, Linton KJ, Rosenberg MF, Ford RC. Structure of the multidrug resistance P-glycoprotein. *Semin Cancer Biol.* 1997;8(3):135-42.
31. Kim Y, Chen J. Molecular structure of human P-glycoprotein in the ATP-bound, outward-facing conformation. *Science.* 2018;359(6378):915-9.
32. Sharom FJ, Liu R, Romsicki Y, Lu P. Insights into the structure and substrate interactions of the P-glycoprotein multidrug transporter from spectroscopic studies. *Biochim Biophys Acta.* 1999;1461(2):327-45.
33. Sharom FJ. Complex interplay between the P-glycoprotein multidrug efflux pump and the membrane: its role in modulating protein function. *Front Oncol.* 2014;4:41.
34. Smith PC, Karpowich N, Millen L, Moody JE, Rosen J, Thomas PJ, et al. ATP binding to the motor domain from an ABC transporter drives formation of a nucleotide sandwich dimer. *Mol Cell.* 2002;10(1):139-49.
35. Jones PM, George AM. Subunit interactions in ABC transporters: towards a functional architecture. *FEMS Microbiol Lett.* 1999;179(2):187-202.
36. Siarheyeva A, Liu R, Sharom FJ. Characterization of an asymmetric occluded state of P-glycoprotein with two bound nucleotides: implications for catalysis. *J Biol Chem.* 2010;285(10):7575-86.
37. Verhalen B, Ernst S, Borsch M, Wilkens S. Dynamic ligand-induced conformational rearrangements in P-glycoprotein as probed by fluorescence resonance energy transfer spectroscopy. *J Biol Chem.* 2012;287(2):1112-27.
38. Aller SG, Yu J, Ward A, Weng Y, Chittaboina S, Zhuo R, et al. Structure of P-glycoprotein reveals a molecular basis for poly-specific drug binding. *Science.* 2009;323(5922):1718-22.
39. Gameiro M, Silva R, Rocha-Pereira C, Carmo H, Carvalho F, Bastos ML, et al. Cellular models and in vitro assays for the screening of modulators of P-gp, MRP1 and BCRP. *Molecules.* 2017;22(4).
40. Abbott NJ. Dynamics of CNS barriers: evolution, differentiation, and modulation. *Cell Mol Neurobiol.* 2005;25(1):5-23.

41. Seelig A. A general pattern for substrate recognition by P-glycoprotein. *Eur J Biochem.* 1998;251(1-2):252-61.
42. Seelig A, Landwojtowicz E. Structure-activity relationship of P-glycoprotein substrates and modifiers. *Eur J Pharm Sci.* 2000;12(1):31-40.
43. Cianchetta G, Singleton RW, Zhang M, Wildgoose M, Giesing D, Fravolini A, et al. A pharmacophore hypothesis for P-glycoprotein substrate recognition using GRIND-based 3D-QSAR. *J Med Chem.* 2005;48(8):2927-35.
44. Huang J, Ma G, Muhammad I, Cheng Y. Identifying P-glycoprotein substrates using a support vector machine optimized by a particle swarm. *J Chem Inf Model.* 2007;47(4):1638-47.
45. Bain LJ, McLachlan JB, LeBlanc GA. Structure-activity relationships for xenobiotic transport substrates and inhibitory ligands of P-glycoprotein. *Environ Health Perspect.* 1997;105(8):812-8.
46. Wang RB, Kuo CL, Lien LL, Lien EJ. Structure-activity relationship: analyses of p-glycoprotein substrates and inhibitors. *J Clin Pharm Ther.* 2003;28(3):203-28.
47. Cascorbi I. Role of pharmacogenetics of ATP-binding cassette transporters in the pharmacokinetics of drugs. *Pharmacol Ther.* 2006;112(2):457-73.
48. Cummins CL, Jacobsen W, Benet LZ. Unmasking the dynamic interplay between intestinal P-glycoprotein and CYP3A4. *J Pharmacol Exp Ther.* 2002;300(3):1036-45.
49. Palmeira A, Sousa E, Vasconcelos MH, Pinto MM. Three decades of P-gp inhibitors: skimming through several generations and scaffolds. *Curr Med Chem.* 2012;19(13):1946-2025.
50. Varma MV, Ashokraj Y, Dey CS, Panchagnula R. P-glycoprotein inhibitors and their screening: a perspective from bioavailability enhancement. *Pharmacol Res.* 2003;48(4):347-259.
51. Robert J, Jarry C. Multidrug resistance reversal agents. *J Med Chem.* 2003;46(23):4805-17.
52. Sharom FJ. Multidrug resistance protein: P-glycoprotein. *Drug transporters: Molecular characterization and role in drug disposition* 2007. p. 223-62.
53. Scotto KW. Transcriptional regulation of ABC drug transporters. *Oncogene.* 2003;22(47):7496-511.
54. Harmsen S, Meijerman I, Febus CL, Maas-Bakker RF, Beijnen JH, Schellens JH. PXR-mediated induction of P-glycoprotein by anticancer drugs in a human colon adenocarcinoma-derived cell line. *Cancer Chemother Pharmacol.* 2010;66(4):765-71.
55. Dinis-Oliveira RJ, Remiao F, Duarte JA, Ferreira R, Sanchez Navarro A, Bastos ML, et al. P-glycoprotein induction: an antidotal pathway for paraquat-induced lung toxicity. *Free Radic Biol Med.* 2006;41(8):1213-24.
56. Silva R, Carmo H, Dinis-Oliveira R, Cordeiro-da-Silva A, Lima SC, Carvalho F, et al. In vitro study of P-glycoprotein induction as an antidotal pathway to prevent cytotoxicity in Caco-2 cells. *Arch Toxicol.* 2011;85(4):315-26.
57. Silva R, Carmo H, Vilas-Boas V, de Pinho PG, Dinis-Oliveira RJ, Carvalho F, et al. Doxorubicin decreases paraquat accumulation and toxicity in Caco-2 cells. *Toxicology letters.* 2013;217(1):34-41.
58. Sterz K, Mollmann L, Jacobs A, Baumert D, Wiese M. Activators of P-glycoprotein: Structure-activity relationships and investigation of their mode of action. *ChemMedChem.* 2009;4(11):1897-911.
59. Vilas-Boas V, Silva R, Palmeira A, Sousa E, Ferreira LM, Branco PS, et al. Development of novel rifampicin-derived P-glycoprotein activators/inducers. synthesis, in

- silico analysis and application in the RBE4 cell model, using paraquat as substrate. *PLoS One*. 2013;8(8):e74425.
60. Lopes A, Martins E, Silva R, Pinto MMM, Remiao F, Sousa E, et al. Chiral Thioxanthenes as Modulators of P-glycoprotein: Synthesis and Enantioselectivity Studies. *Molecules*. 2018;23(3).
61. Silva R, Palmeira A, Carmo H, Barbosa DJ, Gameiro M, Gomes A, et al. P-glycoprotein induction in Caco-2 cells by newly synthesized thioxanthenes prevents paraquat cytotoxicity. *Arch Toxicol*. 2015;89(10):1783-800.
62. Silva R, Sousa E, Carmo H, Palmeira A, Barbosa DJ, Gameiro M, et al. Induction and activation of P-glycoprotein by dihydroxylated xanthenes protect against the cytotoxicity of the P-glycoprotein substrate paraquat. *Arch Toxicol*. 2014;88(4):937-51.
63. Kondratov RV, Komarov PG, Becker Y, Ewenson A, Gudkov AV. Small molecules that dramatically alter multidrug resistance phenotype by modulating the substrate specificity of P-glycoprotein. *Proc Natl Acad Sci U S A*. 2001;98(24):14078-83.
64. Wang EJ, Barecki-Roach M, Johnson WW. Elevation of P-glycoprotein function by a catechin in green tea. *Biochem Biophys Res Commun*. 2002;297(2):412-8.
65. Zhou S, Lim LY, Chowbay B. Herbal modulation of P-glycoprotein. *Drug Metab Rev*. 2004;36(1):57-104.
66. Masters KS, Brase S. Xanthenes from fungi, lichens, and bacteria: the natural products and their synthesis. *Chem Rev*. 2012;112(7):3717-76.
67. Jindarat S. Xanthenes from mangosteen (*Garcinia mangostana*): multi-targeting pharmacological properties. *J Med Assoc Thai*. 2014;97 (2):S196-S201.
68. Marona H, Pekala E, Filipek B, Maciag D, Szneler E. Pharmacological properties of some aminoalkanoic derivatives of xanthone. *Pharmazie*. 2001;56(7):567-72.
69. Pinto MM, Sousa ME, Nascimento MS. Xanthone derivatives: new insights in biological activities. *Curr Med Chem*. 2005;12(21):2517-38.
70. Magistretti PJ, Allaman I. A cellular perspective on brain energy metabolism and functional imaging. *Neuron*. 2015;86(4):883-901.
71. Abbott NJ, Patabendige AA, Dolman DE, Yusof SR, Begley DJ. Structure and function of the blood-brain barrier. *Neurobiol Dis*. 2010;37(1):13-25.
72. Campos-Bedolla P, Walter FR, Veszelka S, Deli MA. Role of the blood-brain barrier in the nutrition of the central nervous system. *Arch Med Res*. 2014;45(8):610-38.
73. Abbott NJ, Ronnback L, Hansson E. Astrocyte-endothelial interactions at the blood-brain barrier. *Nat Rev Neurosci*. 2006;7(1):41-53.
74. Clark DE. In silico prediction of blood-brain barrier permeation. *Drug Discov Today*. 2003;8(20):927-33.
75. Demeule M, Regina A, Jodoin J, Laplante A, Dagenais C, Berthelet F, et al. Drug transport to the brain: key roles for the efflux pump P-glycoprotein in the blood-brain barrier. *Vascul Pharmacol*. 2002;38(6):339-48.
76. Wolburg H, Lippoldt A. Tight junctions of the blood-brain barrier: development, composition and regulation. *Vascul Pharmacol*. 2002;38(6):323-37.
77. Dallas S, Miller DS, Bendayan R. Multidrug resistance-associated proteins: expression and function in the central nervous system. *Pharmacol Rev*. 2006;58(2):140-61.
78. Bodor N, Buchwald P. Brain-targeted drug delivery. *Am J Drug Deliv*. 2003;1(1):13-26.

79. Begley DJ, Brightman MW. Structural and functional aspects of the blood-brain barrier. *Prog Drug Res.* 2003;61:39-78.
80. Pardridge WM. The blood-brain barrier: bottleneck in brain drug development. *NeuroRx.* 2005;2(1):3-14.
81. Glezer I, Simard AR, Rivest S. Neuroprotective role of the innate immune system by microglia. *Neuroscience.* 2007;147(4):867-83.
82. Scholz M, Cinatl J, Schadel-Hopfner M, Windolf J. Neutrophils and the blood-brain barrier dysfunction after trauma. *Med Res Rev.* 2007;27(3):401-16.
83. Qosa H, Miller DS, Pasinelli P, Trotti D. Regulation of ABC efflux transporters at blood-brain barrier in health and neurological disorders. *Brain Res.* 2015;1628(Pt B):298-316.
84. Zhao Y, Hou D, Feng X, Lin F, Luo J. Role of ABC transporters in the pathology of Alzheimer's disease. *Rev Neurosci.* 2017;28(2):155-9.
85. Association As. 2017 Alzheimer's disease facts and figures. *Alzheimers Dement.* 2017;13(4):325-73.
86. Selkoe DJ. Alzheimer's disease: genes, proteins, and therapy. *Physiol Rev.* 2001;81(2):741-66.
87. Huynh TV, Davis AA, Ulrich JD, Holtzman DM. Apolipoprotein E and Alzheimer's disease: the influence of apolipoprotein E on amyloid-beta and other amyloidogenic proteins. *J Lipid Res.* 2017;58(5):824-36.
88. Tanzi RE, Bertram L. Twenty years of the Alzheimer's disease amyloid hypothesis: a genetic perspective. *Cell.* 2005;120(4):545-55.
89. Citron M. Alzheimer's disease: strategies for disease modification. *Nat Rev Drug Discov.* 2010;9(5):387-98.
90. Wenk GL. Neuropathologic changes in Alzheimer's disease. *J Clin Psychiatry.* 2003;64(9):7-10.
91. McInerney MP, Short JL, Nicolazzo JA. Neurovascular alterations in Alzheimer's Disease: Transporter expression profiles and CNS drug access. *AAPS J.* 2017;19(4):940-56.
92. Haass C, Selkoe DJ. Cellular processing of β -amyloid precursor protein and the genesis of amyloid β -peptide. *Cell.* 1993;75(6):1039-42.
93. Zou K, Gong JS, Yanagisawa K, Michikawa M. A novel function of monomeric amyloid beta-protein serving as an antioxidant molecule against metal-induced oxidative damage. *J Neurosci.* 2002;22(12):4833-41.
94. Yao ZX, Papadopoulos V. Function of beta-amyloid in cholesterol transport: a lead to neurotoxicity. *FASEB J.* 2002;16(12):1677-9.
95. Soscia SJ, Kirby JE, Washicosky KJ, Tucker SM, Ingelsson M, Hyman B, et al. The Alzheimer's disease-associated amyloid beta-protein is an antimicrobial peptide. *PLoS One.* 2010;5(3):e9505.
96. Walsh DM, Selkoe DJ. A β oligomers—a decade of discovery. *J Neurochem.* 2007;101(5):1172-84.
97. Hardy JA, Higgins GA. Alzheimer's disease: the amyloid cascade hypothesis. *Science.* 1992;256(5054):184-5.
98. Zlokovic BV, Deane R, Sallstrom J, Chow N, Miano JM. Neurovascular pathways and Alzheimer Amyloid β -peptide. *Brain Pathol.* 2005;15(1):78-83.
99. Zlokovic BV. Neurovascular mechanisms of Alzheimer's neurodegeneration. *Trends Neurosci.* 2005;28(4):202-8.

100. Mucke L. Neuroscience: Alzheimer's disease. *Nature*. 2009;461(7266):895-7.
101. Islam MA, Khandker SS, Alam F, Khalil MI, Kamal MA, Gan SH. Alzheimer's Disease and Natural Products: Future Regimens Emerging from Nature. *Curr Top Med Chem*. 2017;17(12):1408-28.
102. Masters CL, Bateman R, Blennow K, Rowe CC, Sperling RA, Cummings JL. Alzheimer's disease. *Nature reviews Disease primers*. 2015;1:15056.
103. Mawuenyega KG, Sigurdson W, Ovod V, Munsell L, Kasten T, Morris JC, et al. Decreased clearance of CNS β -amyloid in Alzheimer's disease. *Science*. 2010;330(6012):1774.
104. Thal DR. The role of astrocytes in amyloid β -protein toxicity and clearance. *Exp Neurol*. 2012;236(1):1-5.
105. Iliff JJ, Wang M, Liao Y, Plogg BA, Peng W, Gundersen GA, et al. A paravascular pathway facilitates CSF flow through the brain parenchyma and the clearance of interstitial solutes, including amyloid β . *Sci Transl Med*. 2012;4(147).
106. Pahnke J, Langer O, Krohn M. Alzheimer's and ABC transporters--new opportunities for diagnostics and treatment. *Neurobiol Dis*. 2014;72:54-60.
107. Shibata M, Yamada S, Kumar SR, Calero M, Bading J, Frangione B, et al. Clearance of Alzheimer's amyloid- β 1-40 peptide from brain by LDL receptor-related protein-1 at the blood-brain barrier. *J Clin Invest*. 2000;106(12):1489-99.
108. Deane R, Bell RD, Sagare A, Zlokovic BV. Clearance of amyloid-beta peptide across the blood-brain barrier: implication for therapies in Alzheimer's disease. *CNS Neurol Disord Drug Targets*. 2009;8(1):16-30.
109. Deane R, Du Yan S, Subramanian RK, LaRue B, Jovanovic S, Hogg E, et al. RAGE mediates amyloid- β peptide transport across the blood-brain barrier and accumulation in brain. *Nat Med*. 2003;9(7):907-13.
110. Abuznait AH, Cain C, Ingram D, Burk D, Kaddoumi A. Up-regulation of P-glycoprotein reduces intracellular accumulation of beta amyloid: investigation of P-glycoprotein as a novel therapeutic target for Alzheimer's disease. *J Pharm Pharmacol*. 2011;63(8):1111-8.
111. Bruckmann S, Brenn A, Grube M, Niedrig K, Holtfreter S, Und Halbach OVB, et al. Lack of P-glycoprotein results in impairment of removal of Beta-Amyloid and Increased intraparenchymal cerebral amyloid angiopathy after active Immunization in a transgenic mouse model of Alzheimer's disease. *Curr Alzheimer Res*. 2017;14(6):656-67.
112. Cirrito JR, Deane R, Fagan AM, Spinner ML, Parsadanian M, Finn MB, et al. P-glycoprotein deficiency at the blood-brain barrier increases amyloid- β deposition in an Alzheimer disease mouse model. *J Clin Invest*. 2005;115(11):3285-90.
113. Hartz AM, Miller DS, Bauer B. Restoring blood-brain barrier P-glycoprotein reduces brain amyloid- β in a mouse model of Alzheimer's disease. *Mol Pharmacol*. 2010;77(5):715-23.
114. Kuhnke D, Jedlitschky G, Grube M, Krohn M, Jucker M, Mosyagin I, et al. MDR1-P-glycoprotein (ABCB1) mediates transport of Alzheimer's Amyloid- β peptides-implications for the mechanisms of A β Clearance at the Blood-Brain Barrier. *Brain Pathol*. 2007;17(4):347-53.
115. Lam FC, Liu R, Lu P, Shapiro AB, Renoir JM, Sharom FJ, et al. β -Amyloid efflux mediated by p-glycoprotein. *J Neurochem*. 2001;76(4):1121-8.
116. Qosa H, Abuznait AH, Hill RA, Kaddoumi A. Enhanced brain amyloid- β clearance by rifampicin and caffeine as a possible protective mechanism against Alzheimer's disease. *J Alzheimers Dis*. 2012;31(1):151-65.

117. van Assema DM, Lubberink M, Bauer M, van der Flier WM, Schuit RC, Windhorst AD, et al. Blood-brain barrier P-glycoprotein function in Alzheimer's disease. *Brain*. 2012;135(1):181-9.
118. van Assema DM, Lubberink M, Boellaard R, Schuit RC, Windhorst AD, Scheltens P, et al. P-glycoprotein function at the blood-brain barrier: effects of age and gender. *Mol Imaging Biol*. 2012;14(6):771-6.
119. Vogelgesang S, Cascorbi I, Schroeder E, Pahnke J, Kroemer HK, Siegmund W, et al. Deposition of Alzheimer's β -amyloid is inversely correlated with P-glycoprotein expression in the brains of elderly non-demented humans. *Pharmacogenetics*. 2002;12(7):535-41.
120. Wang W, Bodles-Brakhop AM, Barger SW. A role for P-glycoprotein in clearance of Alzheimer amyloid β -peptide from the brain. *Curr Alzheimer Res*. 2016;13(6):615-20.
121. Zhang C, Qin H, Zheng R, Wang Y, Yan T, Huan F, et al. A new approach for Alzheimer's disease treatment through P-gp regulation via ibuprofen. *Pathol Res Pract*. 2018;214(11):1765-71.
122. Qosa H, Abuasal BS, Romero IA, Weksler B, Couraud PO, Keller JN, et al. Differences in amyloid- β clearance across mouse and human blood-brain barrier models: kinetic analysis and mechanistic modeling. *Neuropharmacology*. 2014;79:668-78.
123. Brenn A, Grube M, Peters M, Fischer A, Jedlitschky G, Kroemer HK, et al. Beta-Amyloid downregulates MDR1-P-glycoprotein (Abcb1) expression at the Blood-Brain Barrier in mice. *Int J Alzheimers Dis*. 2011;2011.
124. Kania KD, Wijesuriya HC, Hladky SB, Barrand MA. Beta amyloid effects on expression of multidrug efflux transporters in brain endothelial cells. *Brain Res*. 2011;1418:1-11.
125. Park R, Kook SY, Park JC, Mook-Jung I. A β 1-42 reduces P-glycoprotein in the blood-brain barrier through RAGE-NF- κ B signaling. *Cell Death Dis*. 2014;5(6):e1299.
126. Janelidze S, Stomrud E, Palmqvist S, Zetterberg H, van Westen D, Jeromin A, et al. Plasma β -amyloid in Alzheimer's disease and vascular disease. *Sci Rep*. 2016;6(26801).
127. Poller B, Gutmann H, Krahenbuhl S, Weksler B, Romero I, Couraud PO, et al. The human brain endothelial cell line hCMEC/D3 as a human blood-brain barrier model for drug transport studies. *J Neurochem*. 2008;107(5):1358-68.
128. Weksler BB, Subileau EA, Perriere N, Charneau P, Holloway K, Leveque M, et al. Blood-brain barrier-specific properties of a human adult brain endothelial cell line. *FASEB J*. 2005;19(13):1872-4.
129. Weksler B, Romero IA, Couraud PO. The hCMEC/D3 cell line as a model of the human blood brain barrier. *Fluids Barriers CNS*. 2013;10(1):16.
130. Lowik CW, Alblas MJ, van de Ruit M, Papapoulos SE, van der Pluijm G. Quantification of adherent and nonadherent cells cultured in 96-well plates using the supravital stain neutral red. *Anal Biochem*. 1993;213(2):426-33.
131. Ishiyama M, Tominaga H, Shiga M, Sasamoto K, Ohkura Y, Ueno K. A combined assay of cell viability and in vitro cytotoxicity with a highly water-soluble tetrazolium salt, neutral red and crystal violet. *Biol Pharm Bull*. 1996;19(11):1518-20.
132. Repetto G, del Peso A, Zurita JL. Neutral red uptake assay for the estimation of cell viability/cytotoxicity. *Nat Protoc*. 2008;3(7):1125-31.
133. Mosmann T. Rapid colorimetric assay for cellular growth and survival: application to proliferation and cytotoxicity assays. *J Immunol Methods*. 1983;65(1-2):55-63.

134. Morgan DM. Tetrazolium (MTT) assay for cellular viability and activity. *Methods Mol Biol.* 1998;79:179-83.
135. van Meerloo J, Kaspers GJ, Cloos J. Cell sensitivity assays: the MTT assay. *Cancer cell culture: Springer;* 2011. p. 237-45.
136. Poller B, Wagenaar E, Tang SC, Schinkel AH. Double-transduced MDCKII cells to study human P-glycoprotein (ABCB1) and breast cancer resistance protein (ABCG2) interplay in drug transport across the blood-brain barrier. *Mol Pharm.* 2011;8(2):571-82.
137. Jouan E, Le Vee M, Mayati A, Denizot C, Parmentier Y, Fardel O. Evaluation of P-Glycoprotein Inhibitory Potential Using a Rhodamine 123 Accumulation Assay. *Pharmaceutics.* 2016;8(2).
138. Silva R, Carmo H, Vilas-Boas V, Barbosa DJ, Palmeira A, Sousa E, et al. Colchicine effect on P-glycoprotein expression and activity: in silico and in vitro studies. *Chem Biol Interact.* 2014;218:50-62.
139. Vilas-Boas V, Silva R, Gaio AR, Martins AM, Lima SC, Cordeiro-da-Silva A, et al. P-glycoprotein activity in human Caucasian male lymphocytes does not follow its increased expression during aging. *Cytometry A.* 2011;79(11):912-9.
140. Wongwanakul R, Vardhanabhuti N, Siripong P, Jianmongkol S. Effects of rhinacanthin-C on function and expression of drug efflux transporters in Caco-2 cells. *Fitoterapia.* 2013;89:80-5.
141. Mechetner EB, Schott B, Morse BS, Stein WD, Druley T, Davis KA, et al. P-glycoprotein function involves conformational transitions detectable by differential immunoreactivity. *Proc Natl Acad Sci U S A.* 1997;94(24):12908-13.
142. Shapiro AB, Ling V. Positively cooperative sites for drug transport by P-glycoprotein with distinct drug specificities. *Eur J Biochem.* 1997;250(1):130-7.
143. Oliveira C, Cagide F, Teixeira J, Amorim R, Sequeira L, Mesiti F, et al. Hydroxybenzoic Acid Derivatives as Dual-Target Ligands: Mitochondriotropic Antioxidants and Cholinesterase Inhibitors. *Front Chem.* 2018;6:126.
144. Marin-Argany M, Rivera-Hernandez G, Marti J, Villegas S. An anti-Abeta (amyloid beta) single-chain variable fragment prevents amyloid fibril formation and cytotoxicity by withdrawing Abeta oligomers from the amyloid pathway. *Biochem J.* 2011;437(1):25-34.
145. Zhu J, Fu Q, Xia C, Ma G. Effects of diazoxide on Abeta1-42-induced expression of the NR2B subunit in cultured cholinergic neurons. *Mol Med Rep.* 2015;12(6):8301-5.
146. Tang R, Faussat AM, Perrot JY, Marjanovic Z, Cohen S, Storme T, et al. Zosuquidar restores drug sensitivity in P-glycoprotein expressing acute myeloid leukemia (AML). *BMC Cancer.* 2008;8:51.
147. Zerlin T, Kim YS, Hong SY, Song HY. Protective effect of methylprednisolone on paraquat-induced A549 cell cytotoxicity via induction of efflux transporter, P-glycoprotein expression. *Toxicol Lett.* 2012;208(2):101-7.
148. Abuznait AH, Qosa H, Busnena BA, El Sayed KA, Kaddoumi A. Olive-oil-derived oleocanthal enhances beta-amyloid clearance as a potential neuroprotective mechanism against Alzheimer's disease: in vitro and in vivo studies. *ACS Chem Neurosci.* 2013;4(6):973-82.

8. Supplementary data

Cytotoxicity of the Amyloid- β peptide ($A\beta$) vehicle

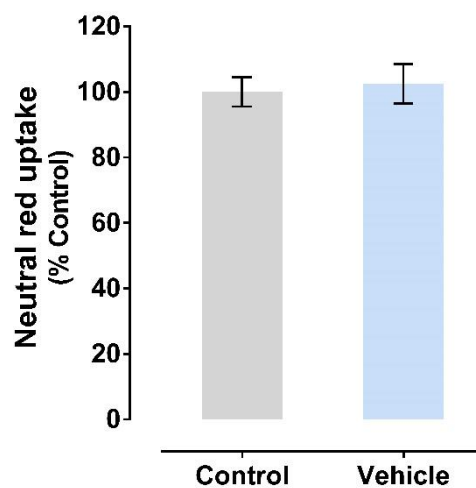


Figure S1. Cytotoxicity of the Amyloid- β peptide 42 ($A\beta_{42}$) vehicle in hCMEC/D3 cells evaluated by the MTT uptake assay, 24 h after exposure. Results are presented as mean \pm SD from at least 3 independent experiments (performed in triplicate). Statistical comparisons were made using the unpaired t test.